



## MPHIL

### **The influence of magnesium stearate and carrier surface on the deposition performance of carrier based dry powder inhaler formulations**

Plastira, Maia

*Award date:*  
2008

*Awarding institution:*  
University of Bath

[Link to publication](#)

## **Alternative formats**

If you require this document in an alternative format, please contact:  
[openaccess@bath.ac.uk](mailto:openaccess@bath.ac.uk)

Copyright of this thesis rests with the author. Access is subject to the above licence, if given. If no licence is specified above, original content in this thesis is licensed under the terms of the Creative Commons Attribution-NonCommercial 4.0 International (CC BY-NC-ND 4.0) Licence (<https://creativecommons.org/licenses/by-nc-nd/4.0/>). Any third-party copyright material present remains the property of its respective owner(s) and is licensed under its existing terms.

### **Take down policy**

If you consider content within Bath's Research Portal to be in breach of UK law, please contact: [openaccess@bath.ac.uk](mailto:openaccess@bath.ac.uk) with the details. Your claim will be investigated and, where appropriate, the item will be removed from public view as soon as possible.

**The influence of Magnesium Stearate and carrier  
surface on the deposition performance of carrier  
based Dry Powder Inhaler formulations**

**Volume 1**

**Maia Plastira**

**A thesis submitted for the degree of Master of Philosophy**

**University of Bath  
Department of Pharmacy and Pharmacology**

**May 2008**

**COPYRIGHT**

Attention is drawn to the fact that copyright of this thesis rests with its author. A copy of this thesis has been supplied on condition that anyone who consults it is understood to recognize that its copyright rests with the author and they must not copy it or use material from it except as permitted by law or with the consent of the author.

This thesis may be made available for consultation within the University Library and may be photocopied or lent to other libraries for the purposes of consultation.

*Plastira*

## **Acknowledgments**

I would like to express my deepest gratitude to my supervisor Dr Robert Price for his guidance, enthusiasm, support and encouragement throughout the course of my research. My sincere thanks to him for the advice and help and especially his much appreciated advice during the writing up of my thesis.

I would also like to thank all the members of the Pharmaceutical Surface Science Research Group: Jag, Chonladda, Amandeep, Haggis for their help and advice during the course of my research. Thanks also to the Optical Electronic Group (SEM).

Finally, words cannot express my sincere gratitude and love to my godfather Dr Andreas Pittas for giving me the opportunity to extend my knowledge, my father Dr Yiannakis Plastiras and my mother Evie Plastira for supporting and encouraging me through all the way, providing me everything I needed. A special thank you to my brother Christis, for his moral support and for making me laugh at times when I needed it. A very big and special thank you to them for their endless love and for being there for me.

## Abstract

This study investigated the influence of the addition of Magnesium Stearate (MgSt) with commercial grade (Lactochem®) and smoothed carrier lactose particles (Nanolac®) on the performance of a budesonide-lactose dry powder inhaler (DPI) formulation. A Multi Stage Liquid Impinger (MSLI) was used to investigate the *in vitro* deposition profile of the budesonide-lactose formulations containing different concentrations of Magnesium Stearate (MgSt), a widely used lubricant in the manufacture of pharmaceutical solid dosage forms. Upon pre-blending Magnesium Stearate using high shear blending process the aerosolisation performance of the DPI generally increased. This study suggested that the addition of 0.25% w/w MgSt in the formulation with Lactochem (63-90 m sieved lactose) resulted in the greatest aerosolisation efficiency amongst the other Lactochem formulations, while for the Nanolac formulations the addition of 0.5% w/w MgSt resulted in the most efficient aerosolisation. This difference could be attributed to the different surface morphology between the two carriers used and therefore the difference in their interparticulate forces between the drug particles and the surface of the carrier. The study suggested that an optimum concentration of the MgSt needs to be reached in order to get balanced interparticulate forces between the drug particles and the carrier surface which will enable maximum aerosolisation deposition. The influence of storage humidity on the aerosolisation efficiency and therefore the adhesion properties of the same formulations were also investigated. The formulations were stored for 3 months at 25°C, 75%RH and 40°C, 75%RH. Storage humidity had a significant effect on the aerosolisation efficiency of all formulations except from the formulation containing 0.5% w/w MgSt. This could be due to the formation of a hydrophobic layer on the surface of the powder formulation, making it less sensitive to moisture. In addition, at high humidity, surface amorphous regions may have the ability to re-crystallize and effectively fuse to the lactose carrier surface, reducing the ability for the powder to be aerosolized and decreasing the FPF. This study suggests therefore, that an optimum concentration of the MgSt needs to be reached in order not only increase aerolisation efficiency but to maintain formulation stability upon exposure to elevated conditions of temperature and relative humidity.

The use of a novel optical technology, the VariDose, was also investigated in order to obtain a system which can lead to an effective and efficient system for testing aerosol based systems for design, cycling, manufacturing and therapeutic management.

# Contents

<b>Acknowledgements</b>	<b>i</b>
<b>Abstract</b>	<b>ii</b>
<b>List of Figures</b>	<b>iii</b>
<b>List of Tables</b>	<b>iv</b>
<b>List of Abbreviations</b>	<b>v</b>
<b>Chapter 1: Introduction</b>	<b>1</b>
1.1 General introduction	1
1.1.1 Respiratory tract delivery	2
1.1.2 Particle deposition in the lungs	3
1.1.2.1 Inertial Impaction	4
1.1.2.2 Gravitational Sedimentation	4
1.1.2.3 Brownian Diffusion	5
1.1.2.4 Interception and Electrostatic Deposition	5
1.1.3 Drug delivery systems	5
1.2 Inter-particulate interactions	9
1.2.1 Electrostatic forces	9
1.2.2 Effect of humidity on electrostatic forces	10
1.2.3 Van der Waals forces	11
1.2.3.1 Casimir-orientation van der Waals forces	12
1.2.3.2 Debye-induction van der Waals forces	12
1.2.3.3 Dispersive or London van der Waals forces	12
1.2.4 Effect of humidity on van der Waals forces	12
1.2.5 Capillary forces	13
1.2.6 Effect of humidity on capillary forces	14
1.3 Factors affecting interparticulate factors	14
1.3.1 Particle size	14
1.3.2 Particle shape	15
1.3.3 Surface roughness of particles	15
1.3.4 Surface free energy	16
1.3.5 Relative humidity	16
1.3.5.1 Effect of storage and exposure to a high relative humidity	17
1.4 Novel developments in improving aerosol delivery performance	17
1.4.1 Addition of Magnesium stearate to DPI formulations	18
1.4.2 Effect of fine excipient particles on carrier based DPI formulations	21
1.4.2.1 The influence of lactose fines on a carrier based DPI formulations	21
1.4.2.2 Removal of intrinsic fine particles from a lactose carrier	21
1.4.2.3 Addition of lactose fines in a formulation	22
1.5 Current pharmaceutical aerosol testing devices	23
1.6 Aim of the study	24
1.7 References	25

## **Chapter 2: General materials and methods**

2.1	Materials	30
2.1.1	Drug material	31
2.1.2	Carrier structure	31
2.2	Methods	32
2.2.1	Scanning electron microscopy	32
2.2.2	Particle size analysis	33
2.2.3	In vitro apparatus for determination of drug concentration	34
2.2.4	Chemical determination of drug concentration	36
2.2.4.1	Preparation of mobile phase	36
2.2.4.2	Preparation of standard solutions of budesonide	36
2.2.4.3	Preparation of powder formulations	36
2.2.4.4	Capsule filling and storage	37
2.2.4.5	Drug content uniformity	37
2.2.5	Drug content determination	38
2.2.5.1	High Performance Liquid Chromatography	38
2.2.6	Statistical analysis	39
2.3	Conclusions	40
2.4	References	40

## **Chapter 3: The effect of different concentrations of Magnesium stearate on the aerosolisation performance of DPI formulations.**

3.1	Introduction	41
3.2	Materials	43
3.3	Methods	43
3.3.1	Scanning electron microscopy	43
3.3.2	Particle size analysis	44
3.3.3	Preparation of surface etched $\alpha$ -lactose monohydrate	45
3.3.4	Preparation of carrier based DPI formulation blends	45
3.3.4.1	Drug content uniformity	47
3.3.4.2	Capsule filling and storage	48
3.3.5	In vitro aerosolisation studies	48
3.3.5.1	Analysis of budesonide	49
3.3.6	Statistical analysis	49
3.4	Results and Discussion	49
3.4.1	Scanning electron microscopy	49
3.4.2	Particle size analysis	54
3.4.2.3	Particle size analysis of MgSt-lactose pre-blends	56
3.4.2.4	Processed formulations	60
3.4.3	Drug content uniformity	66
3.4.4	In vitro aerosolisation studies	67
3.5	Conclusion	89
3.6	References	91

## **Chapter 4: Effects of environmental conditions on the aerosol deposition performance of DPI formulations containing different concentrations of MgSt.**

4.1	Introduction	94
4.2	Materials	96
4.3	Methods	96
4.3.1	Scanning electron microscopy	96
4.3.2	Particle size analysis of aerosol cloud	96
4.3.3	In vitro aerosolisation studies	97
4.3.4	Analysis of budesonide	97
4.3.5	Optical imaging of powder samples	97
4.3.6	Statistical analysis	98
4.4	Results and Discussion	98
4.4.1	Scanning electron microscopy	98
4.4.2	Particle size analysis	104
4.4.3	In vitro aerosolisation studies	107
4.4.3.1	The influence of storage conditions on the in vitro aerolisation performance of Lactochem and Nanolac formulations	107
4.4.3.2	The influence of storage conditions on the in vitro aerolisation performance of 0.25% w/w MgSt formulations	112
4.4.3.3	The influence of storage conditions on the in vitro aerolisation performance of 0.5% w/w MgSt formulations	114
4.4.3.4	The influence of storage conditions on the in vitro aerolisation performance of 1.0% w/w MgSt formulations	117
4.4.4	Summary of deposition performance of the formulations upon storage at different conditions	124
4.4.5	Optical imaging of powder samples	139
4.5	Conclusions	142
4.6	References	143

## **Chapter 5 : Influence of carrier lactose particles modifications on dry powder inhalers performance directly monitored by in line optical measurements**

5.1	Introduction	146
5.1.1	Laser diffraction	146
5.1.2	Varidose device	148
5.1.3	Basic components of a Varidose	151
5.1.4	Sensor position	152
5.1.5	Data acquisition	153
5.1.6	Acquisition frequency	153
5.1.7	Data analysis	153
5.2	Aims of the study	154
5.3	Methods	154
5.3.1	Preparation of Magnesium stearate- lactose blend	155
5.3.2	VariDose experimental set up	155
5.3.3	In vitro aerosolisation studies	156
5.3.3.1	Preparation of carrier based formulations containing fines	157
5.4	Results and discussion	158



5.4.1	Scanning electron microscopy	158
5.4.2	In vitro aerosolisation studies	159
5.5	Conclusion	165
5.6	References	166

## **Chapter 6 : Conclusions**

6.1	Introduction	168
6.2	Summary	169
6.3	Suggested future work	170
6.4	References	172

## List of Figures

Figure 1.1 Diagrammatic representation of the structure of a human lung

Figure 1.2 Chemical structure of Magnesium stearate.

Figure 1.3 Schematic representation of the distribution of lubricant within a formulation

Figure 2.1 Chemical structure of budesonide.

Figure 2.2 Chemical structure of  $\alpha$ -lactose monohydrate.

Figure 2.3 Representative SEMs of the micronised budesonide at A) x3000 and B) x8500 magnification.

Figure 2.4 Schematic representation of a Twin Stage Impinger, adapted from the British Pharmacopoeia, 2001, Volume II.

Figure 2.5 An example of a HPLC calibration graph.

Figure 3.1 Representative scanning electron micrographs of Lactochem at A) x650 and B) x1600 magnifications.

Figure 3.2 Representative scanning electron micrographs of Nanolac at x1200 magnification.

Figure 3.3 Representative scanning electron micrographs showing the control formulation at 25°C, 44%RH containing Nanolac and budesonide at A) x650 and B) x2200 magnifications.

Figure 3.4 Representative scanning electron micrographs showing the control formulation at 25°C, 44%RH containing Lactochem and budesonide at A) x650 and B) x2200 magnifications.

Figure 3.5 Representative scanning electron micrographs of Lactochem and budesonide pre-conditioned with A) 0.125%, B) 0.25%, C) 0.5% and D) 1.0% w/w MgSt at x650 and x2200 magnifications.

Figure 3.6 Representative scanning electron micrographs of Nanolac and budesonide pre-conditioned with A) 0.125%, B) 0.25%, C) 0.5% and D) 1.0% w/w MgSt at x650 and x2200 magnifications.

Figure 3.7 Cumulative particle size distribution of Lactochem<sup>®</sup>.

Figure 3.8 Cumulative particle size distribution of Nanolac<sup>®</sup>.

Figure 3.9 Cumulative particle size distributions of A) blend containing Nanolac and 0.125% MgSt and B) blend containing Lactochem and 0.125% MgSt.

Figure 3.10 Cumulative particle size distributions of A) blend containing Nanolac and 0.25% MgSt and B) blend containing Lactochem and 0.25% MgSt.

Figure 3.11 Cumulative particle size distributions of A) blend containing Nanolac and 0.5% MgSt and B) blend containing Lactochem and 0.5% MgSt.

Figure 3.12 Cumulative particle size distributions of A) blend containing Nanolac and 1.0% MgSt and B) blend containing Lactochem and 1.0% MgSt.

Figure 3.13 Representative particle size distributions of the aerosol clouds generated by the formulations of A) Lactochem and budesonide and B) Nanolac and budesonide at 25°C, 44%RH.

Figure 3.14 Representative particle size distributions of the aerosol clouds generated by the formulations of Lactochem and budesonide pre-conditioned with A) 0.125% B) 0.25%, C) 0.5%, D) 1.0% w/w MgSt at 25°C, 44%RH.

Figure 3.15 Representative particle size distributions of the aerosol clouds generated by the formulations of Nanolac and budesonide pre-conditioned with A) 0.125%, B) 0.25% C) 0.5% and D) 1.0% w/w MgSt at 25°C, 44%RH.

Figure 3.16 The deposition of budesonide, as a percentage of total recovered dose, for Lactochem and MgSt-Lactochem formulations at 25°C, 44%RH. (Mean  $\pm$  S.D, n=3).

Figure 3.17 The deposition of budesonide, as a percentage of recovered dose, for Nanolac formulations at 25°C, 44%RH. (Mean  $\pm$  S.D, n=3).

Figure 3.18 A graph showing the relationship between the recovered dose and the concentration of Magnesium stearate of both types of formulations. (Mean  $\pm$  SD, n=3).

Figure 3.19 A graph showing the relationship between the emitted dose and the concentration of Magnesium stearate of both types of formulations. (Mean  $\pm$  SD, n=3).

Figure 3.20 A graph showing the relationship between the fine particle dose and the concentration of Magnesium stearate of both types of formulations. (Mean  $\pm$  SD, n=3).

Figure 3.21 A graph showing the relationship between the fine particle fraction as a percentage of recovered dose and the concentration of Magnesium stearate of both types of formulations. (Mean  $\pm$  SD, n=3).

Figure 4.1 Representative scanning electron micrographs showing the control formulation at 25°C, 75%RH containing Lactochem and budesonide at A) x1200 and B) x2200 magnifications.

Figure 4.2 Representative scanning electron micrographs showing the control formulation at 25°C, 75%RH containing Nanolac and budesonide at A) x1200 and B) x2200 magnifications.

Figure 4.3 Representative scanning electron micrographs of the formulations containing Lactochem and budesonide pre-conditioned with A) 0.25%, B) 0.5% and C) 1.0% w/w MgSt at 25°C, 75%RH.

Figure 4.4 Representative scanning electron micrographs of the formulations containing Nanolac and budesonide pre-conditioned with A) 0.25%, B) 0.5% and C) 1.0% w/w MgSt at 25°C, 75%RH.

Figure 4.5 Representative scanning electron micrographs showing the control formulation at 40°C, 75%RH containing Lactochem and budesonide at A) x650 and B) x2200 magnifications.

Figure 4.6 Representative scanning electron micrographs showing the control formulation at 40°C, 75%RH containing Nanolac and budesonide at A) x650 and B) x1200 magnifications.

Figure 4.7 Representative scanning electron micrographs of the formulations containing Lactochem and budesonide pre-conditioned with A) 0.25%, B) 0.5%, C) 1.0% w/w MgSt at 40°C, 75%RH.

Figure 4.8 Representative scanning electron micrographs of the formulations containing Nanolac and budesonide pre-conditioned with A) 0.25%, B) 0.5%, C) 1.0% w/w MgSt at 40°C, 75%RH.

Figure 4.9a The deposition of budesonide, as a percentage of recovered dose, throughout the MSLI for the Lactochem control formulations at the different environmental conditions. (Mean  $\pm$  S.D, n=3).

Figure 4.9b The deposition of budesonide, as a percentage of recovered dose, throughout the MSLI for the Nanolac control formulations at the different environmental conditions. (Mean  $\pm$  S.D, n=3).

Figure 4.10a The deposition of budesonide, as a percentage of recovered dose, throughout the MSLI for the 0.25% w/w MgSt+Lactochem+budesonide formulation at the different environmental conditions. (Mean  $\pm$  S.D, n=3).

Figure 4.10b The deposition of budesonide, as a percentage of recovered dose, throughout the MSLI for the 0.25% w/w MgSt+Nanolac+budesonide formulation at the different environmental conditions. (Mean  $\pm$  S.D, n=3).

Figure 4.11a The deposition of budesonide, as a percentage of recovered dose, throughout the MSLI for the 0.5% w/w MgSt+Lactochem+budesonide formulation at the different environmental conditions. (Mean  $\pm$  S.D, n=3).

Figure 4.11b The deposition of budesonide, as a percentage of recovered dose, throughout

the MSLI for the 0.5% w/w MgSt+Nanolac+budesonide formulation at the different environmental conditions. (Mean  $\pm$  S.D, n=3).

Figure 4.12a The deposition of budesonide, as a percentage of recovered dose, throughout the MSLI for the 1.0% w/w MgSt+Lactochem+budesonide formulation at the different environmental conditions. (Mean  $\pm$  S.D, n=3).

Figure 4.12b The deposition of budesonide, as a percentage of recovered dose, throughout the MSLI for the 1.0% w/w MgSt+Nanolac+budesonide formulation at the different environmental conditions. (Mean  $\pm$  S.D, n=3).

Figure 4.13a A graph showing the relationship between the recovered dose and the Lactochem formulations at the different environmental conditions. (Mean  $\pm$  SD, n=3).

Figure 4.13b A graph showing the relationship between the recovered dose and the Nanolac formulations at the different environmental conditions. (Mean  $\pm$  SD, n=3).

Figure 4.14a A graph showing the relationship between the emitted dose and the Lactochem formulations at the different environmental conditions. (Mean  $\pm$  SD, n=3).

Figure 4.14b A graph showing the relationship between the emitted dose and the Nanolac formulations at the different environmental conditions. (Mean  $\pm$  SD, n=3).

Figure 4.15a A graph showing the relationship between the fine particle dose and the Lactochem formulations at the different environmental conditions. (Mean  $\pm$  SD, n=3).

Figure 4.15b A graph showing the relationship between the fine particle dose and the Nanolac formulations at the different environmental conditions. (Mean  $\pm$  SD, n=3).

Figure 4.16a A graph showing the relationship between the fine particle fraction of recovered dose and the Lactochem formulations at the different environmental conditions. (Mean  $\pm$  SD, n=3).

Figure 4.16b A graph showing the relationship between the fine particle fraction of recovered dose and the Nanolac formulations at the different environmental conditions. (Mean  $\pm$  SD, n=3).

Figure 4.17 Optical images of A) Lactochem and budesonide at 25°C, 75%RH and B) at 40°C, 75%RH, C) 0.25%w/w MgSt+Lactochem+budesonide at 25°C,75%RH and D) at 40°C,75%RH, E) 0.5%w/w MgSt+Lactochem+budesonide at 25°, 75%RH and F) at 40°C, 75%RH, G) 1.0%w/w MgSt+Lactochem+budesonide at 25°C,75%RH and H) at 40°C,75%RH.

Figure 4.18 Optical images of A) Nanolac and budesonide at 25°C, 75%RH and B) at 40°C, 75%RH, C) 0.25%w/w MgSt+Nanolac +budesonide at 25°C,75%RH and D) at 40°C,75%RH, E) 0.5%w/w MgSt+Nanolac +budesonide at 25°C, 75%RH and F) at 40°C,

75%RH, G) 1.0%w/wMgSt +Nanolac + Budesonide at 25°C, 75%RH and H) at 40°C, 75%RH.

Figure 5.1 A diagram showing the principle of the laser light diffraction.

Figure 5.2 Images of the A) VariDose device with the sensor rings and B) the Varidose tube intersected by co-planar beams of infrared light.

Figure 5.3 Schematic diagram for optical characterization of the pulmonary drug delivery.

Figure 5.4 An image of the VariDose-TSI experimental set up.

Figure 5.5 Representative scanning micrographs of blend containing budesonide and lactose pre-conditioned with A)1% w/w MgSt at x1500 and B) x2700 magnifications.

Figure 5.6 A graph showing the light obscuration values for each actuation estimated by the varidose apparatus.

Figure 5.7 A graph showing the FPD for each actuation calculated with the TSI.

Figure 5.8 The correlation graph showing the relationship between the FPD estimated by the Varidose and calculated by the TSI.

Figure 5.9 A graph showing the light obscuration values for each actuation estimated by the Varidose for the formulation containing Lactochem +10% fines +budesonide.

Figure 5.10 A graph showing the FPD for each actuation calculated with the TSI for the formulation containing Lactochem+10%fines+budesonide.

Figure 5.11 A graph showing the light obscuration values for each actuation estimated by the Varidose for the formulation containing Nanolac+10%fines+budesonide.

Figure 5.12 A graph showing the FPD for each actuation calculated with the TSI for the formulation containing Nanolac+10%fines+budesonide.

## List of Tables

Table 2.1 Materials used throughout this study.

Table 3.1 Blend masses and concentrations of lactose and MgSt for the prepared blends.

Table 3.2 Blend masses of the pre-blend and drug for the study.

Table 3.3 Particle size distribution statistics summary for budesonide.

Table 3.4 Particle size distribution statistics summary of the carriers.

Table 3.5 Particle size distribution statistics summary of the MgSt-Lactochem pre-blends.

Table 3.6 Particle size distribution statistics summary of the MgSt-Nanolac pre-blends.

Table 3.7 Particle size distribution statistics summary of the Lactochem formulations at 25°C, 44%RH for the Helios Inhaler module.

Table 3.8 Particle size distribution statistics summary of the Nanolac formulations at 25°C, 44%RH for the Helios Inhaler module.

Table 3.9 The content uniformity of the five Lactochem formulations of budesonide analysed by HPLC duplicate.

Table 3.10 The content uniformity of the five Nanolac formulations of budesonide analysed by HPLC in duplicate.

Table 3.11 The deposition of budesonide as mean drug weight per shot ( $\mu\text{g}$ ) at 25°C, 44% RH in the different stages of the MSLI for the Lactochem formulations and standard deviations (Mean  $\pm$  SD), n=3.

Table 3.12 The deposition of budesonide as mean drug weight per shot ( $\mu\text{g}$ ) at 25°C, 44% RH in the different stages of the MSLI for the Nanolac formulations and standard deviations (Mean  $\pm$  SD), n=3.

Table 3.13 The deposition of budesonide in the MSLI from the Lactochem formulations at 25°C, 44%RH via a Cyclohaler (Mean  $\pm$  S.D), n=3).

Table 3.14 The deposition of budesonide in the MSLI from the Nanolac formulations at 25°C, 44%RH via a Cyclohaler (Mean  $\pm$  S.D), n=3).

Table 4.1 Particle size distribution statistics summary of the Lactochem formulations at 25°C, 75%RH.

Table 4.2 Particle size distribution statistics summary of the Nanolac formulations at 25°C, 75%RH.

Table 4.3 Particle size distribution statistics summary of the Lactochem formulations at 40°C, 75%RH.

Table 4.4 Particle size distribution statistics summary of the Nanolac formulations at 40°C,

75%RH.

Table 4.5 The deposition of budesonide as mean drug weight per shot ( $\mu\text{g}$ ) at  $25^{\circ}\text{C}$ , 75%RH in the different stages of the MSLI for the Lactochem formulations and standard deviations (Mean  $\pm$  SD),  $n=3$ .

Table 4.6 The deposition of budesonide as mean drug weight per shot ( $\mu\text{g}$ ) at  $25^{\circ}\text{C}$ , 75%RH in the different stages of the MSLI for the Nanolac formulations and standard deviations (Mean  $\pm$  SD),  $n=3$ .

Table 4.7 The deposition of budesonide as mean drug weight per shot ( $\mu\text{g}$ ) at  $40^{\circ}\text{C}$ , 75%RH in the different stages of the MSLI for the Lactochem formulations and standard deviations (Mean  $\pm$  SD),  $n=3$ .

Table 4.8 The deposition of budesonide as mean drug weight per shot ( $\mu\text{g}$ ) at  $40^{\circ}\text{C}$ , 75%RH in the different stages of the MSLI for the Nanolac formulations and standard deviations (Mean  $\pm$  SD),  $n=3$ .

Table 4.9 The deposition of budesonide in the MSLI from the Lactochem formulations at  $25^{\circ}\text{C}$ , 75%RH via a Cyclohaler (Mean  $\pm$  S.D),  $n=3$ ).

Table 4.10 The deposition of budesonide in the MSLI from the Nanolac formulations at  $25^{\circ}\text{C}$ , 75%RH via a Cyclohaler (Mean  $\pm$  S.D),  $n=3$ ).

Table 4.11 The deposition of budesonide in the MSLI from the Lactochem formulations at  $40^{\circ}\text{C}$ , 75%RH via a Cyclohaler (Mean  $\pm$  S.D),  $n=3$ ).

Table 4.12 The deposition of budesonide in the MSLI from the Nanolac formulations at  $40^{\circ}\text{C}$ , 75%RH via a Cyclohaler (Mean  $\pm$  S.D),  $n=3$ ).



## List of Abbreviations

ACI	Andersen cascade impactor
ANOVA	Analysis of variance
AUC	Area under the curve
BP	British Pharmacopoeia
Bud	Budesonide
C	Constant in Coulomb's law (Equation 1.1)
°C	Degrees centigrade
CAB	Cohesive-adhesive balance
C & D	Capsules and device
CFC	Chlorofluorocarbons
cm	Centimetre
COPD	Chronic obstructive pulmonary disease
CV	Coefficient of variance
d	Distance (Equation 1.1,1.2,1.3)
d <sub>ae</sub>	Aerodynamic diameter of particle
d <sub>50</sub>	50 <sup>th</sup> of particle diameter
DPI	Dry powder inhaler
ED	Emitted dose
F	Capillary force
F <sub>ad</sub>	Force of adhesion
F <sub>el</sub>	Electrostatic force
FPD	Fine particle dose
FPF	Fine particle fraction
FPF <sub>ED</sub>	Fine particle fraction as a percentage of emitted dose
F <sub>vdw</sub>	Van der Waals force
g	Grams
HFA	Hydrofluoroalkanes
HPLC	High performance liquid chromatography
KeV	Kilo electron volts
L	Litres
m	Metre
mg	Milligram
min	Minute
ml	Millilitre
mm	Millimetre
MMAD	Mass median aerodynamic diameter
MSLI	Multi-stage liquid impinger
NGI	Next generation impactor
nm	Nanometre
pMDI	Pressurised metered-dose inhaler
q	Electrical charge
r	Radius
R <sup>2</sup>	Coefficient of determination
RH	Relative humidity
rpm	Revolutions per minute
RSD	Relative standard deviation
s	Stage
s1	Stage 1 of the MSLI

s2	Stage 2 of the MSLI
s3	Stage 3 of the MSLI
s4	Stage 4 of the MSLI
SD	Standard deviation
SEM	Scanning electron microscope
T	Temperature
TSI	Twin-stage impinger
uv	Ultraviolet
<b>x</b>	Arithmetic mean
$\alpha$	Contact angle, anomeric form of lactose
$\beta$	Contact angle, anomeric form of lactose
$\gamma$	Surface tension
$\varepsilon$	Permittivity of free space
$\eta$	Air viscosity
$\theta$	Diffraction angle
$\lambda$	Wavelength
$\mu$	Microgram
$\mu\text{m}$	Micrometre
$\pi$	Constant of proportionality
% v/v	Percentage volume for volume
% w/w	Percentage weight for weight

# Chapter 1

## Introduction

### 1.1 General introduction

Respiratory diseases such as asthma, chronic obstructive pulmonary disease (COPD) and cystic fibrosis have increased dramatically over the last decade. The increase need to develop novel ways of administering inhaled drugs has led to increasing attention to the field of pulmonary delivery. Pulmonary drug delivery is an attractive route of administering drugs to the lungs since it is non-invasive and thus increases patient acceptance and compliance. In addition, relative small doses are required (compared to oral or parenteral administration), minimises side effects and the drug action onset is rapid since the drug is delivered directly to the target thereby reducing systemic exposure.

Furthermore, delivery via the inhalation route provides a portal entry for systemically acting drugs, since it offers a large absorptive surface area for the rapid drug absorption in the peripheral airways<sup>1</sup>. The first drug to be delivered via the lungs was ergotamine for the treatment of migraine in the 1960's. More recently, the first inhalable formulation of insulin was approved for use in Europe and the United States<sup>2</sup>.

One of the major issues with the drug delivery via inhalation, however, is in the inefficiency of the drug delivery systems particularly with issues relating to device related losses, large deposition of the therapeutic dose in the mouth and throat by inertia and rapid particle removal from the lungs by various clearance mechanisms. However, these problems may be addressed by modifying the different factors that influence drug deposition, such as physico-chemical properties of the drug formulation (particle size and shape), its delivery characteristics (aerodynamic diameter), charge, density, hygroscopicity

etc. Furthermore, new inhaler devices are continually being developed to increase deaggregation efficiency.

There are currently three major drug delivery systems: pressurized metered-dose inhalers (pMDIs), dry powder inhalers (DPIs) and nebulisers. These types of systems have been extensively investigated and undergone significant technological advancements in terms of their engineering and in the preparation of their respective formulations.

### **1.1.1 Respiratory tract delivery**

The primary function of the respiratory system is to supply a rich supply of oxygen to the blood which is delivered to all the organs, muscles etc. of the body. It achieves this by a respiratory breathing cycle. During an inhalation/exhalation cycle, an exchange in gases occurs; oxygen is being inhaled and supplied to the heart via the peripheral airways and carbon dioxide is subsequently exhaled. In humans, it is the main two bronchi (produced by the bifurcation of the trachea) that enter the roots of the lungs. The bronchi continue to divide within the lung and after multiple divisions give rise to bronchioles. The bronchial tree continues branching until it reaches the level of terminal bronchioles which lead to the alveolar sacs. Human lungs are located in two cavities and are separated into lobes with three lobes on the right and two on the left<sup>3</sup>.

The respiratory tract is divided into three regions: 1) the upper respiratory tract which includes the nose and nasal passages, the paranasal sinuses and throat or pharynx, 2) the respiratory, or conducting, airways which includes the trachea, bronchi and bronchioles and 3) the peripheral airways, which includes the respiratory bronchiole, the alveolar ducts, the alveolar sacs and the alveoli. In addition to the main function of the transport of oxygen into and carbon dioxide out of the body, the respiratory tract has also evolved into a very effective filter of airborne materials, particularly as it comes into contact with the environment and is exposed to micro organisms in the air. In addition, it is also exposed to many potential pathogens via dust and smoke which are inhaled from the air<sup>4</sup>. In most cases, asthma is caused by inhaling an allergen that sets off the chain of biochemical and tissue changes leading to inflammation of the smooth muscle of the airways and

bronchoconstriction<sup>3</sup>. A schematic diagram of the branching airways of the human respiratory tract is shown in figure 1.1.

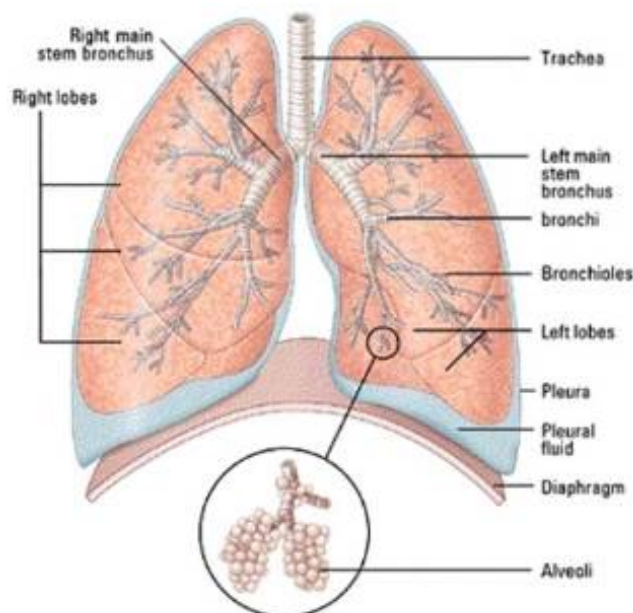


***Figure 1.1 Diagrammatic representation of the structure of a human lung  
(Copyright © 1996 Johns Hopkins University)***

### **1.1.2 Particle deposition in the lungs**

The deposition of inhaled drug aerosol in the respiratory system is influenced by many factors such as inertial impaction, gravitational sedimentation, Brownian diffusion, interception and electrostatic forces<sup>5</sup>. The degree of lung deposition is strongly affected by the aerodynamic diameter of the particles and their distribution. Aerodynamic particle size is the most important physicochemical parameter influencing deposition in the lung. The optimum size range of particulates for inhalation therapy has been shown to be between 1 and 5 $\mu$ m depending on the desired target site<sup>6</sup>.

The aerodynamic particle size influences where in the respiratory tract the aerosol particles will be deposited. Particles with an aerodynamic diameter ( $d_{ac}$ ) larger than  $6\text{ }\mu\text{m}$  deposit mainly in the oropharyngeal region, particles with a  $d_{ac}$  between  $4$  and  $6\text{ }\mu\text{m}$  deposit in the conducting airways (e.g bronchioles), while particles with  $d_{ac}$  less than  $2\text{ }\mu\text{m}$  deposit in the peripheral regions of the lung (e.g. alveoli).

Aerosols come in a variety of shapes and sizes therefore different particles characteristics will be affected by different particle deposition mechanisms. This effect is taken into account by determining their aerodynamic particle diameter of the aerosol particles. The main mechanisms of particle removal from an inhaled dose are summarised below:

#### **1.1.2.1 Inertial Impaction**

Large particles ( $d_{ac} > 6\text{ }\mu\text{m}$ ) are affected by inertial impaction when the gas air stream is fast, changing direction or turbulent<sup>7</sup>. The impaction is caused by the inertial properties of the particles, which tends to resist a change in the direction of its path. Thus, particles of a certain mass travelling in an air stream at a sufficient velocity will not lose momentum sufficiently quickly to be able to relax into a new direction of the airflow and so will impact in the upper airways. Inertial impaction is the main mode of particle removal in oropharynx, larynx and at bifurcations in the upper airways<sup>7</sup>.

#### **1.1.2.2 Gravitational Sedimentation**

When the air velocity in respiratory tract is low and the residence time is high, particles are affected by gravitational sedimentation. It is dependant on the terminal settling velocity of the particle and is an important deposition in the bronchioles, where residence time is high and velocity is low. This process is time dependant, as particles must have sufficient residence time in the airway to settle from their initial position to deposit on the respiratory surface<sup>7</sup>.

### 1.1.2.3 Brownian Diffusion

Small particles ( $d_{ae} < 0.1 \mu\text{m}$ ) are affected by Brownian diffusion, which is caused when particles are randomly bombarded by air molecules giving rise to a “random walk.”

Brownian motion results in particles following a random and variable path and for the particles  $< 0.5 \mu\text{m}$  in diameter it will tend to cause greater displacement than sedimentation and so the primary mechanism of deposition in the terminal bronchioles and alveolar regions<sup>7</sup>.

### 1.1.2.4 Interception and Electrostatic Deposition

Other particle deposition mechanisms include *interception* where particles travelling within the air stream are intercepted by contact with the respiratory airway and electrostatic deposition where deposition where highly charged particles may be efficiently deposited if the electric field induced by an image charge on the airways is sufficient to direct the aerosol particles towards the airway walls<sup>7</sup>.

### 1.1.3 Drug delivery systems

**Pressurised metered dose inhalers** have been the system of choice for delivery of inhaled therapies for airway diseases for decades, but recent environmental concerns over the use of chlorofluorocarbon (CFC) propellants, which have been directly linked to the depletion of the ozone layer, has forced the pharmaceutical industry to re-address their long term use. Following the Montreal protocol in 1987, the use of CFC driven aerosols, have been phased out, although an extension was provided for inhaler devices until an alternative formulation could be obtained<sup>8</sup>. This led to the reformulation of pMDIs using hydrofluoroalkanes (HFAs) as alternative propellants.

Formulation of the active pharmaceutical ingredients in these propellants have been fraught with difficulties particularly because of crucial differences in densities and solubilities of

drugs and excipients<sup>9</sup>. As a result of the significant issues in formulating new chemical entities as pMDI formulations, several of the major pharmaceutical companies have favoured their development of new inhalation products away from the pMDI platform<sup>8</sup>. In pMDIs, a high vapour pressure gas, typically a liquid propellant (CFC) and a solution or suspension of fine drug particles is contained within a pressurised canister<sup>10</sup>. Actuation of an inhaler valve results in the release of a metered volume of this solution or suspension which is driven at high speed through a narrow orifice by the volatile expansion of the pressurised liquid, resulting in the delivery of the dose to the respiratory tract<sup>10</sup>.

**Nebulisers** provide a means of delivering high doses of a drug directly to the lungs<sup>7</sup> and are usually prescribed to people with severe, life-threatening asthma or COPD. A compressor is traditionally used to provide sufficient energy to a solution to make a fine mist of the solute material. The mist is being continually aerolised via the nebuliser which allows the patient to continually inhale the aerosol without the requirements for device-patient co-ordination with pMDI devices and the forced inhalation breathing manoeuvre required for passive DPI devices.

The aerosol droplets produced have typically a smaller aerodynamic particle size than DPIs and pMDIs, making them capable of penetrating the deeper regions of the airways. However, the use of nebulisers is limited due to the length of time needed to deliver the required dose (usually 10 to 15 minutes), they are not portable and the nebuliser are costly<sup>7,11</sup>.

The problems and limitations with nebulisers and pMDIs has led to the increasing development and acceptability of the use of **Dry powder inhalers** (DPIs) for the delivery of therapeutic agents to the respiratory tract.

The use of DPIs for inhalation therapy for obstructive airway disease management such as asthma and chronic obstructive airway disease (COPD) has gained significant popularity during the early part of the 21<sup>st</sup> century<sup>12</sup>. DPIs were firstly used in the treatment of asthma in the 1960's and the 1970's, for the delivery of high powder loads. The first marketed



passive unit-dose DPI device was the Fisons Intal Spinhaler device for the delivery of sodium cromoglycolate. This was soon followed by the development of the Glaxo Rotahaler device for the delivery of the  $\beta$ 2-agonist salbutamol sulphate.<sup>13</sup>

DPI formulations typically involve a blend of the drug particles ( $<5\mu\text{m}$ ) and coarse excipient particles ( $63\text{--}90\mu\text{m}$ ). Drug particulates are blended with the inert crystalline carrier materials to reduce the cohesive interactions between the primary drug particles and to improve formulation flowability for device filling and subsequently the fluidisation of the formulation during device activation<sup>14</sup>. Carrier based systems also allow accurate metering of very small quantities of potent drug ( $>6\mu\text{g}$ ).

The blend forms an ordered mixture of the drug and excipient<sup>15</sup> and is typically referred to as a binary or carrier-based DPI formulation. The most commonly used carrier in DPI formulations is  $\alpha$ -lactose-monohydrate which is relatively cheap and pharmacologically inert<sup>16</sup>. During a forced inhalation manoeuvre, the resistance to the air flow generated via the passive DPI device may generate sufficient drag and shear forces to overcome the interparticulate attractive force between the drug particles and carrier particle surface leading to the re-suspension of the drug particles for lung delivery<sup>17</sup>. If the drug particles are strongly adhering to the lactose surface the aerodynamic forces generated within the DPI device may not be sufficient for efficient drug re-suspension leading to a low fine particle dose delivery. The larger carrier particles and the drug particles which have not been re-suspended during aerolisation impact in the oropharynx and the upper airways and eventually are swallowed<sup>14</sup>.

This process of aerolisation is key to understanding the performance (how much drug reaches the target site of action) of the formulation and is dependant upon a fine balance of the adhesive and cohesive forces between the drug and carrier particles<sup>18,19</sup>. The adhesive forces between the drug and carrier particles are known to be dependant upon many factors such as size, shape, surface roughness and morphology of the particles, the presence of electrostatic charging, the environmental conditions (relative humidity and temperature) and the process (e.g. low shear versus high shear processing) by which the blend is formed<sup>16,19,20</sup>.

To achieve the optimum particle size distribution of the drug particles for inhalation therapy, energy intensive comminution techniques (e.g. air-jet milling) are commonly used. However, these micronised powders, have a high bulk volume and exhibit very poor flow characteristics due to the highly cohesive interactive forces between particles, making them difficult to handle and process. This problem is effectively overcome by the use of carriers, as mentioned above<sup>21</sup>.

The deposition of inhaled drug aerosol in the respiratory system is also influenced by the variability of the energy source (i.e. the patient) and their inhalation technique, the device used, the drug substance and the formulation. The performance of a DPI is a direct function of the energy supplied by the forced inhalation breath of patients to de-aggregate and deliver the active ingredient to the site of action<sup>6</sup>.

There are three primary forces in a dry powder inhalation system which influence the total adhesion and cohesion of the system. These are van der Waals forces, electrostatic and capillary interactions and their characteristics such as magnitude, total interaction and subsequent aerolization efficiency which will depend on the physicochemical characteristics of the drug and the carrier, and the environmental conditions in which they are stored and delivered, ie humidity, temperature<sup>12</sup>.

The engineering of the DPI devices are designed to provide sufficient resistance to the inspiration and the inspiratory flow of the patient to induce the energy required for de-aggregation and aerosolisation of the medication. High resistance devices, such as the reservoir based Clickhaler, require a considerable inspiratory flow to produce a dose and provides effective drug delivery to the lower respiratory tract<sup>22</sup>. The main problem with the majority of marketed DPIs is in the variability of the source (i.e. the patient) and its dependence on the inspiratory flow to deliver the payload. Patients, in particular the elderly people and/or children, cannot provide sufficient inspiratory flow for efficient drug re-suspension, thus influencing the possible therapeutic effect<sup>9</sup>.

## **1.2 Interparticulate interactions**

In order to increase the degree of particle de-aggregation there is a need to understand the physical forces which may directly influence the particulate interactions within a formulation and the requirements for overcoming the forces to effectively de-aggregate the particles. The interparticulate interactions are one of the most important factors in determining the performance and behaviour of carrier-based DPI formulations.

Particle interactions are primarily dictated by van der Waals forces, electrostatic forces and capillary forces. The effect of these three forces to the total interaction have been shown to be dependant on the physicochemical properties of the materials and environmental conditions such as temperature and humidity. The effect of the environmental conditions on the interparticulate forces and therefore aerosolization performance, will be drug specific signifying that a detailed understanding of the DPI and its properties are required for formulation development.

### **1.2.1 Electrostatic forces**

One of the major problems associated with the DPIs is the generation of electrostatic charges, which have been shown to influence the performance of the inhaler device<sup>23</sup>. Electrostatic charges are generated when two different materials are brought together and then separated<sup>23</sup>. Such a charge build-up develops an electric field that has an effect on other subjects at a distance.

During aerosolisation processes like shaking, priming, metering and dispersion, the movement of particles and droplets with the surface of the inhaler device provides the ideal conditions for the development of charge by triboelectrification<sup>24</sup>.

Triboelectrification is whereby an electrostatic charge is generated by the contact and separation of two dissimilar materials, resulting in oppositely charged surfaces<sup>24</sup>.

Electrostatic effects were first reported almost 2500 years ago but it was only in 1780's when Coulomb described the electrostatic force:

Equation 1.1

$$F = \frac{Cq^2}{d^2}$$

This equation shows that the force (F) between two materials carrying a charge (q) is inversely proportional to the square of the distance (d) between the materials and C is constant<sup>7</sup>. In the simplest case of two point electric charges, the magnitude of the electrostatic force,  $F_{el}$ , between them can be described by Coulomb's law:

Equation 1.2

$$F_{el} = \frac{q_1 q_2}{4\pi\epsilon_0\epsilon_r d^2}$$

Where  $F_{el}$  : the force of attraction or repulsion (N)

$q_1$ : electric charge on the first particle in Coulomb (q)

$q_2$ : electric charge on the second particle in Coulomb (q)

$4\pi$ : constant of proportionality

$\epsilon_0$ : permittivity of free space ( $Fm^{-1}$ )

d: distance between the charge points in meters (m)

For a single charged particle near a flat (plane) conducting surface the relationship becomes:

Equation 1.3

$$F_{el} = \frac{q_1^2}{16\pi\epsilon d^2}$$

Equation 1.3 shows that a charged particle will always be attracted to an uncharged conducting surface<sup>7</sup>.

### 1.2.2 Effect of humidity on electrostatic forces

At low relative humidity, electrostatic forces predominate in particle interactions. As previously stated, the multiple contacts between drug particles and surfaces during handling

and aerosolization will lead to triboelectric charging. These charges lead to an increase in the attractive forces between the micronized materials, resulting in an increase in the contact area and therefore causing a greater degree of cohesion. However, in the presence of moist air, water can adsorb onto the surface of the material, allowing mobilization of electrons, increasing surface conductivity and subsequently reducing specific charge<sup>25</sup>.

### 1.2.3 van der Waals forces

The van der Waals force is the fundamental quantum mechanical inter-molecular force that results when molecules come very close to one another. It is a finite attractive force which is present between all atoms and is short range force<sup>26</sup>. The adhesive van der Waals force ( $F_{vdw}$ ) between a spherical particle and a plane surface is determined by the following equation:

$$\text{Equation 1.4} \quad F_{vdw} = \frac{Ad}{6r^2}$$

Where d: diameter of particle

r: distance between particle and plane surface

A: Hamaker constant which represents the interaction energy that is dependant on the molecular properties of both interacting materials

$$\text{Equation 1.5} \quad \text{Where: } A = \pi^2 v_1 v_2 \lambda_{1,2}^d$$

Where  $v_1$  &  $v_2$ : number of atoms per unit volume of particles 1 and 2

$\lambda_{1,2}^d$ : constant of dispersion

$$\text{Equation 1.6} \quad \text{Where: } \lambda_{1,2}^d = -3/4 h f \alpha^2$$

Where h: Planck's constant

f: vibration frequency of the interacting electronic oscillators

$\alpha$ : polarisability of the molecules

The van der Waals force between two ideally smooth spherical particles in vacuum is expressed by the equation:

Equation 1.7

$$F_{vdw} = \frac{A}{12r^2} \left( \frac{d_1 d_2}{d_1 + d_2} \right)$$

As can be seen from both equations, the separation distance (r) of the interacting materials is a critical parameter<sup>7</sup>.

#### **1.2.3.1 Casimir-orientation van der Waals forces**

These forces arise between two polar molecules each of which has the electric dipole moment.

#### **1.2.3.2 Debye-induction van der Waals forces**

These forces arise between polar and non polar molecules.

#### **1.2.3.3 Dispersive or London van der Waals forces**

These are weak intermolecular forces that arise from the attractive force between transient dipoles in molecules without permanent multiple moments. These forces are finite between all atoms and are of predominant importance between macroscopic bodies. They are the most ubiquitous of the van der Waals forces.

#### **1.2.4 Effect of humidity on van der Waals forces**

The presence of moisture increases the van der Waals forces as a decrease of the interparticle distance will occur due to the fact that the adsorbed layers may be considered as part of the particle<sup>25</sup>.

### 1.2.5 Capillary forces

Capillary forces result from trapped liquid that produce an attractive force due to Laplace pressure differences and surface tension forces. If the condensation of the water vapour is significant, usually at high relative humidities, the formation of a liquid bridge may arise between two conducting surfaces due to capillary interaction, leading to the formation of the force. In addition, this structure leads to an increased force of adhesion between the particles due to the surface tension of water. At high humidities, (above 65%), capillary forces become the dominant force responsible for adhesion<sup>7</sup>.

The magnitude of the capillary force ( $F_C$ ) between two identical smooth spheres (radius  $r$ ) may be simply calculated as:

$$\text{Equation 1.8} \quad F_C = 2\pi\gamma_L r \cos\alpha$$

Where:  $\gamma_L$  is the surface tension of water

$\alpha$  is the contact angle between water and the spheres

The capillary force resulting from the condensation of water in the interface in the case of a sphere (radius  $r$ ) is calculated by:

$$\text{Equation 1.9} \quad F_C = 2\pi\gamma_L r (\cos\alpha + \cos\beta)$$

The formation of capillary forces by condensation leads to undesirable events such as an increase in the strength of granules, which leads to flow problems and/or caking of powder samples during storage and handling. The prediction and control of the magnitude of capillary forces is necessary for eliminating or minimizing these undesirable events. In addition, volume reduction with evaporation of the liquid can produce sufficient strength to collapse fragile suspended structures, resulting in the damage of the devices and the promotion of the adhesion that results from van der Waals and electrostatic forces<sup>7</sup>.

### **1.2.5 Effect of humidity on capillary forces**

At high relative humidity, capillary forces predominate in particle interactions. The presence of water on the surface of the powders causes attractive forces due to the capillary action of adsorbed water layers. At high humidities, water vapour can condense in the capillaries which are present between individual powder particles forming liquid bridges. The presence of these liquid bridges increases the cohesive forces between particles leading in an increase in tensile strength. In addition, in extreme cases, where the materials are highly hydrophilic and hygroscopic, deliquescence and subsequent solidification of the particle surfaces could potentially lead to the formation of solid-liquid bridges, therefore increasing the particle size and decreasing the fine particle fraction<sup>25</sup>.

## **1.3 Factors affecting interparticulate factors**

The interparticulate forces are influenced by many factors such as the particle size, shape, surface roughness of the particles, surface free energy and relative humidity. Each of these factors will be described in detail below.

### **1.3.1 Particle size**

Of all the physical parameters that influence the delivery of dry powder inhaler formulations to the lung, the most critical one is the particle aerodynamic diameter. As mentioned previously in 1.1.2 section, only particles within the narrow size range of 0.5 to 5µm can reach the deep lung and avoid impaction in the upper airways. In some cases, if the dry powder particles adsorb moisture, they grow in the presence of a humid environment or even agglomerate, therefore getting deposited to a different location in the respiratory tract and affecting the efficacy of the formulation. Furthermore, larger particles tend to be highly adhesive/cohesive and are influenced by particle interactions.



The van der Waals, capillary and electrostatic forces all increase with increasing particle size.

As particle size decreases, the adhesion forces experienced by a particle become more and more significant when compared to the gravitational forces to which it is exposed<sup>51</sup>. The cohesive and adhesive properties of particles with a diameter less than 10  $\mu\text{m}$  are governed by the van der Waals forces and the relative influence of the dynamic capillary and electrostatic forces.

### **1.3.2 Particle shape**

Particle shape is one of the most uncontrollable factors which may influence interparticulate interactions, due to the fact that the methods used to produce particles give rise to particles with various geometrical parameters. The van der Waals and electrostatic forces both decrease as a function of the square of the separation distance between particles. Thus, any effect on particle shape, will therefore have a significant effect on interparticulate forces.

### **1.3.3 Surface roughness of particles**

Particle roughness is another important factor that affects the interparticulate forces by determining the level of adhesion to other active particles, excipients and inhaler device surfaces, via its effect on contact area<sup>21</sup>. Smoother particles are likely to reduce particle self-adhesion, therefore reducing agglomerate formation<sup>21</sup>. When the particle surfaces are rough, the force of adhesion between the drug particles and the carrier surface is low due to the small surface contact area and therefore a reduced amount of force is required to detach the drug particles from the carrier surface. A perfect sphere sitting on top of a perfectly flat surface will have the maximum contact area. Microscopic asperities on particle surfaces would dramatically decrease the effective contact area of contiguous surfaces, resulting in a concomitant reduction in particle interactions.

### 1.3.4 Surface free energy

The surface free energy of a solid material can be defined as the free energy change during the formation of a surface by one unit area in vacuo and is analogous to the surface tension of a liquid<sup>52,53</sup>. The amount of work required to separate two surfaces is termed the work of adhesion ( $W_a$ ) and is related to the surface free energy of the surfaces by the following equation:

$$\text{Equation 1.10} \quad W_a = A (\gamma^1 + \gamma^2 - \gamma^{12})$$

Where A: is the area of surface produced by separation

$\gamma^1$  and  $\gamma^2$ : are the surface free energy of the 2 surfaces

$\gamma^{12}$ : is the free energy of the 1-2 interface per unit area

The work of cohesion ( $W_c$ ), which is the work required to separate two surfaces of the same material is given by the equation:

$$\text{Equation 1.11} \quad W_c = 2A \gamma^1$$

In general, solids exhibiting high surface energy are more likely to form strong inter-surface forces. Therefore, the adhesion and cohesion of respirable drug particles will be affected by the surface free energies of the interacting particles<sup>7</sup>.

### 1.3.5 Relative humidity

In order to get drug delivery into the lungs from a DPI formulation, the drug particles have to detach from the carrier particle surface and penetrate into the lungs. The key factors affecting the de-agglomeration and aerosolisation of respirable particles are the interparticulate forces between contiguous particle surfaces and the physicochemical stability of DPI formulations upon storing and handling at variable environmental

conditions of temperature and relative humidity.

DPIs are particularly susceptible to interparticulate forces because micronized powders have a high specific surface area. Interparticulate forces are affected by relative humidity via two mechanisms. Firstly, the presence of humidity allows the dissipation of electrostatic charge from particles, by increasing the conductivity of both the atmosphere and the materials themselves, thus decreasing the electrostatic forces<sup>7</sup>. In addition, relative humidity changes induce changes in water activity; at high RH water can condensate at the contact points between particles leading to the formation of liquid bridges and an increase in capillary forces<sup>7</sup>.

#### **1.3.5.1 Effect of storage and exposure to a high relative humidity**

The interparticulate interactions in adhesive mixtures may change with time, depending on the storage conditions. Braun et al (1996)<sup>54</sup> showed that two formulations with different strengths of disodium cromoglycate had higher fine particle fractions when stored for 27 days at 33%RH than the formulations which were stored at 55%RH. In addition, it has also been found that the relative humidity of the air during inhalation may influence the fraction of the drug detached from the carrier surface<sup>54</sup>. This can be explained by the fact that humidity influences the energy necessary to separate the drug particles from the carrier particles.

### **1.4 Novel developments in improving aerosol delivery performance**

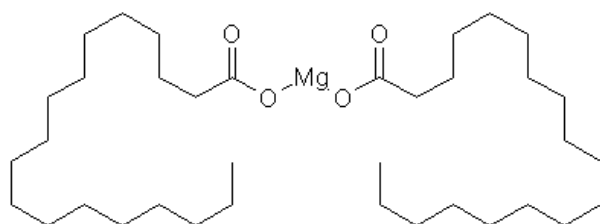
Numerous techniques have been applied in modifying the interparticulate interactions in DPI formulations and thereby increasing aerosolisation performance. The majority have targeted the physical properties of the carrier such as the particle size, shape and surface roughness. Other techniques applied include engineering drug particles to produce more

uniform drug particulates, using methods such as spray drying and supercritical fluids. Addition of a wetting agent or an anti-adherent material to improve the dispersibility of the formulation has been investigated<sup>27,28</sup>.

In addition, it has been reported that the co-processing of the carrier particles with low surface free energy materials like magnesium stearate, leucine, lecithin, increases the aerosolisation efficiencies of dry powder inhaler formulations<sup>29</sup>, by decreasing the drug-excipient adhesion and thus facilitating the drug detachment upon device actuation. The increase in performance is achieved by the anti-adherent and/or anti-friction properties of these force control agents (FCAs).

#### 1.4.1 Addition of Magnesium Stearate to DPI formulations

Magnesium stearate is the most widely used lubricant in the manufacture of pharmaceutical solid dosage forms<sup>30</sup>. The structure of magnesium stearate is shown in figure 1.2.



**Molecular formula: C<sub>36</sub>H<sub>70</sub>MgO<sub>4</sub>**

***Figure 1.2 Chemical structure of Magnesium stearate***

During powder formulation, various adjuvants are added to the formulations to form a bulk mixture in achieving uniform mixing and flow of the powders in capsules or tablets<sup>31</sup>. The adjuvants influence the physical properties of the tablets; the crushing strength of the tablet decreases and the disintegration time increases<sup>32</sup>. Lubrication involves adding small quantities of an antifriction agent to powders or granules and mixing them for a specified time<sup>31</sup>. In general, a lubricant is used to eliminate adherence of the tablet compact to the die,

and minimise sticking and picking of the punch face surfaces in contact with the compressed tablet<sup>31</sup>.

As mentioned, MgSt is an effective lubricant, anti-adherent and glidant<sup>33</sup> and is a critical excipient for processing tablets<sup>34</sup>. MgSt has also been proven to be a functional excipient in dry powder inhaler formulations for inhalation. Studies have shown that the addition of MgSt improves the powder flow of carrier based ordered mixtures, promotes the release and dispersion of the drug particles from the carrier surface and manipulates and modifies the interparticulate forces within a DPI formulation<sup>30</sup>. In addition, it has also been shown that MgSt improves the moisture resistance of DPI formulations under high humidity conditions<sup>30</sup>.

In contrast, MgSt is commonly known to cause de-stabilization of ordered powder mixtures if not carefully controlled. Furthermore, due to the variability in source, its lubricant properties may vary from batch to batch due to the fact that it primarily consists of a mixture of magnesium stearate, magnesium palmitate in various proportions together with very small amounts of magnesium laurate and myristate<sup>35</sup>.

As shown for conventional solid dosage forms, the process of blending and the time of introduction of MgSt is quite critical to the performance of the formulation. The duration of mixing in the lubricant component affects the properties of the compact as well as the properties of the blended mixture by changing the apparent bulk volume, the compression force required to make a prescribed compact and the hydrophobic character of the mixture<sup>31</sup>.

It is suggested that after a mixing time of 1 min there is a good correlation between the lubricant surface area and the coverage of the base of the material. The distribution of MgSt in a powder mass upon mixing is shown in Figure 1.3, below<sup>36</sup>.

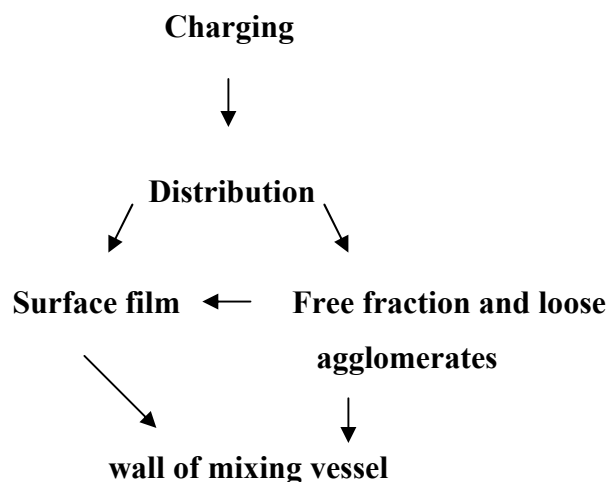


***Figure 1.3 Schematic representation of the distribution of lubricant within a formulation***

When MgSt is used within a powder blend, it is either distributed as a free fraction and loose agglomerates or it gets deposited as a surface film on the base material. If the mixing time is prolonged, then more lubricant will be transferred from the free fraction to the surface film and would therefore affect the lubricating properties of the MgSt since both free fraction and surface film is required in order to form the die wall<sup>36</sup>.

The mechanism of lubrication for MgSt involves covering the surface through physical mixing upon the initial mixing and the subsequent forming of a film if there is sufficient shear. As the mixing continues, the shear effects continue to cause delamination or deagglomeration of the lubricant to harness more stearate particles which slide or adhere on the excipient surface<sup>36</sup>. Therefore, the adhered particles, once delaminated, no longer spread over the excipient surface during mixing. This tendency of the particles to delaminate may make some forms of MgSt perform better as a lubricant than others under given mixing times<sup>31</sup>.

The lubricant properties of pure MgSt are influenced by many factors such as the particle size, the surface area, the crystal structure of the compound and more specifically the crystal spacing which is dependent on the hydration state<sup>37</sup>.

According to Ertel and Carstensen<sup>38</sup> the lubrication properties of pure MgSt depend on the moisture content and the crystal structure. Furthermore, studies suggest that the batch with smaller particle size and larger surface area has considerably better performance<sup>38</sup>.

#### **1.4.2 Effect of fine excipient particles on carrier based DPI formulations**

The amount of fine carrier particles, the shape of the particle size distributions and the surface roughness of the coarse carrier particles in a dry powder inhaler formulation play a key role in drug deposition. It has been reported in the literature that the addition of fine carrier particles in a powder mixture improves the drug deposition through optimizing the drug-carrier interaction. Fine carrier particles may form agglomerates with micronized drug and therefore effective respiratory delivery will require the dispersion of the drug from the agglomerate using energy generated from the inspiratory airflow of the patients<sup>39,40</sup>.

##### **1.4.2.1 The influence of lactose fines on a carrier based DPI formulation**

The inclusion of fines in carrier-based DPI systems is an extensively investigated and useful technique for the improvement of formulation performance. Carriers containing greater proportions of intrinsic fines give better performance<sup>41,42</sup>, and can be decreased by their removal.

The addition of fine particles of lactose or one of many excipients to a formulation increases performance, although this may be at the cost of decreasing emission of drug from the device. The optimum median particle size for additional fines appears to be approximately 5-10 $\mu\text{m}$ <sup>43</sup>.

##### **1.4.2.2 Removal of intrinsic fine particles from a lactose carrier**

A number of studies conducted have incorporated pre-treatment of a coarse lactose carrier to remove any existing intrinsic fine particles, in order to allow a more accurate

quantification of the effects of adding fines to a formulation. In such cases, the removal of intrinsic fines resulted in a decrease in the performance of the formulations and the findings were in accordance with findings of studies suggesting that formulations containing the highest proportions of intrinsic fines have the greatest aerosol deposition performance<sup>41,42</sup>. study conducted by Islam et al (2004)<sup>44</sup> investigated the performance of salmeterol xinafoate containing different grades of carrier lactose modified by wet decantation. The results suggested that as the number of lactose particles  $<5\mu\text{m}$  in the carrier increased, the fine particle fraction (FPF) increased up to the maximum when the proportion of the intrinsic lactose fines was 15% where thereafter no improvement in performance was observed<sup>44</sup>.

In this study, two types of carriers were used in preparing the formulations. The first type was Lactochem which was used as-supplied as a sieve fraction in the range 63-90 $\mu\text{m}$  and the second type was Nanolac which is etched lactose. The removal of fine lactose particles in Nanolac was performed by an etching process and the effect of the fines was investigated in formulations containing MgSt to examine any improvement in the performance.

#### **1.4.2.3 Addition of lactose fines in a formulation**

As the presence of fines in the carrier material is one of the most important factors influencing the formulation performance, extended research has been conducted. Zeng et al (1996)<sup>45</sup> investigated the effect of the addition of 6% fines to a carrier-based formulation containing 1.5% salbutamol sulphate and lactose, which resulted in an increase in the FPF by up to 116%.

In addition, another study performed by Zeng et al (2001)<sup>46</sup> using a formulation containing again salbutamol sulphate, lactose ad lactose fines resulted in an increase in fine particle dose (FPD) by up to 51%. The majority of the studies performed, found that the addition of lactose fines to the formulations resulted in an increase in FPF or in FPD of the



drug. Furthermore, the concentration of the fines in the formulation has also an effect in the performance of the formulation. However, each study performed on the variation of the amount of lactose fines, suggested a different optimum concentration which could be due to the different methods and materials used.

### **1.5 Current pharmaceutical aerosol testing devices**

An in vitro apparatus is used as a substitute for the respiratory tract, acting as a surrogate particle collector. They reproduce, to a reasonable degree, the aerosol deposition characteristics within the respiratory tract. These devices classify the particles collected according to their aerodynamic diameters, therefore indicating the extent to which the sample would have penetrated the respiratory tract. Impactors are the instruments of choice for the in vitro assessment of delivery efficiency of inhalation products and the reason is because they allow the aerodynamic size distribution of the entire inhaled dose to be characterised in a way that is specific to the drug and which ignores the size of any excipient particles that are present<sup>47</sup>. Pharmacopoeia acceptable in vitro testing apparatus include the Andersen Cascade Impactor (ACI), the Marple Miller Impactor, the Multi Stage Liquid Impinger (MSLI), the Twin Stage Impinger (TSI) and the recently developed Next Generation Impactor (NGI).

The MSLI and TSI which are used in this study will be described in more detail in Chapter 2, Section 2.2.3.

## 1.6 Aims of the study

As mentioned, different strategies have been employed in order to improve the aerosol deposition performance of carrier-based DPI formulations by affecting the interparticulate interactions between particles in them. It is clear that the investigation of the interparticulate interactions between the variable formulations compared to their aerosol performance may be useful to find out the mechanism by which MgSt and fines improve the formulation performance. A better understanding of these mechanisms is important to determine the optimum concentration of MgSt and fines of lactose to achieve better aerosol performance and more efficient protection at different environmental conditions, as well as promote faster formulation development.

The primary aim of this study is to investigate the influence of the addition of MgSt and the presence of lactose fines on the aerosol deposition performance of DPI formulations and consequently the drug-excipient adhesion properties. In addition, investigative work was also conducted to investigate and understand the prospective influence of the environmental conditions such as relative humidity and temperature on the stability of the DPI formulations and if the addition of MgSt would protect the formulations from de-stabilising under these conditions. By employing different concentrations of MgSt on carriers with different morphology, formulations with varying adhesive and cohesive interactions were produced, enabling the exploration of their relationship to in-vitro formulation performance.

In addition, the potential use of an in-line optical sensing technology, the VariDose, is investigated (Chapter 5) which could rapidly test the performance and predict the variability in the delivery characteristics of both nasal and inhalation based formulations. The VariDose device, could lead to an effective and efficient system for testing aerosol based systems for design, cycling, manufacturing and therapeutic management.

## 1.7 References

1. Byron P.R, Patton J.S, “Drug delivery via the respiratory tract”, *Journal of Aerosol Medicine* 1994;7:49-75.
2. Lenzer J, “Inhaled insulin is approved in Europe and United States”, *British Medical Journal* 2006;332:321.
3. Stille D.R, “The Respiratory System”, New York: Children’s Press 1997.
4. Chamberlain N, “Respiratory tract infections” Phd thesis, 2005, Kirksville College of Osteopathic Medicine, Missouri, USA.
5. Murtomaa M, Mellin V, Harjunen P, Lankinen T, Laine E, Lehto V.S, “Effect of particle morphology on the triboelectrification in dry powder inhalers”, *International Journal of Pharmaceutics* 2004;282:107-114.
6. Zeng X.M, Martin G.P, Tee S.K, Marriott C, “The role of fine particle lactose on the dispersion and deaggregation of salbutamol sulphate in an air stream in vitro”, *International Journal of Pharmaceutics* 1998;176:99-110.
7. Zeng X.M, Martin G.P, Marriott C, “Particulate interactions in dry powder formulations for inhalation”, 2001, London: Taylor and Francis.
8. Atkins P.J, “Transition to HFA MDIs: how did we get here and where are we going?” In *Proceedings of Respiratory Drug Delivery 10*, 2006, Boca Raton, Florida, USA (R.N Dalby et al eds.) p.83-90, Davis Healthcare International Publishing.
9. Ashurst I, Malton A, Prime D, Sumbly B, “Latest advances in the development of dry powder inhalers”, *Pharmaceutical Science and Technology Today* 2000;3:246-256.
10. Smith I.J, Parry-Billings M, “The inhalers of the future? A review of dry powder devices on the market today”, *Pulmonary Pharmacology & Therapeutics* 2003;16(2):79-95.
11. Dalby R, Suman J, “Inhalation therapy: technological milestones in asthma treatment”, *Advanced Drug Delivery Reviews* 2003;55:779-791.
12. Young P.M, Cocconi D, Colombo P, Bettini R, Price R, Steele D.F, Tobyn M.J, “Characterization of a surface modified dry powder inhalation carrier prepared by Particle smoothing”, *Journal of Pharmacy and Pharmacology* 2002;54:1339-1344.

13. Atkins P.J, Crowder T.M, Hickey A.J, Johnson K.A, Kraabel S.A, Mckinney D.D, "Recent Technical Advances and Formulation Strategies in Pulmonary Drug Delivery", *Drug Delivery*, p.22-26.
14. Schiavone H, Palakodaty S, Clark A, York P, Tzannis S.T, "Evaluation of SCF-engineered particle-based lactose blends in passive dry powder inhalers", *International Journal of Pharmaceutics* 2004;281:55-66.
15. Hersey J.A, "Ordered mixing: a new concept on powder mixing practice", *Powder Technology* 1975;11:41-44.
16. Timsina M.P, Martin G.P, Marriott C, Ganderton D, Yianneskis M, "Drug delivery to the respiratory tract using dry powder inhalers", *International Journal of Pharmaceutics* 1994;101:1-13.
17. Srichana T, Martin G.P, Marriott C, "On the relationship between drug and carrier deposition from dry powder inhalers in vitro", *International Journal of Pharmaceutics* 1998;167:13-23.
18. Frijlink H.W, De Boer A.H, "Dry powder inhalers for pulmonary drug delivery", *Expert Opinion on Drug Delivery* 2004;1:67-86.
19. Ganderton D, Kassem N.M, "Dry powder inhalers", In *Advances in Pharmaceutical Sciences* 1992, (Ganderton D. and Jones T, eds), p.165-191, London, UK: Academic Press.
20. Malcomson R.J, Embleton J.K, "Dry powder formulations for pulmonary delivery", *Pharmaceutical Science & Technology Today* 1998;1:394-398.
21. Ebbens S, Luk Shen, Patel N, "Advanced surface characterisation of inhalation microparticles", *The Drug Delivery Companies Report Autumn/Winter 2002 at PharmaVentures Ltd.*
22. Fink J.B, "Metered-dose inhalers, Dry powder inhalers and Transitions", *Respiratory Care* 2000;45:623-635.
23. Cross J.A, "Electrostatics: Principles, Problems and Applications", IOP Publishing Limited, Bristol, 1987, UK.
24. Murtomaa M, Mellin V, Harjunen P, Lankinen T, Laine E, Lehto V.-P, "Effect of particle morphology on the triboelectrification in dry powder inhalers", *International Journal of Pharmaceutics* 2004;282:107-114.

25. Young P.M, Price R, Tobyn M.J, Buttrum M, Dey F, “Effect of humidity on aerosolization of micronized drugs”, *Drug development and industrial pharmacy* 2003a;29:959-966.
26. Visser J, “Particle adhesion and removal: A review”, *Particulate Science and Technology* 1995;13:169-196.
27. Staniforth J.N, “Powders comprising anti-adherent materials for use in Dry Powder Inhalers 6”, 2002, p.475-523.
28. Poochikian G & Bertha C.M, “Inhalation drug product excipient controls:Significance and pitfalls”, *Drug Delivery VII*, Dalby R.N, Byron P.R, Farr S.J, Peart J, Serentec Press Inc, 2000, p.109-115.
29. Begat P, Price R, Harris H, Morton D.A.V, Staniforth J.N, “The influence of force control agents on the cohesive-adhesive balance in dry powder inhaler formulations”, *KONA* 2005;23:109-119.
30. Müller-Walz R, Fueg L.M, Niederlaender C, Piele U, Wirth A, “Ternary additives: manipulation and control with magnesium stearate”, *Respiratory Drug Delivery* 2006;32:343-350.
31. Shah C, Mlodozieniec A.R, “Mechanism of surface lubrication: Influence of duration of lubricant-excipient mixing on processing characteristics of powders and properties of compressed tablets, *Journal of Pharmaceutical Sciences* 1977;12:1377-1382.
32. Pintye-Hódi K, Tóth I, Kata M, “Investigation of the formation of magnesium stearate film by energy dispersive X-ray microanalysis”, *Pharmaceutical Acta Helv.* 1981;56:320-323.
33. Butcher A.E, Jones T.M, “Some physical characteristics of magnesium stearate”, *Journal of Pharmacy and Pharmacology* 1972;24:1P-9P.
34. Andrès C, Bracconi P, Pourcelot Y, “On the difficulty of assessing the specific surface area of magnesium stearate”, *International Journal of Pharmaceutics* 2001;218:153-163.
35. Marwaha S.B, Rubinstein M.H, “Structure-lubricity evaluation of magnesium stearate”, *International Journal of Pharmaceutics* 1988;43:249-255.
36. Bolhuis G.K, Holzer A.W, (1995), Influence of mixing time, particle size and colloidal silica on the surface coverage and lubrication of magnesium stearate .In:

- Alderborn G, Nyström C, (eds), "Pharmaceutical Powder Compaction Technology", Marcel Dekker, New York, p.43-49.
37. Leinonen I, Jalonen H.U, Vihervaara P.A, Laine E.S.U, "Physical and lubrication properties of magnesium stearate", *Journal of Pharmaceutical Sciences* 1992;81:1194-1198.
  38. Ertel K.D, Carstensen J.T, "Chemical, physical and lubricant properties of magnesium stearate", *Journal of Pharmaceutical Sciences* 1988;77:625-629.
  39. Lucas P, Anderson K, Staniforth J.N, "Protein deposition from dry powder inhalers: fine particle multiplets as performance modifiers", *Pharmaceutical Research* 1998;15:562-569.
  40. Louey M.D, Stewart P.J, "Particle interactions involved in aerosol dispersion of ternary interactive mixtures", *Pharmaceutical Research* 2002;19:1524-1531.
  41. Tee S.K, Marriott C, Zeng X.M, Martin G.P, "The use of different sugars as fine and coarse carriers for aerosolised salbutamol sulphate", *International Journal of Pharmaceutics* 2000;208:111-123.
  42. Lambregts D, Gruben K, De Boer A.H, "Importance of the choice of lactose in combination with dry powder inhalers", In *Drug Delivery to the Lungs* 15, 2004, London, p.157-160, The Aerosol Society.
  43. Jones M.D, "An investigation into the dispersion mechanisms of ternary dry powder inhaler formulations by the quantification of interparticulate forces", PhD thesis, University of Bath 2006.
  44. Islam N, Stewart P, Larson I, Hartley P, "Lactose surface modification by decantation: are drug-fine lactose ratios the key to better dispersion of salmeterol xinafoate from lactose-interactive mixtures?", *Pharmaceutical Research* 2004;21:492-499.
  45. Zeng X.M, Tee S.K, Martin G.P, Marriott C, "Improving the delivery efficiency of dry powder inhalers by adding fine carrier particles to powder formulations", *Thorax* 1996;51:A74.
  46. Zeng X.M, Martin G.P, Marriott C, Pritchard J, "Lactose as a carrier in dry powder formulations: the influence of surface characteristics on drug delivery", *Journal of Pharmaceutical Sciences* 2001;90:1424-1434.

47. de Boer A.H, Gjaltema D, Hagedoorn P, Frijlink H.W, “Characterization of inhalation aerosols: a critical evaluation of cascade impactor analysis and laser diffraction technique”, *International Journal of Pharmaceutics* 2002;249:219-231.
48. European Pharmacopoeia 5.0 volume 1 (01/2005) – European Pharmacopoeia (EP), Test Chapter 2.9.18, Multi stage liquid impinger, Published by the Directorate for the Quality of Medicines of the Council of Europe (EDQM), available online at <http://www.pheur.org>
49. Taylor K.M.G, Pancholi K, Wong D.Y.T, “In-vitro evaluation of dry powder inhaler formulations of micronized and milled nedocromil sodium”, *Pharm. Pharmacol. Commun.* 1999;5:255-257.
50. B.P.C British Pharmacopoeia, 2001, Volume II, London.
51. Visser J, “Van der Waals and other cohesive forces affecting powder fluidization”, *Powder Technology* 1989;58:1-10.
52. Podzeck F, “Particle-particle adhesion in pharmaceutical powder handling”, London: Imperial College Press, 1998.
53. Grimsey I.M, Feeley J.C, York P, “Analysis of the surface energy of pharmaceutical powders by inverse gas chromatography”, *Journal of Pharmaceutical Sciences* 2002;91:571-583.
54. Braun M.A, Oschmann R, Schmidt P.C, “Influence of excipients and storage humidity on the deposition of disodium cromoglycate (DSG) in the twin impinger”, *International Journal of Pharmaceutics* 1996;135:53-62.

# Chapter 2

## General materials and methods

### 2.1 Materials

All the materials and their source used during this study are listed in table 2.1. Materials were first characterised in terms of sample morphology and particle size. All organic solvents used in this study were of at least analytical grade. Ceramic balls of 10mm diameter were used for high shear ball milling. The lactose was vibrated through a nest of sieves to obtain a 60-90 $\mu$ m sieve fraction, which was used throughout the study.

Materials	Source
Micronized budesonide	Sicor, BN:6157/M1, Santhia, Italy
$\alpha$ -lactose monohydrate (Lactochem <sup>®</sup> )	Lactochem, Borculo, Holland 63-90 $\mu$ m fraction obtained by sieving
10% etched $\alpha$ -lactose monohydrate (Nanolac <sup>®</sup> )	University of Bath, BN: DINA01
Sorbolac 400 (milled $\alpha$ -lactose monohydrate)	Meggle GmbH, Wasserburg, Germany
Magnesium Stearate	Fischer Chemicals, BN:9880836, Loughborough, UK
Acetonitrile	Fischer Scientific Ltd, Loughborough, UK
Methanol	Fischer Scientific Ltd, Loughborough, UK
Water	Obtained by reverse osmosis MilliQ, Molsheim, France

***Table 2.1 Materials used throughout this study.***

It should be stated that for the remainder of this thesis  $\alpha$ -lactose monohydrate and 10% etched  $\alpha$ -lactose monohydrate will be referred to as Lactochem and Nanolac, respectively.



### 2.1.1 Drug material

Budesonide is an inhaled glucocorticosteroid which is widely used in the treatment of asthma. It has potent anti-inflammatory actions and thus reduces the inflammation and hyper-reactivity (spasm) of the airways caused by asthma. The chemical structure of budesonide is shown in figure 2.1.

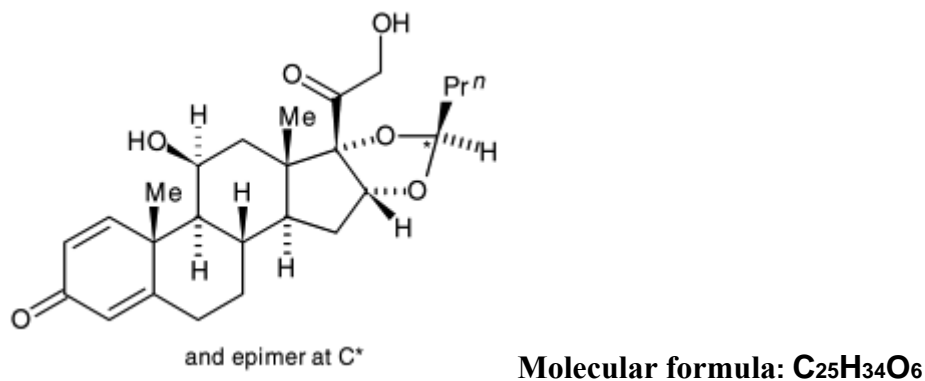


*Figure 2.1 Chemical structure of budesonide.*

### 2.1.2 Carrier structure

Lactose is a disaccharide, widely used as a carrier in inhalation formulations. Figure 2.2 shows the chemical structure of  $\alpha$ -lactose monohydrate.

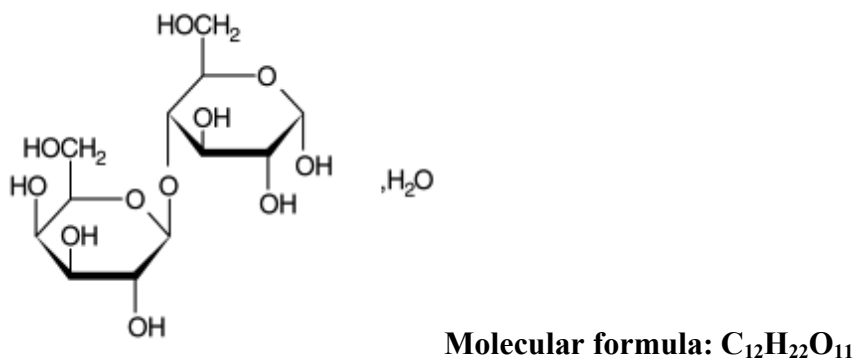


*Figure 2.2 Chemical structure of  $\alpha$ -lactose monohydrate.*

## 2.2 Methods

### 2.2.1 Scanning electron microscopy (SEM)

The morphology of the drug particle surfaces used throughout the investigation was investigated by SEM, which is a microscope that uses electrons rather than light to generate a high resolution image of a conducting sample. It achieves this by collecting and analysing secondary electrons emitted as a result of high energy electron beam collisions. Scanning electron microscopy is used to make a qualitative analysis of the particle shape and size of the various materials used.

Samples were fixed to sticky carbon tabs mounted on aluminium stubs. They were then coated with gold using a sputter coater (model S150B, Edwards High Vacuum, Sussex, UK) and examined using a scanning electron microscope (model JSM6310 or JSM6480, Japanese Electron Optics Ltd, Tokyo, Japan) at 10 KeV. Inspection of the SEM images of the micronised drug (Figure 2.3) showed the budesonide particles to have both columnar and irregular plate-like crystal shape. Budesonide particles were present in the form of agglomerates of many particles suggesting that the powder was relatively cohesive.

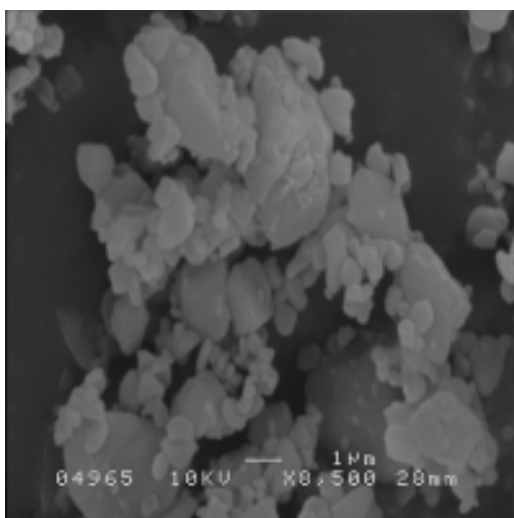


***Figure 2.3 Representative SEMs of the micronised budesonide at A) x3000 and B) x8500 magnification.***

### 2.2.2 Particle size analysis

The particle size distribution (PSD) of the materials was investigated using laser light scattering. Particle size characterisation is critical for inhalation preparations since they may influence the stability, flowability and aerolisation performance of the formulations. Laser light scattering involves measuring the intensity pattern of scattered light from a laser passing through a particulate sample<sup>1</sup>.

Light scattering is a popular technique used for determining the particle size distribution of a material. The diffraction of the laser light results from the interaction of the light with the particles and can be described mathematically by Fraunhofer or Mie theory. The Mie theory is the rigorous solution for light scattered from a sphere<sup>2</sup>. For particles smaller than the wavelength of the incident light, the Mie theory is reduced to the Rayleigh theory. When particles are much larger than the wavelength of the incident light, the Mie theory simplifies to the Fraunhofer theory<sup>3</sup>.

Gustav Mie in 1908 published a solution to the problem of light scattering by homogeneous spherical particles of any size. The Mie theory is a complete mathematical-physical theory of the scattering of electromagnetic radiation by spherical particles. It takes into account both the diffraction and diffusion of the light around the particle, in its medium. According to the Mie theory, the scattering angular pattern is symmetrical along the axis of incident light for perfect spheres<sup>1</sup>. However, to use this model it is necessary to know certain parameters like the complex refractive index ( $m$ ) of both the sample and the medium<sup>3</sup>.

The Fraunhofer theory is applied to large particles, typically  $>30\mu\text{m}^3$ . When the particle is much larger than the wavelength of light or the materials are highly absorptive, the edge effect (diffraction) of particles contributes more to the total scattered light. In this theory, a particle is assumed to be producing a scattering pattern as it were an opaque circular disk of the same projected area placed normally to the axis of the incident beam. The Fraunhofer theory provides a much easier analytical solution for particle sizing as compared to the Mie theory.

For particles smaller than the wavelength the incident light, the scattered light is not concentrated in the forward direction but spreads to the side and rear. Modern light scattering instruments used for measuring particle size distribution rely mainly on the Mie theory to obtain analytical results. Thus, the basic assumption for the instruments is that particles are perfect spheres<sup>1</sup>.

Particle size analysis was carried out in the dry state. Powders were dispersed with compressed air at 3 bar through a RODOS dry disperser fed by an ASPIROS micro-dosing unit before sizing with a HELOS laser diffraction sensor (all from Sympatec GmbH, Clausthal-Zellerfeld, Germany). The particle size analysis was performed using WINDOX 4.0 software (Sympatec GmbH, Clausthal-Zellerfeld, Germany).

The particle size distribution was calculated and represented as a volume distribution, and was also characterized by the 10<sup>th</sup>, 50<sup>th</sup> and 90<sup>th</sup> percentile of the cumulative particle undersize frequency distribution. All samples were prepared and analysed in triplicate.

### **2.2.3 In vitro apparatus for determination of aerodynamic properties of inhalation formulations**

- **Multi Stage Liquid Impinger (MSLI)**

The multi stage liquid impinger (MSLI) is a five-stage cascade impactor for determining the aerodynamic size distribution of DPIs and pMDIs. The MSLI has no interstage loss and is suitable for use throughout the range 30 to 100 L/min. It consists of four classifying stages and a filter. The collection stages are kept moist by the addition of mobile phase, which helps avoid the problem of re-entrainment of powder sometimes experienced when using more conventional impactors. It separates the particles into five fractions with cut off diameters ranging from 18 down to 3µm. The MSLI apparatus consists of a throat, four classifying stages into which 20ml of mobile phase is introduced such that the entire surfaces of all the glass plates are completely wetted and a fifth dismantled stage on top of which a filter paper is placed<sup>48</sup>. The MSLI is described in more detail in section 3.4.5.

- **Twin Stage Impinger (TSI)**

The TSI is the first device which was used to assess pulmonary drug delivery through inertial impaction. It has two stages and a representative throat. It first appeared in the British Pharmacopoeia and is used for the initial screening of inhalation devices and formulations. 30 ml of the mobile phase is introduced into the conical measure (stage 2) of the apparatus and 7 ml of the mobile phase into stage 1. These wet stages of the impinger make it less prone to errors resulting from particle re-entrainment and they also create a humid environment similar to that in the lungs<sup>49</sup>. However, the TSI has inherent limitations in the adequacy of size distribution, since it has an effective cut-off diameter of  $6.4\ \mu\text{m}$ <sup>49</sup> but it still is a useful and convenient method of in vitro assessment of delivery efficiency of inhalation products.

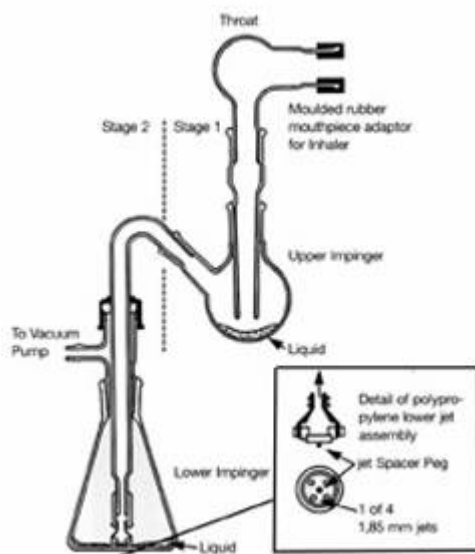


**Figure 1.4** Schematic representation of a Twin stage impinger, adapted from the *British Pharmacopoeia, 2001, Volume II*<sup>50</sup>.

## **2.2.4 Chemical determination of drug concentration**

### **2.2.4.1 Preparation of mobile phase**

The mobile phase used for analysing budesonide was 45 % Methanol, 35% Acetonitrile and 20% Water.

### **2.2.4.2 Preparation of standard solutions of budesonide**

Stock solutions of budesonide of concentrations 0.1, 0.25, 0.5, 2, 10, 50 mcg /ml were prepared. The stock standard solution was prepared by accurately weighing out 0.0205g of budesonide into a 500ml volumetric flask, which was made up with 150ml of water and methanol. Each stock solution was sonicated for 20 minutes to ensure dissolution and allowed to cool at room temperature and made up to the mark with 30% water and methanol. Serial dilutions of the stock standard solution were carried out using calibrated (class A) volumetric laboratory pipettes, to produce the stock solutions with the concentrations stated above.

### **2.2.4.3 Preparation of powder formulations**

Lactochem<sup>®</sup> was sieve fractioned using a sieve shaker (Endecotts sieve and sieve shaker, London,UK). A test sieve with an aperture width of 90 $\mu$ m was placed over a test sieve with an aperture width of 63 $\mu$ m. The 63-90 $\mu$ m sieve fractioned lactose was subsequently blended with micronised budesonide in a ratio of 67.5:1 w/w. The blending procedure involved initially adding a mass of lactose, approximately double the amount of budesonide to be incorporated in the powder blend into a stoppered sample glass vial. The total mass of budesonide was then directly weighed on top of the layer of lactose. The glass vial was then placed on a Whirlymixer (Fisons Scientific Equipment, Loughborough, UK) in a slanting position at 45° and mixed for 1 minute. The blend was further diluted by the addition of lactose. The amount of lactose was equivalent to the total amount of drug and lactose in the

glass vial and mixed again on the Whirlymixer. The geometric addition of the lactose and mixing was repeated until all of the lactose was incorporated into the blend.

The glass vial was then placed in a Turbula mixer and mixed at 46 rev/min for 30 minutes. The same procedure as above (geometric mixing) was carried out for preparing the Nanolac formulations.

#### **2.2.4.4 Capsule filling and storage**

Hydroxypropyl methylcellulose (HPMC) capsules, size 3, (Qualicaps, BN: EO404632, Shiongi Qualicaps, Madrid, Spain) were filled with  $25 \pm 3$  mg of the powder blends, such that each capsule contained a nominal dose of approximately  $200 \pm 20\mu\text{g}$  of budesonide. The filling was performed manually and filled capsules were stored in a sealed container at a controlled environment of 44% RH created by a saturated solution of potassium carbonate.

#### **2.2.4.5 Drug content uniformity**

Uniformity testing can be used as an indirect method of evaluating the interaction between the drug and the carrier particles. For example, if the uniformity is low, the drug has not been well dispersed. This may occur because the cohesive forces between the drug particles are high and more energy is required to break up agglomerates of drug particles. Alternatively, it may be that the cohesion between drug particles is much higher than the adhesion to the carrier particles leading to an unstable formulation. In this case, the drug distribution becomes less uniform over time as the drug particles will tend to re-agglomerate as they detach from the carrier.

## 2.2.5 Drug content determination

### 2.2.5.1 High Performance Liquid Chromatography (HPLC)

The HPLC system consisted of a JASCO AS950 intelligent sampler, a JASCO PU-980 intelligent HPLC pump, a JASCO 975 UV/VIS detector and a Waters Spherisorb 15 cm, 5 $\mu$ m ODSI column. The detection wavelength was  $\lambda=244$  nm, the flow rate was 1.5 ml/min, the pressure was less than 500 kg/m<sup>2</sup>, the injection volume was 100 $\mu$ l, the analysis time was 5 minutes, the retention time was 3.15 minutes and the mobile phase was that described above. Injections of all solutions analysed were made in duplicate.

The standard solutions of budesonide prepared, were analysed using the HPLC method. Data were recorded and integrated using AZUR-0SIRIS Chromatography Software V3.0 (Theix, France) The mean value of the area under the curve (AUC) of the two injections for each solution was calculated for the peak which represented budesonide and a calibration graph was constructed. An example of the calibration graph is shown in figure 2.5.

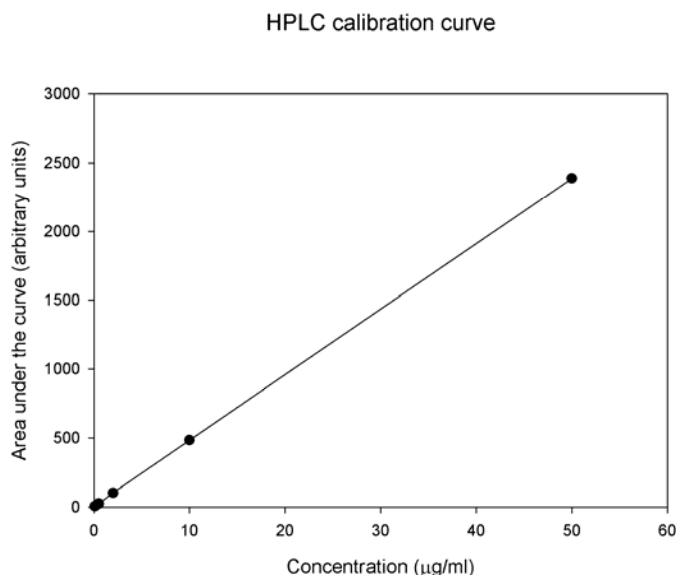


**Figure 2.5** *An example of a HPLC calibration graph.*



### 2.2.6 Statistical analysis

Statistical analysis of data was carried out using Minitab for Windows. One-way ANOVA (analysis of variance) was used to determine the variance of data. Fisher's pair-wise analysis was carried out to determine the level of significance. Statistical significance was defined at either a limit of  $P < 0.05$  or  $P < 0.01$ .

The average and deviation of normal distribution populations were expressed as arithmetic mean ( $\bar{x}$ ) and standard deviation (SD). Arithmetic mean ( $\bar{x}$ ) was calculated by equation 2.1:

$$\text{Equation 2.1} \quad \bar{x} = \frac{1}{n} \sum_{i=1}^n x_i$$

The standard deviation (SD) was calculated by equation 2.2:

$$\text{Equation 2.2} \quad SD = \sqrt{\frac{1}{n-1} \sum_{i=1}^n (\bar{x} - x_i)^2}$$

The relative standard deviation RSD (%) also known as the coefficient of variation was calculated by equation 2.3:

$$\text{Equation 2.3} \quad RSD = \frac{100SD}{\bar{x}}$$

## **2.3 Conclusions**

As described, the materials used throughout the study underwent an extensive physicochemical characterisation. The physicochemical properties of the materials could possibly be modified during their processing, handling and storage and therefore their characterisation would further help gain a better understanding on the changes and the reasons behind them for occurring.

## **2.4 References**

1. Mitchell J.P, Nagel M.W, “Particle size analysis of aerosols from medicinal inhalers”, KONA 2004;22:32-32-65.
2. Johnson R.W, Thiele E.S, French R.H, “Light scattering efficiency of white pigments: Titania-coated silica relative to rutile  $\text{TiO}_2$ ”, TAPPI 1997;11:233-239.
3. de Boer A.H, Gjaltema D, Hagedoorn P, Frijlink H.W, “Characterization of inhalation aerosols: a critical evaluation of cascade impactor analysis and laser diffraction technique”, International Journal of Pharmaceutics 2002;249:219-231.

# Chapter 3

## **The effect of the addition of Magnesium Stearate on the aerosolisation performance of DPI formulations**

### **3.1 Introduction**

Magnesium stearate (MgSt) is widely used as a lubricant in the manufacture of pharmaceutical solid dosage forms<sup>1</sup>. Previous studies have shown that the addition of MgSt to pharmaceutical DPI formulations increased aerosol deposition performance by modifying the adhesive interaction between the drug and the carrier, thus facilitating the detachment of the drug particles from the coarse carrier during aerolisation<sup>2</sup>. It has been reported that MgSt can displace the fine active ingredient from coarse monodisperse carriers in mixtures based on its influence on the force balance of particle interactions. Magnesium stearate as suggested by these studies, should form weaker drug-lactose interactions within the blends. It is well established that drug dispersion within the dry powder formulation is the key factor in efficient pulmonary drug delivery. Without the introduction of a force lowering agent, such as lubricant, a larger amount of energy would be required to overcome the adhesive interaction for the dispersion of the drug from the lactose surface<sup>2</sup>.

In a related study, the coating of MgSt to a lactose surface by mechanofusion modified the interfacial interactions between budesonide-lactose to such a degree that the drug completely segregated from the carrier leading to a high coefficient of variation in content uniformity and variable drug delivery performance<sup>2</sup>

In solid dosage forms, magnesium stearate is used as a lubricant to aid the efficient ejection of tablets through reducing the frictional forces exhibited between the compressed tablet

and the die wall during operation. If there is sufficient shear forces generated during the mixing process MgSt may form a thin film around host particles, which can interfere with the bonding and adhesive properties of the host particles by acting as a physical barrier.<sup>3</sup>

Depending on the shear forces induced during powder mixing and processing time. MgSt may coat the host particles with varying thicknesses of the lubricant, from a molecular film up to a particulate film. The formation of a MgSt film will lead to a significant decrease in the adhesive tendency of the host particle due to the lowering of its surface free energy and the coefficient of friction. The use of force control agents, in particular MgSt, on the behaviour and performance of model DPI formulations has been investigated by Begat et al. (2005)<sup>2</sup>. Their work highlighted the potential advantages and disadvantages for the introduction of MgSt in DPI formulations. However, they used a highly intensive co-processing system “*Mechanofusion*” to ensure the liberation of the MgSt layers in forming a complete coating over the host particles. The high degree of shear was sufficient to modify the adhesive interactions between budesonide-lactose and salbutamol sulphate-lactose to such an extent that there was no observable interaction between the drug and excipient. This led to the segregation of the drug from the excipient and the formation of a cohesively led drug-drug system, which is undesirable<sup>2</sup>.

The aim of this study was to investigate the influence of various concentration of MgSt on the properties and behaviour of carrier based DPI formulations but through a medium-high shear process, where the degree of lubrication and anti-adhesive properties of the excipient should not be sufficient to completely segregate the active pharmaceutical ingredient from the excipient surface. An inhaled corticosteroid, budesonide, was used as a model drug for the study.

## 3.2 Materials

$\alpha$ -Lactose monohydrate (Lactochem<sup>®</sup>) was supplied by Borculo Whey (Chester, UK). The as supplied lactose was vibrated through a nest of sieves to obtain 63-90  $\mu$ m sieve fraction, which was used throughout the study. Micronised budesonide was supplied by Sicor (Batch no. 6157/M1, Santhia, Italy). A 10% etched lactose (Nanolac) was produced according to the procedure outlined by El-Sabawi et al. (2006). Magnesium stearate was supplied by Fisher chemicals (Batch no. 9880836, Loughborough, UK). The acetonitrile and methanol were of HPLC grade and were obtained from Fisher Scientific (Loughborough, UK). Water was purified by reverse osmosis (MilliQ, Millipore, Molsheim, France). Hydroxypropyl methylcellulose (HPMC) capsules (size 3) were supplied by Qualicaps (Batch no. EO404632, Shiongi Qualicaps, Madrid, Spain). Potassium carbonate anhydrous was supplied by Acros Organics (Batch no. A018189301, New Jersey, USA) and was used to maintain a constant relative humidity of 44% RH for the storage of the formulations in hermetically sealed containers. Ceramic balls of 10mm diameter were used to create high shear energy during blending.

## 3.3 Methods

### 3.3.1 Scanning electron microscopy

The morphology of each blend, the lactose and budesonide were investigated using a scanning electron microscope, (JEOL 6310, Japanese Electron Optics Ltd, Tokyo, Japan) at 10 KeV. The samples were sprinkled onto adhesive black carbon tabs, which were pre-mounted on aluminium stubs and coated with gold using a sputter coater (S150B, Edwards High Vacuum, Sussex, UK) prior to analysis.

### 3.3.2 Particle size analysis

The particle size distribution of the non processed samples were determined by laser light scattering, using a Sympatec laser light diffraction particle size analyser (Sympatec, Clausthal-Zellerfeld, Germany). The instrument was equipped with a RODOS powder dispenser and depending on the powder particle size to be analysed an R3 lens or an R4 lens was used. The R4 lens could be used to observe large particles (size range of 0.5 to 350µm) that could not be detected by an R3 lens. The inlet pressure on the equipment was set at 2 bars and a speed of 50mm/s. A RODOS dispenser (Sympatec) was used for a consistent fluidisation of the powder sample, which was fed with an ASPIROS micro-dosing unit before sizing with a HELOS laser diffraction sensor.

The particle size analysis was performed using WINDOX 4.0 software. (Sympatec, Clausthal-Zellerfeld, Germany). Size distributions and values presented are the average of 3 determinations. The particle size distribution of the aerosol cloud, emitted from a Cyclohaler<sup>®</sup> by each of the ten processed formulations described was determined using a HELOS laser diffraction sensor and an INHALER module (both from Sympatec GmbH, Clausthal-Zellerfeld, Germany). The flow rate through the INHALER module was set at 60L/min and the mouthpiece of the Cyclohaler<sup>®</sup> was fitted directly to the measuring chamber, to enable measurement of the particle size distribution of the aerosol cloud immediately after emission. For each measurement, a size 3 HPMC capsule filled with  $25 \pm 1$  mg of the test formulation was inserted into the Cyclohaler<sup>®</sup> opened by piercing it and its contents aerosolised through the laser of the diffraction sensor for 10 ms. Particle size analysis was performed using WINDOX 4.0 software (Sympatec GmbH, Clausthal-Zellerfeld, Germany). Particle size distributions and values presented are the average of 5 determinations.

### **3.3.3 Preparation of surface etched $\alpha$ -lactose monohydrate (Nanolac<sup>®</sup>)**

A saturated solution of lactose in water was prepared by the addition of 300g lactose to 1000ml of water and continually stirred at a temperature of 25°C for 30 minutes. The temperature within the vessel was controlled to within 0.1°C via a refrigerated controlled water bath (Haake, DC5, Fisons Scientific Equipment, Loughborough, UK). After the 30 minutes, 400 ml of the saturated solution was removed from the vessel, filtered under vacuum through a 0.2 $\mu$ m filter, and transferred to a dissolution cell, which was maintained at the saturation temperature. An accurately weighed mass of 63-90 $\mu$ m sieved  $\alpha$ -lactose monohydrate (250mg) was added to the saturated solution in the dissolution cell and continually stirred as the temperature within the vessel was gradually raised to 35°C for 2 hours. A well-controlled etching of the lactose particles was achieved by forming an undersaturated solution of the lactose with increasing temperature. The difference between the initial temperature (25°C) and the final (35°C) is referred to as the etching temperature, and with knowledge of the solubility of the lactose at various temperatures and the initial amount of mass added the percentage of this mass which had been etched can be pre-determined and controlled. After the 2 hours, the solution in the dissolution cell was filtered through a 0.2 $\mu$ m filter and washed out thoroughly with ethanol, in which lactose is practically insoluble. The resulting lactose was collected in a Petri dish and left to air dry for a week and then sieved again through a nest of sieves for 1 hour to obtain 63-90 $\mu$ m sieve fraction<sup>4</sup>. The 10% etched lactose produced will be referenced as Nanolac throughout this study. In addition to the efficient dissolution of fine lactose particles from the surfaces of the coarser particles, the process further etches the surface asperities present on the excipient producing a highly smooth lactose surface, hence the name Nanolac.

### **3.3.4 Preparation of carrier based DPI formulation blends**

Budesonide was blended with both forms of lactose (Lactochem<sup>®</sup> or Nanolac<sup>®</sup>) in the ratio of 1:67.5% w/w. The formulations were blended through geometric mixing. Firstly, the Nanolac<sup>®</sup> or Lactochem<sup>®</sup> was either processed with or without various concentrations of the

MgSt and then budesonide was added to the blend. The concentrations of MgSt in the pre-blend were 0.125, 0.25, 0.5, and 1.0 %w/w. The processing of the MgSt with the lactose involved initially adding a mass of lactose which was approximately double the amount of MgSt to be incorporated into a glass vial. The total amount of MgSt was then added onto the layer of lactose. Three ceramic ball bearings (10mm in diameter) were then added to the blend. The ball bearings were used to induce the shear forces required in the mixing process to liberate and to coat the lactose with the force control agent. The vial containing the excipients and the ball bearings were mixed for 1 minute on a Whirlimixer (Fisons Scientific Apparatus, Loughborough, UK) at a slanting position at 45°. The blend was further diluted by lactose. The amount of lactose was equivalent to the total amount of the MgSt and the lactose in the glass vial. The glass vial was then stoppered and mixed via the whirlimixer, using the settings described above. The geometric addition of the lactose and the mixing were repeated until all the lactose had been incorporated into the blend. The final formulation was then put in the Turbula mixer (Glen Creston, Stanmore, UK) for 40 minutes at 46 revolutions per minute.

Upon the preparation of the pre-blend, 3.968g of the processed lactose was accurately weighed into a separate container. The budesonide was then blended geometrically with the MgSt-lactose pre-blend, following the same procedure as above. Briefly, a small amount of the pre-blend and a fixed amount of budesonide (0.032g) was mixed for 1 minute using a Whirlimixer (Fisons Scientific Apparatus, Loughborough, UK). More of the processed lactose was added in geometric quantities, followed by mixing with the Whirlimixer for 1 minute after each addition. This was done until all the blend weighed out was added to the test tube. The blend was then mixed in a turbula mixer (Turbula, Glen Creston Ltd, Stanmore, UK) at 46 revolutions per minute for thirty minutes. Geometrically produced blends of the unprocessed (Lactochem) lactose with budesonide were also produced using the procedure discussed above.

The blend masses and concentrations for the various formulations prepared for both Lactochem and Nanolac preparations are tabulated in tables 3.1 and 3.2, together with their characteristic letter designated for each blend prepared.



**Table 3.1 Blend masses and concentrations of lactose and MgSt for the prepared blends.**

Blend	Carrier	MgSt concn (w/w%)	Amount of Nanolac/Lactochem(g)	Amount of MgSt (g)
A	Nanolac	0.125%	7.9901	0.0100
B	Lactochem	0.125%	7.9900	0.0100
C	Nanolac	0.25%	7.9800	0.0203
D	Lactochem	0.25%	7.9802	0.0202
E	Nanolac	0.5%	7.9607	0.0403
F	Lactochem	0.5%	7.9609	0.0404
G	Nanolac	1.0%	7.9200	0.0800
H	Lactochem	1.0%	7.9200	0.0800

**Table 3.2 Blend masses of the pre-blend and drug for the study.**

Blend	Amount of Nanolac/Lactochem-MgSt blend (g)	Amount of budesonide (g)
A	3.9682	0.0320
B	3.9685	0.0320
C	3.9684	0.0325
D	3.9686	0.0320
E	3.9680	0.0322
F	3.9689	0.0322
G	3.9687	0.0324
H	3.9683	0.0320
I (control)	Nanolac only- 3.9685	0.0325
J (control)	Lactochem only- 3.9686	0.0321

#### **3.3.4.1 Drug content uniformity**

Drug content uniformity was performed to ensure that the budesonide was blended uniformly with the lactose upon powder mixing. Content uniformity measurements were undertaken by evenly spreading the formulation on a piece of paper and randomly sampling ten samples of approximately  $25 \pm 2$  mg from the powder blend. The samples were accurately weighed into 100ml volumetric flasks and made up with the HPLC mobile phase. The samples were then sonicated for 20 minutes to ensure that the powder was completely dissolved before the testing for drug uniformity.

The concentration of budesonide was measured by high performance liquid chromatography (HPLC). Each solution was run in duplicate through the HPLC machine. The ratio of budesonide to lactose of each sample was determined and the drug uniformity of the mixture was measured by the percentage relative standard deviation (%RSD). A value less than 6.0% is generally regarded as acceptable.

#### **3.3.4.2 Capsule filling and storage**

Hydroxypropyl methylcellulose (HPMC) capsules, size 3, (Qualicaps, BN: EO404632, Shiongi Qualicaps, Madrid, Spain) were filled with  $25 \pm 3$  mg of the powder blends. Thirty capsules were filled for each powder blend. The filled capsules were then stored under a controlled relative humidity of 44% and stored for at least 24 hours before testing, to allow the electrostatic charges induced during processing to decay.

#### **3.3.5 In vitro aerosolisation studies**

The pulmonary deposition of budesonide from each blend was assessed by the use of a Multi Stage Liquid Impinger (MSLI) (Copley Instruments Ltd, Nottingham, UK). A general description of the MSLI and the conditions set for its operation are described in section 2.2.8.1 in Chapter 2. Ten capsules were fired from the Cyclohaler at 60 L/min with a 4 second exposure for each capsule. The capsule shells were removed from the cyclohaler and used in the analysis of device retention. The capsules and device were washed out with mobile phase into the same 100ml volumetric flask. The mouthpiece and throat were analysed together and stages 1 - 5 were washed out and analysed individually. All of these samples were analysed for their budesonide content using the HPLC method described above. The deposition of each formulation was measured in triplicates and a variety of parameters were utilized to characterise the deposition profiles of the budesonide.

#### **3.3.5.1 Analysis of budesonide**

The concentrations of budesonide collected on the various stages of the MSLI apparatus were analysed using high performance liquid chromatography (HPLC). The HPLC system consisted of a 5µm Hypersil column (Hypersil MOS C8, Jones Chromatography Ltd, Hengoed, UK), a pump (Jasco PU-980, JASCO Corp., Tokyo, Japan) and a UV detector (Jasco UV-975). The mobile phase consisted of acetonitrile 35%, methanol 45% and MilliQ water 20%, running at a flow rate of 1.5 ml/min. The detector was set at a wavelength of 244nm. The data were recorded and integrated using AZUR-OSIRIS Chromatography Software V3.0 (Theix, France).

#### **3.3.6 Statistical analysis**

Statistical analysis of the data was carried out using Minitab for Windows. One-way ANOVA (analysis of variance) was used to determine the variance of data. Fisher's pair-wise analysis was carried out to determine if the differences were significant. Statistical significance was defined within 95% ( $P < 0.05$ ) and 99% ( $P < 0.01$ ) confidence limits. The levels of significance obtained are indicated in the key on individual graph.

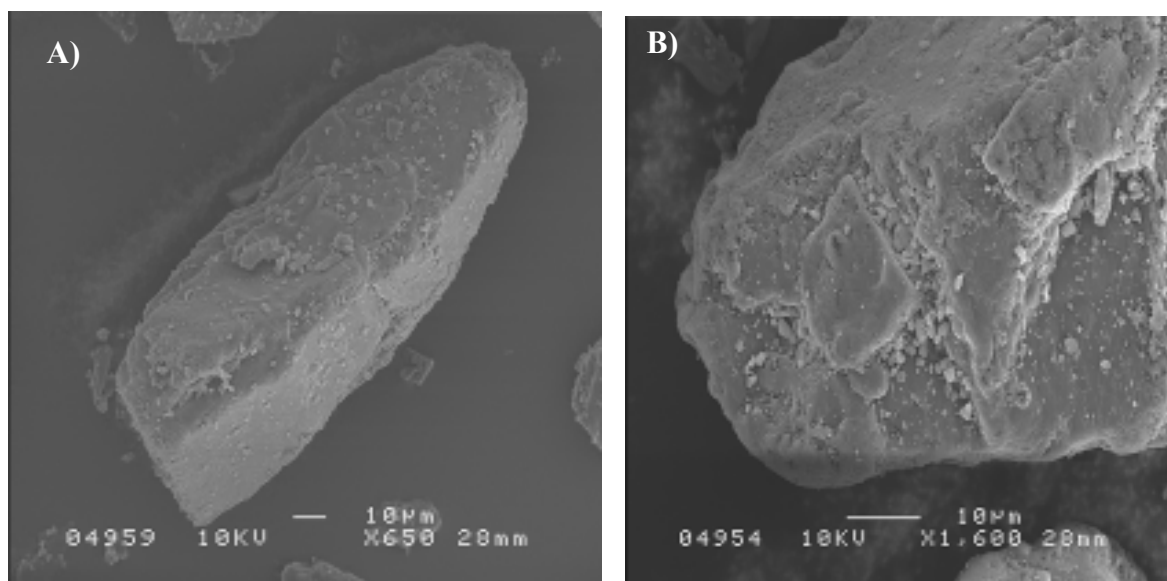
### **3.4 Results and Discussion**

#### **3.4.1 Scanning electron microscopy (SEM)**

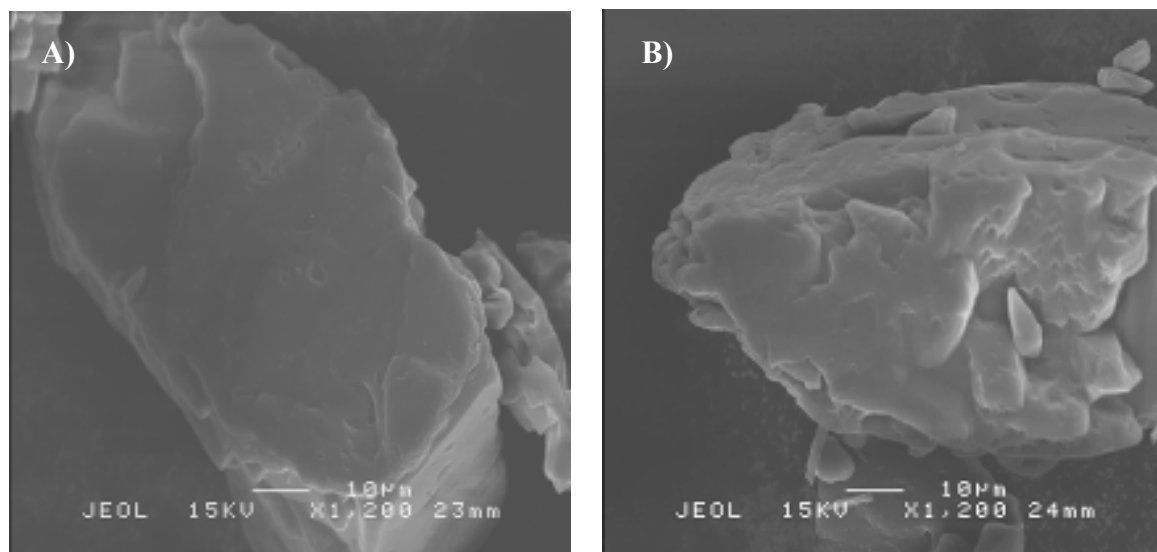
Representative SEM micrographs of Lactochem and Nanolac particles are shown in Figures 3.3 and 3.4, respectively. The figures suggest distinct variations in the amount of intrinsic fines adhering to the surface of the as-received Lactochem with respect to the surface etched lactose (Nanolac). Furthermore, the SEM images indicate a significant increase in the degree of surface smoothness of Nanolac (figure 3.4) in comparison to Lactochem, whose morphology is characterised by a series of ridges and clefts (figure 3.3). These differences are also apparent upon processing with MgSt, where the formulations containing Nanolac having smooth edges (figure 3.8) and formulations containing Lactochem having rough edges and clefts (figure 3.7). This suggests that a smooth

continuous coating of the MgSt over the surface of the lactose particles may be more likely to occur for the Nanolac formulations.

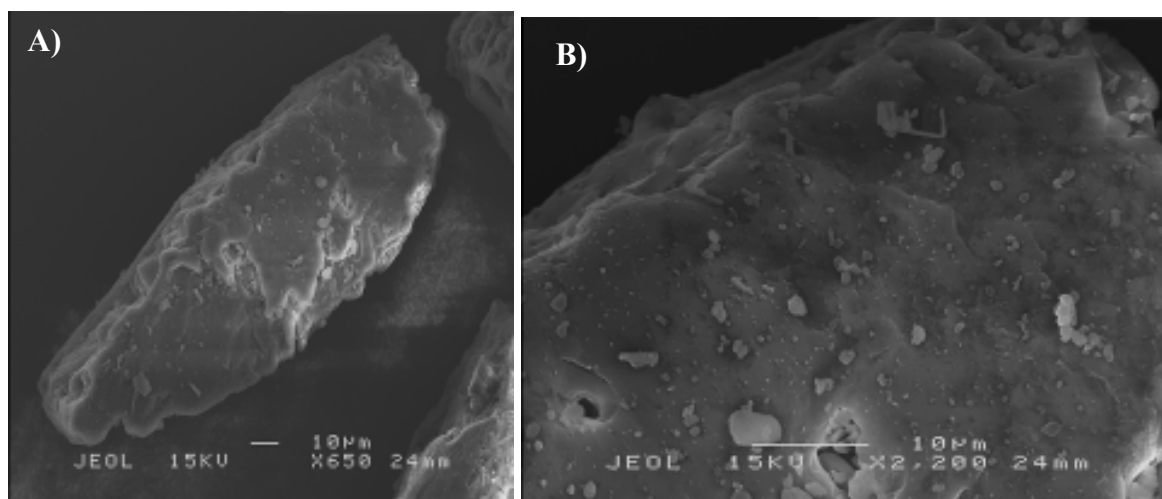
Clear differences in the degree of fine particulates were observed between blends from the lowest to the highest dose level. Lactochem formulations demonstrated a relatively higher presence of fine particulates on the larger lactose particles when compared to the equivalent dose level of Nanolac formulation, as well as a rougher surface topography of the lactose particle. As anticipated, the scanning electron micrographs of the formulation blends highlighted a high degree of agglomeration of the drug and increased segregation of the drug from the lactose surfaces with increasing concentrations of MgSt. This can be clearly observed for the highest concentration of MgSt (1%w/w), where loose and segregated agglomerates can be observed. This may suggest that such a high concentration of MgSt may reduce the force of adhesion between the drug particles and carrier excipient to such an extent that the drug segregation and agglomeration is favoured, as suggested by Begat et al.<sup>2</sup>



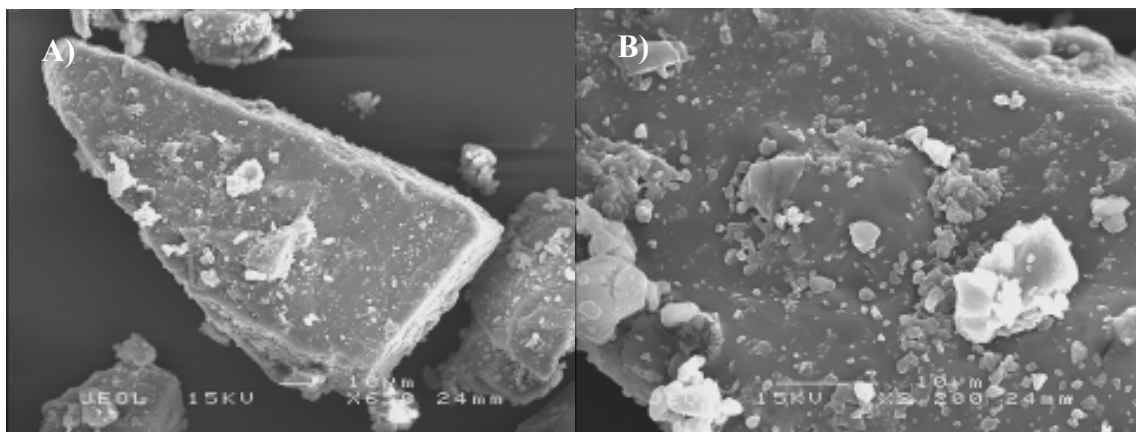
***Figure 3.1 Representative scanning electron micrographs of Lactochem at A) x650 and B) x1600 magnifications.***



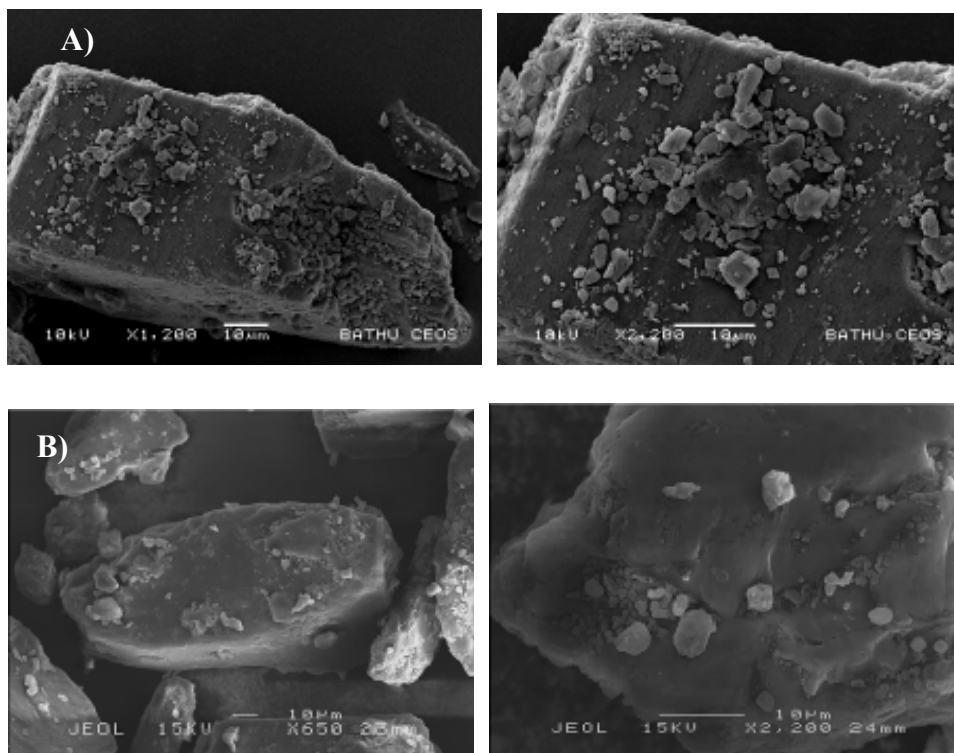
***Figure 3.2 Representative scanning electron micrographs of Nanolac at x1200 magnification.***

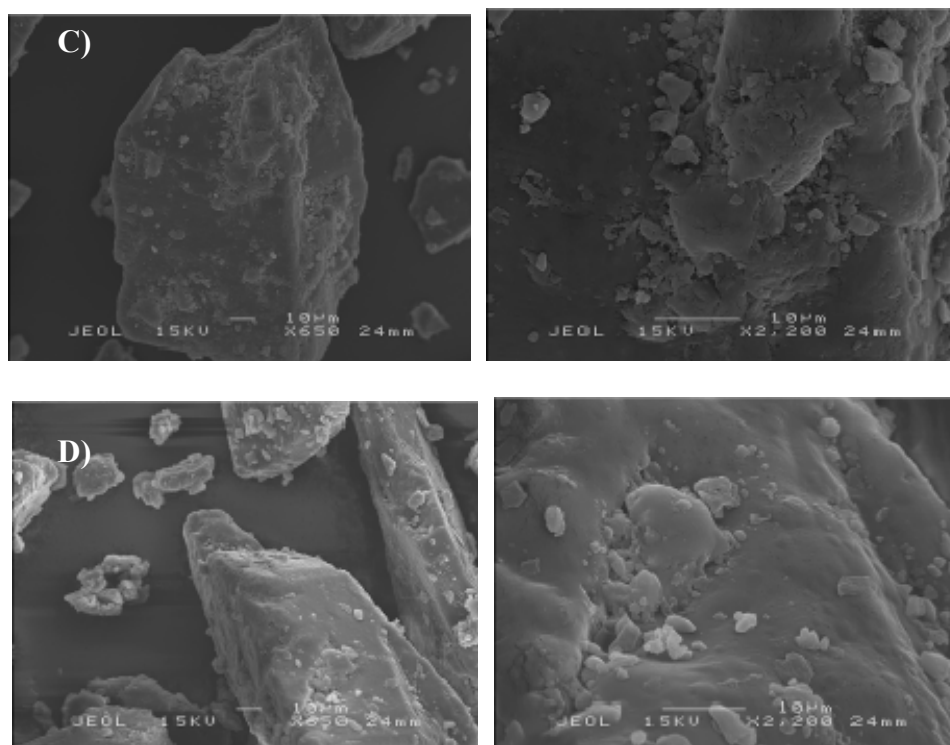


***Figure 3.3 Representative scanning electron micrographs showing the control formulation at 25°C, 44%RH containing Nanolac and budesonide at A) x650 and B) x2200 magnifications.***

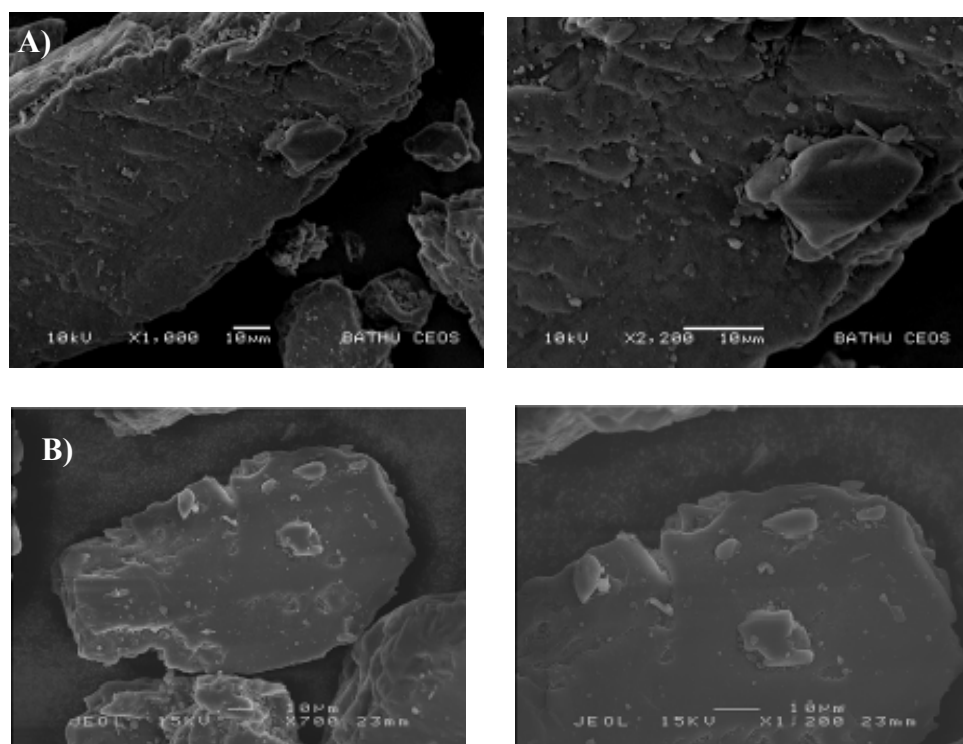


*Figure 3.4 Representative scanning electron micrographs showing the control formulation at 25°C, 44%RH containing Lactochem and budesonide at A) x650 and B) x2200 magnifications.*





**Figure 3.5** Representative scanning electron micrographs of Lactochem and budesonide pre-conditioned with A) 0.125%, B) 0.25%, C) 0.5% and D) 1.0% w/w MgSt at x650 and x2200 magnifications.



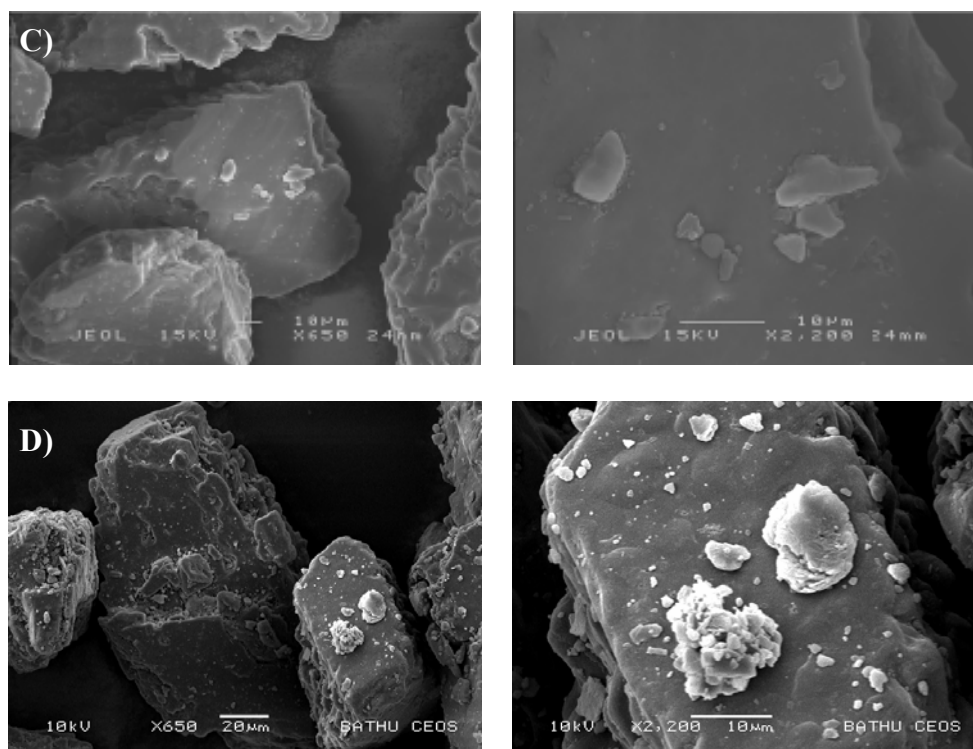


**Figure 3.6** Representative scanning electron micrographs of Nanolac and budesonide pre conditioned with A) 0.125%, B) 0.25%, C) 0.5% and D) 1.0% w/w MgSt at x650 and x2200 magnifications.

### 3.4.2 Particle size analysis

The particle size distribution of budesonide in table 3.3 followed a log-normal distribution, which is common for pharmaceutical materials. The table of data suggests that the micronised batch of budesonide was suitable for inhalation applications.

**Table 3.3** Particle size distribution statistics summary for budesonide.

Material	d <sub>10</sub> (µm ± SD)	d <sub>50</sub> (µm ± SD)	d <sub>90</sub> (µm ± SD)	% <5 µm (µm ± SD)
Micronised budesonide	0.88 ± 0.01	5.52 ± 0.25	11.61 ± 2.15	48.45 ± 0.77



A graphical representation of the particle size and cumulative undersize distributions of the pre-blends for both Lactochem and Nanolac carriers are shown in figures 3.7 – 3.12.

The sieved Lactochem sample and all MgSt processed Lactochem was found to have a considerably higher level of fine particles, compared to the Nanolac blends.

These data suggest, however, that the surface etching process did not significantly modify the coarse particle size but significantly reduced the percentage of intrinsic fines. The cumulative particle size distributions of the Lactochem and Nanolac samples are shown in figures 3.7 and 3.8, respectively and particle size distribution analysis summarised in table 3.4. Although the d<sub>50</sub> and d<sub>90</sub> values of the carrier before and after etching were similar, the d<sub>10</sub> value was approximately double after the etching process, indicating that the etching procedure preferably dissolved the fine lactose particles present. This is further demonstrated by the proportion of particles in the carrier <10µm and < 5µm diameter, which were reduced by ~50% by etching. Thus, any apparent change in functionality may be a consequence of this removal of fines which is known to significantly influence the deaggregation and delivery of drug particulates within a carrier based DPI formulation.<sup>20,21,24,25</sup>

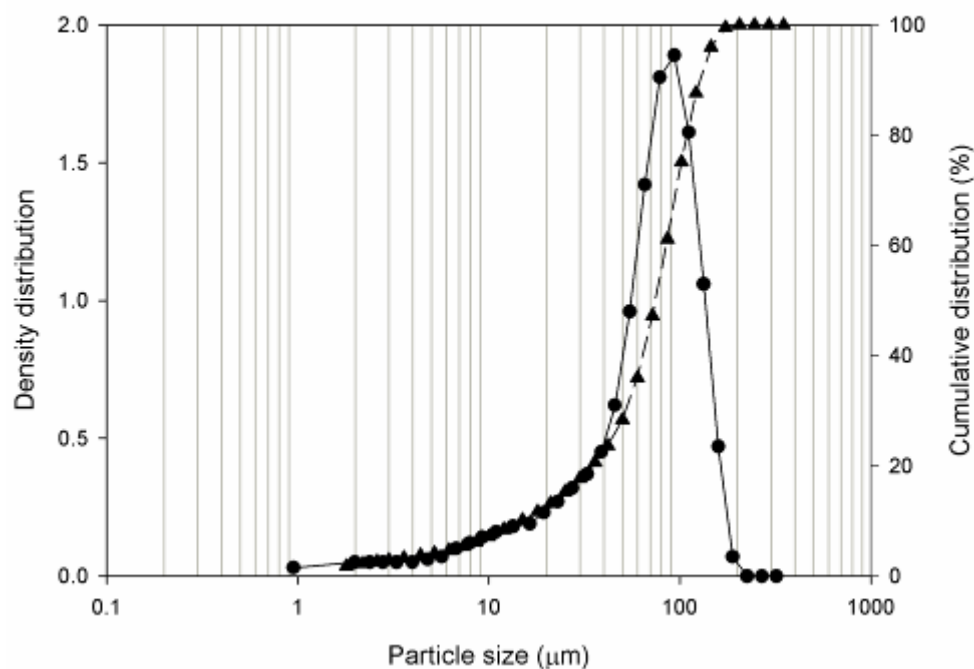


**Figure 3.7 Cumulative particle size distribution of Lactochem®.**

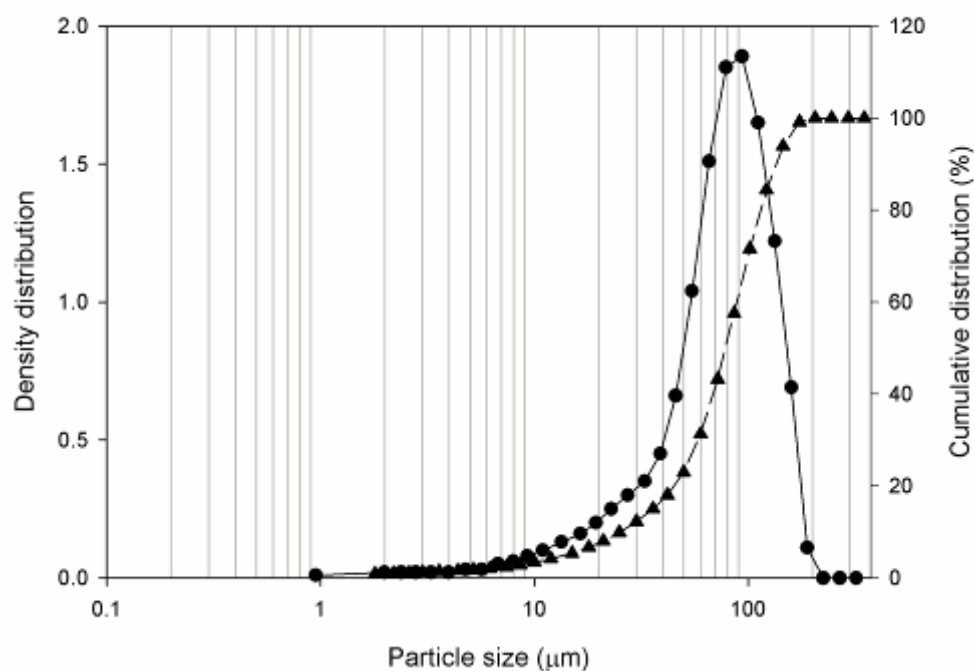


**Figure 3.8 Cumulative particle size distribution of Nanolac®.**

**Table 3.4 Particle size distribution statistics summary of the carriers.**

Materials	d <sub>10</sub> (μm ± SD)	d <sub>50</sub> (μm ± SD)	d <sub>90</sub> (μm ± SD)	% < 10μm (μm ± SD)	% < 5 μm (μm ± SD)
<b>Lactochem®</b>	14.72 ± 0.01	74.92 ± 0.17	129.70 ± 1.19	7.08 ± 0.07	3.84 ± 0.17
<b>Nanolac®</b>	24.48 ± 0.22	76.59 ± 0.89	126.74 ± 4.43	3.50 ± 0.03	1.84 ± 0.04

### 3.4.2.3 Particle size analysis of MgSt-lactose pre-blends

The d<sub>10</sub>, d<sub>50</sub> and d<sub>90</sub> percentiles and % of lactose particles less than 10 and 5μm for the processed MgSt-Lactochem and MgSt-Nanolac pre-blends, shown in Figures 3.11 to 3.14 are summarised in Tables 3.5 and 3.6, respectively.

**Table 3.5 Particle size distribution statistics summary of the MgSt-Lactochem pre-blends.**

<b>Blend</b>	<b>Materials</b>	<b>d<sub>10</sub> (µm ± SD)</b>	<b>d<sub>50</sub> (µm ± SD)</b>	<b>d<sub>90</sub> (µm ± SD)</b>	<b>% &lt; 10 µm (µm ± SD)</b>	<b>% &lt; 5 µm (µm ± SD)</b>
B	0.125% MgSt+Lactochem	16.24±0.92	75.69±0.06	129.42±3.08	6.59±0.3 6	3.68±0.16
D	0.25% MgSt + Lactochem	10.48±0.60	68.41±0.60	130.35±3.20	9.60±0.53	5.19±0.25
F	0.5% MgSt + Lactochem	18.63±0.51	76.84±0.64	132.44±1.11	5.43±0.11	2.55±0.05
H	1.0% MgSt + Lactochem	14.61±0.58	74.89±0.98	129.03±1.42	7.10±0.21	3.58±0.09

**Table 3.6 Particle size distribution statistics summary of the MgSt- Nanolac pre blends.**

<b>Blend</b>	<b>Materials</b>	<b>d<sub>10</sub> (µm ± SD)</b>	<b>d<sub>50</sub> (µm ± SD)</b>	<b>d<sub>90</sub> (µm ± SD)</b>	<b>% &lt; 10 µm (µm ± SD)</b>	<b>% &lt; 5 µm (µm ± SD)</b>
A	0.125% MgSt+Nanolac	25.83±0.38	77.19±0.31	127.79±0.92	3.41±0.03	1.83±0.02
C	0.25% MgSt + Nanolac	56.46±1.39	92.39±0.92	140.95±1.19	2.02±0.23	1.27±0.12
E	0.5% MgSt + Nanolac	54.64±1.54	92.23±0.43	140.67±0.79	3.16±0.52	1.99±0.30
G	1.0% MgSt + Nanolac	56.29±0.38	92.15±0.61	139.8±1.60	2.42±0.15	1.51±0.11

Due to the removal of the fines, the d10 and d50 for the Nanolac formulations are larger. Furthermore, there are significant differences in the amount of fine particle present in all MgSt-Nanolac blends with respect to the lactochem formulations.

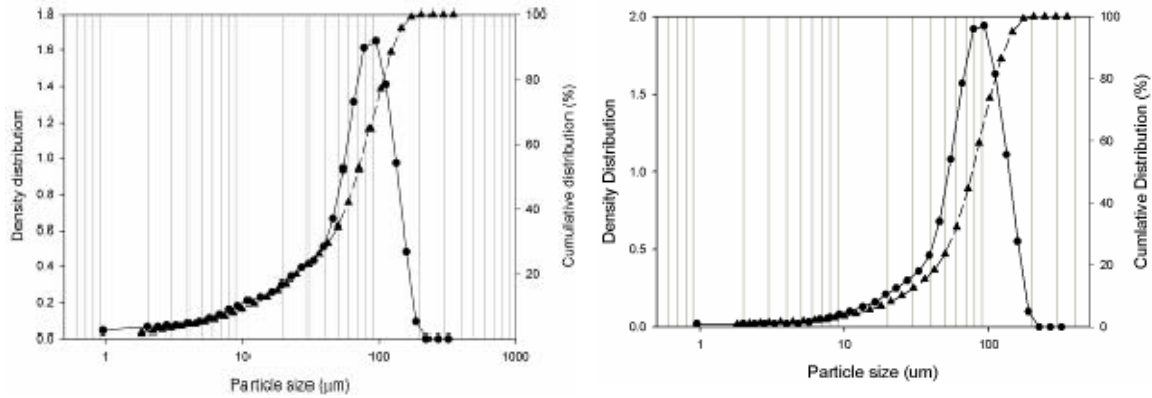


**Figure 3.9** Cumulative particle size distributions of A) blend containing Nanolac and 0.125% MgSt and B) blend containing Lactochem and 0.125% MgSt.

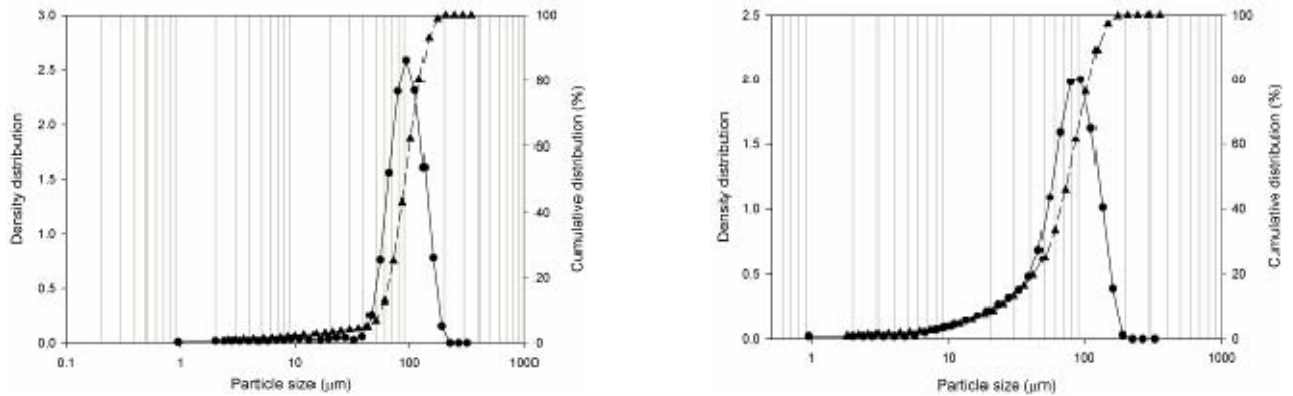


**Figure 3.10** Cumulative particle size distributions of A) blend containing Nanolac and 0.25% MgSt and B) blend containing Lactochem and 0.25% MgSt.

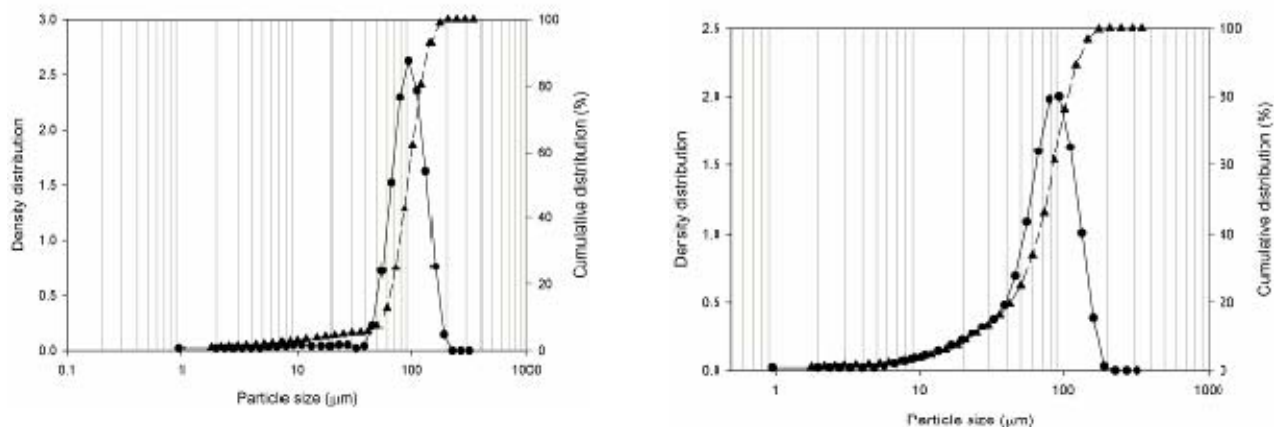


**Figure 3.11** Cumulative particle size distributions of A) blend containing Nanolac and 0.5% MgSt and B) blend containing Lactochem and 0.5% MgSt.

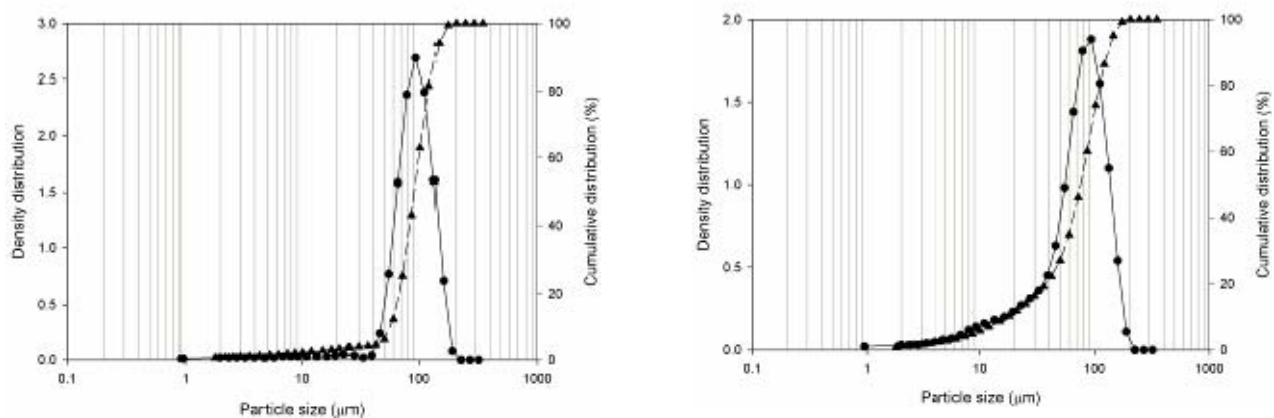


**Figure 3.12** Cumulative particle size distributions of A) blend containing Nanolac and 1.0% MgSt and B) blend containing Lactochem and 1.0% MgSt

#### 3.4.2.4 Processed formulations

Figure 3.13 show the particle size distributions of the aerosol clouds characterised by the Helios system at 60L/min for the Nanolac and Lactochem formulations following actuation from the single shot Cyclohaler DPI device. These data suggest that the Lactochem formulations exhibited a significant distribution of sub-20µm fine particulates within the formulation and the presence agglomerates with a size range between 20 and 40µm, relative to the Nanolac formulations, which only indicated a small inflection between the 2 and 3 microns followed by the presence of the coarse PSD.

With the addition of increasing concentrations of MgSt to the Lactochem formulations there are differences in the particle size distributions of the aerosol clouds with respect to the Lactochem formulation. As show in Figure 3.14, while there are no observable differences in the particle size profiles with the addition of very low concentrations of MgSt (0.125%), there is a marked influence upon the addition of 0.25% MgSt (Figure 3.14(B)). The profile suggests that there is relative increase in the detection of particles in the respirable size range together with an increase in the amount of agglomerates in the 20-40 µm size range. While there are similar effects for the addition of increasing concentrations MgSt their influence appear to be not as significant as the addition of 0.25% MgSt with Lactochem. These observations are supported by particle size distribution statistics shown in Table 3.17 for the Lactochem formulations, where the percentage of particles below 5µm was highest for the addition of 0.25%w/w MgSt.

The addition of MgSt to the Nanolac formulations had a marked influence on the particle size distribution for all concentrations. Upon the addition of 0.125% MgSt there was an observable increase in the size distribution data both in the respirable size range and in the 20-40 µm size range (Figure 3.15(A)). However, with increasing addition of MgSt the influence on the particle size distribution was observed only in the respirable particle size range (Figures 3.15 (B-D)). The particle size distribution statistics for the addition of MgSt with Nanolac, shown in Table 3.18, further supports these observations.

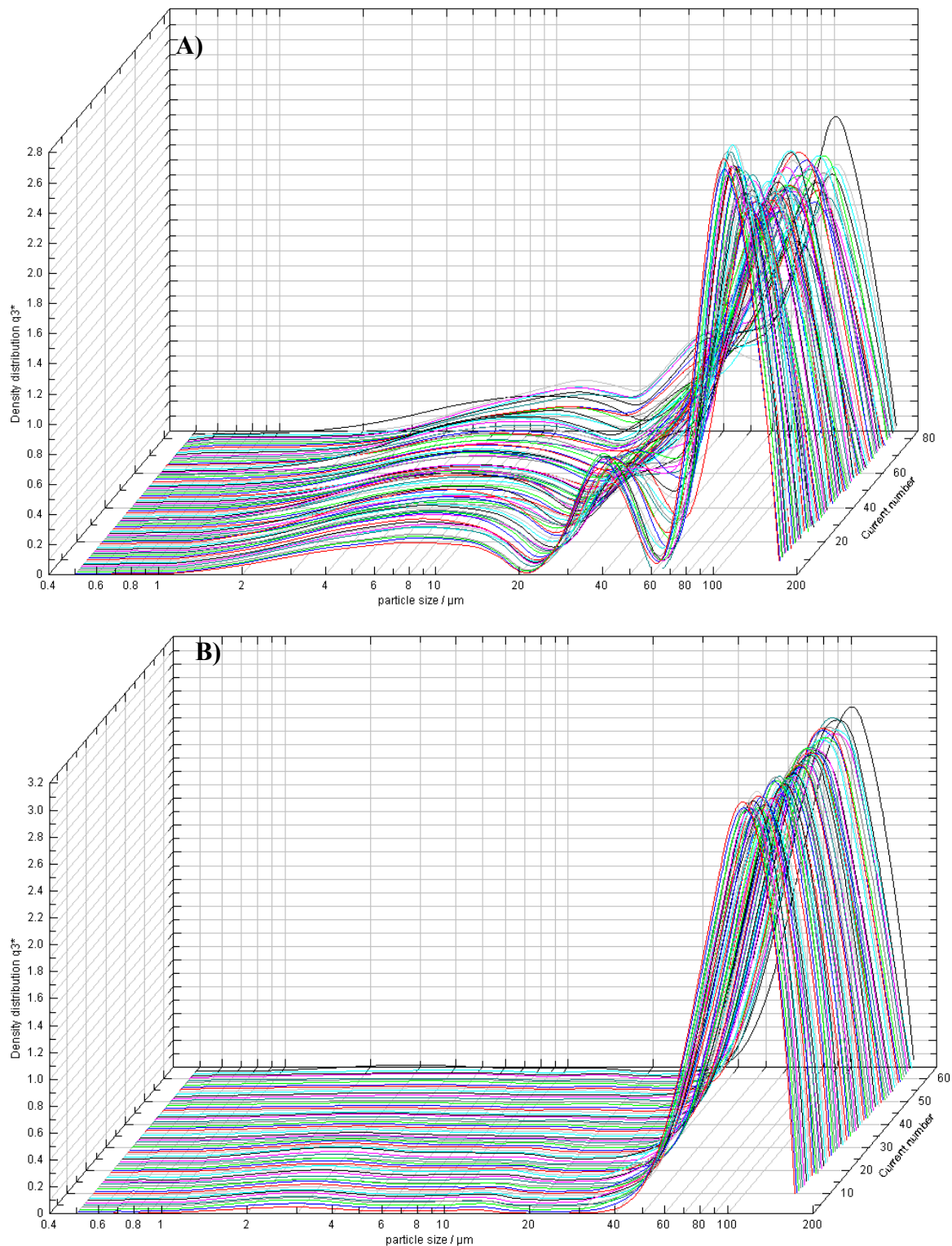


**Figure 3.13 Representative particle size distributions of the aerosol clouds generated by the formulations of A) Lactochem and budesonide and B) Nanolac and budesonide at 25°C, 44%RH.**

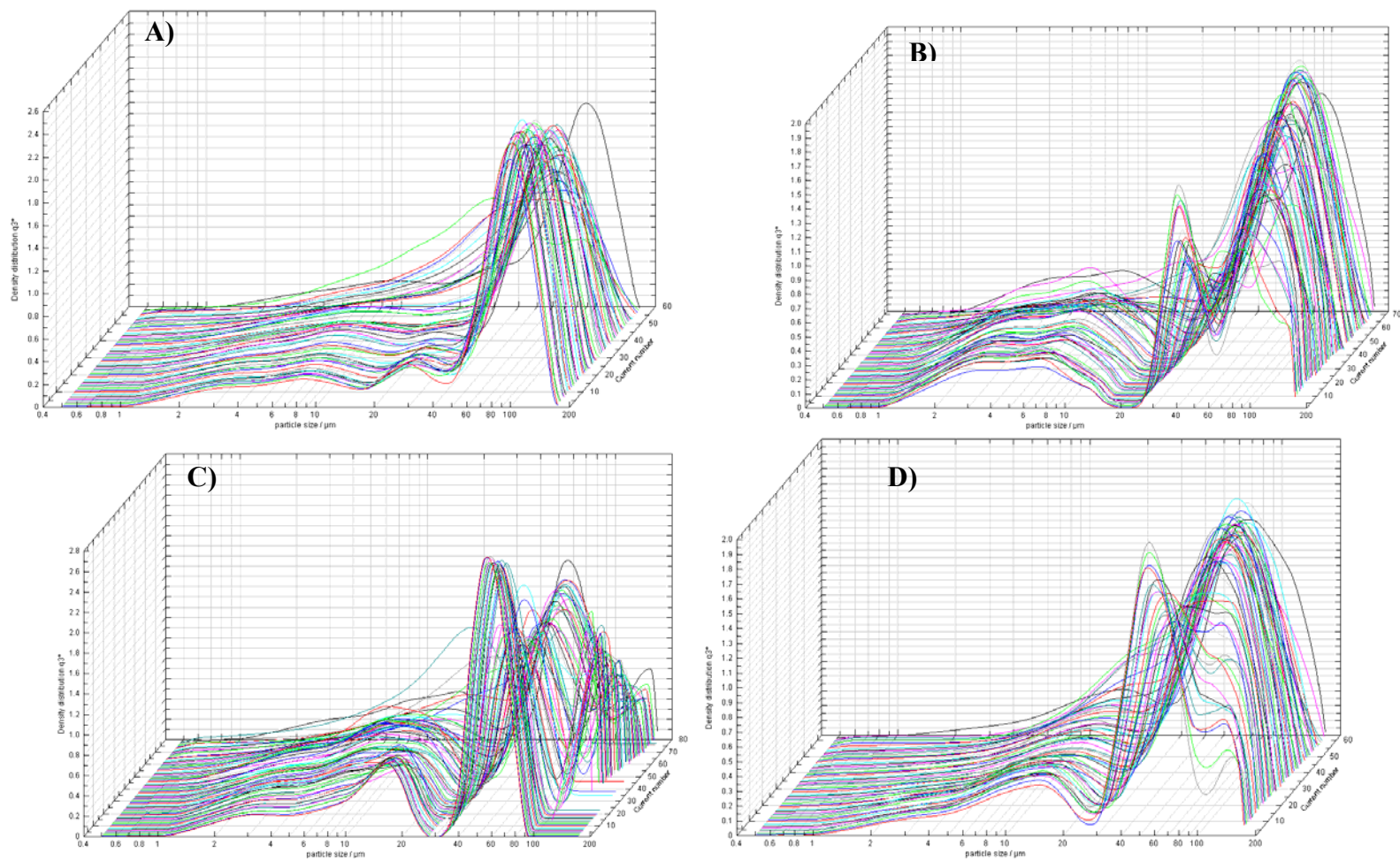


**Figure 3.14** Representative particle size distributions of the aerosol clouds generated by the formulations of Lactochem and budesonide pre-conditioned with A) 0.125% B) 0.25%, C) 0.5%, D) 1.0% w/w MgSt at 25°C, 44%RH.



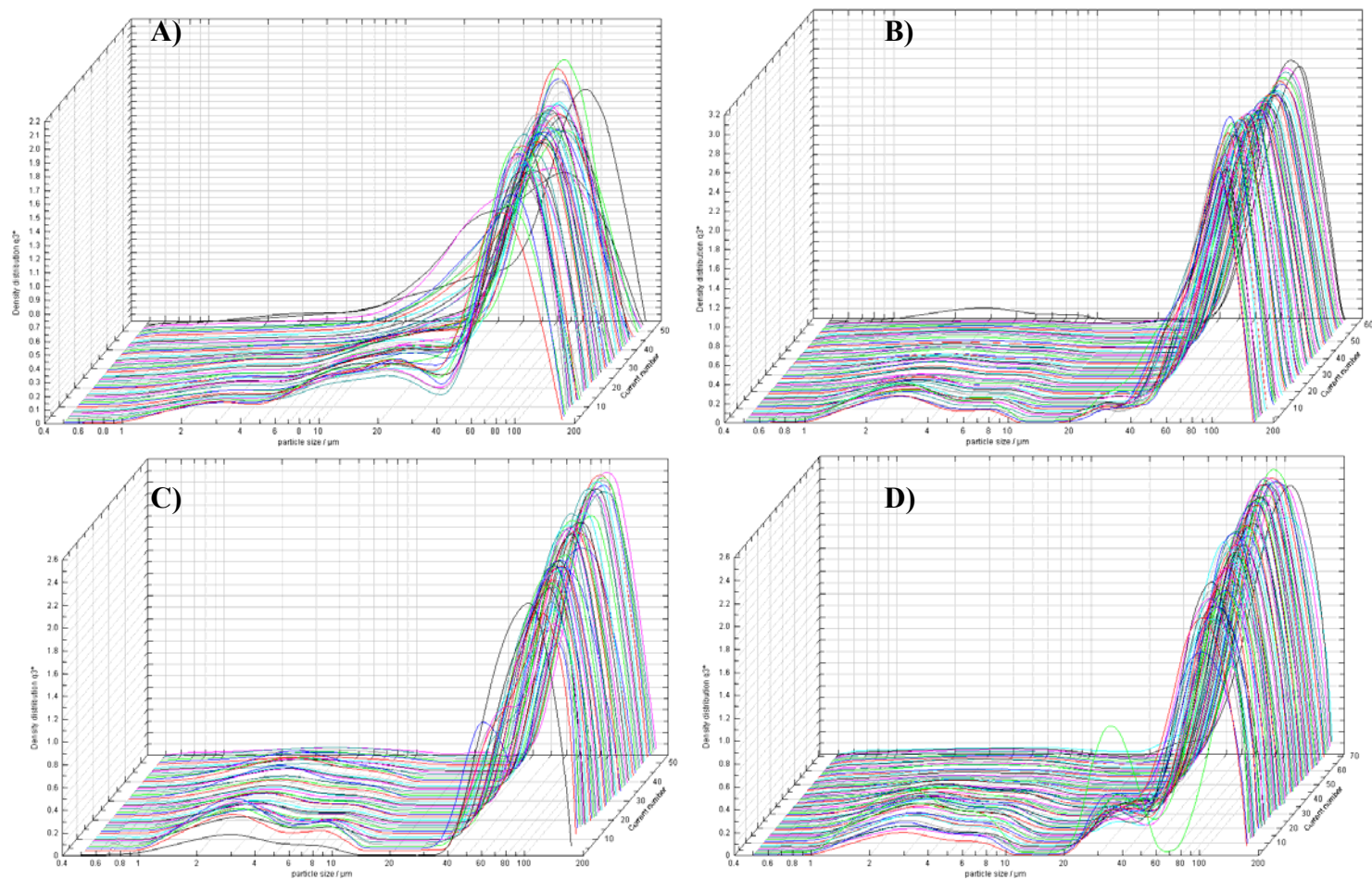


**Figure 3.15** Representative particle size distributions of the aerosol clouds generated by the formulations of Nanolac and budesonide pre-conditioned with A ) 0.125%, B) 0.25% C) 0.5% and D) 1.0% w/w MgSt at 25°C, 44%RH.

**Table 3.7 Particle size distribution statistics summary of the Lactochem formulations at 25°C, 44%RH for the Helios Inhaler module.**

<b>Blend</b>	<b>Materials At 25°C, 44%RH</b>	<b>d<sub>10</sub> (µm ± SD)</b>	<b>d<sub>50</sub> (µm ± SD)</b>	<b>d<sub>90</sub> (µm ± SD)</b>	<b>% &lt; 10 µm (µm ± SD)</b>	<b>% &lt; 5 µm (µm ± SD)</b>
J	Lactochem+budesonide	13.51±2.63	71.41±13.64	120.87±6.78	6.98±1.21	2.00±0.29
B	0.125%MgSt+Lactochem + budesonide	7.29±1.04	71.85±11.59	119.65±9.12	13.69±2.29	7.18±1.10
D	0.25%MgSt+Lactochem + budesonide	4.36±0.70	80.11±3.65	110.58±2.17	19.82±3.26	11.68±1.87
F	0.5% MgSt +Lactochem + budesonide	5.02±1.54	47.29±12.08	97.80±7.09	20.49±3.16	10.52±1.71
H	1.0% MgSt +Lactochem + budesonide	8.67±1.70	56.61±4.52	119.48±9.68	12.18±2.44	5.31±1.21

**Table 3.8 Particle size distribution statistics summary of the Nanolac formulations at 25°C, 44%RH for the Helios Inhaler module.**

<b>Blend</b>	<b>Materials At 25°C, 44%RH</b>	<b>d<sub>10</sub> (µm ± SD)</b>	<b>d<sub>50</sub> (µm ± SD)</b>	<b>d<sub>90</sub> (µm ± SD)</b>	<b>% &lt; 10 µm (µm ± SD)</b>	<b>% &lt; 5 µm (µm ± SD)</b>
I	Nanolac+budesonide	52.78±1.88	90.26±2.48	135.13±2.60	4.68±0.90	3.61±0.69
A	0.125% MgSt + Nanolac + budesonide	14.90±1.99	67.24±8.50	116.28±7.68	7.31±0.77	4.18±0.46
C	0.25% MgSt + Nanolac + budesonide	34.62±2.89	85.35±2.24	130.66±2.95	8.30±0.88	6.56±0.72
E	0.5% MgSt + Nanolac + budesonide	36.95±2.63	87.23±1.47	131.07±3.30	8.18±1.02	5.94±0.77
G	1.0% MgSt + Nanolac + budesonide	23.38±4.61	88.69±1.68	139.36±2.26	11.52±1.10	8.57±1.23

### 3.4.3 Drug content uniformity

The drug content uniformity of all the Lactochem and Nanolac formulations are summarised in table 3.9 and 3.10, respectively. While all formulations have an acceptable %RSD the content uniformity for the non-MgSt processed lactose has a significant lower coefficient of variation. No significant differences in the content uniformity were measured with increasing concentrations of MgSt.

Blend	Formulation	%RSD	SD
B	0.125%MgSt+Lactochem +budesonide	3.07	0.03
D	0.25%MgSt+Lactochem +budesonide	3.48	0.04
F	0.5%MgSt+Lactochem +budesonide	2.76	0.03
H	1%MgSt+Lactochem +budesonide	3.36	0.01
J (control)	Lactochem+budesonide	1.35	0.01

***Table 3.9 Content uniformity of the five Lactochem formulations of budesonide, analysed by HPLC in duplicate. RSD is the relative standard deviation (Mean  $\pm$  SD, n=10).***

As shown in tables 3.9 and 3.10 the content uniformity analysis of the formulations indicated that all the formulations were well blended, showing a uniform distribution of the drug throughout the matrix, since their %RSD was <6%, which is the value commonly taken as sufficiently uniform for a carrier based DPI formulation.

Blend	Formulation	%RSD	SD
A	0.125%MgSt+Nanolac +budesonide	3.14	0.02
C	0.25%MgSt+Nanolac +budesonide	3.61	0.02
E	0.5%MgSt+Nanolac +budesonide	2.95	0.01
G	1%MgSt+Nanolac +budesonide	3.64	0.02
I (control)	Nanolac+budesonide	1.99	0.02

***Table 3.10 The content uniformity of the five Nanolac formulations of budesonide analysed by HPLC in duplicate. RSD is the relative standard deviation (Mean  $\pm$  SD,  $n=10$ )***

As can also be seen from the tables, the % RSD values of the control formulations which did not contain any MgSt are significantly less than the %RSD values of the other formulations. However, there is no significant difference in the %RSD values between the formulations containing MgSt.

#### **3.4.4 In vitro aerosolisation studies**

Stage-by-stage deposition data for the Lactochem formulations containing increasing concentrations of MgSt are shown in Figure 3.16 and summarised in Table 3.11. These data show striking differences in the amount of drug delivered in each stage depending on formulation preparation.

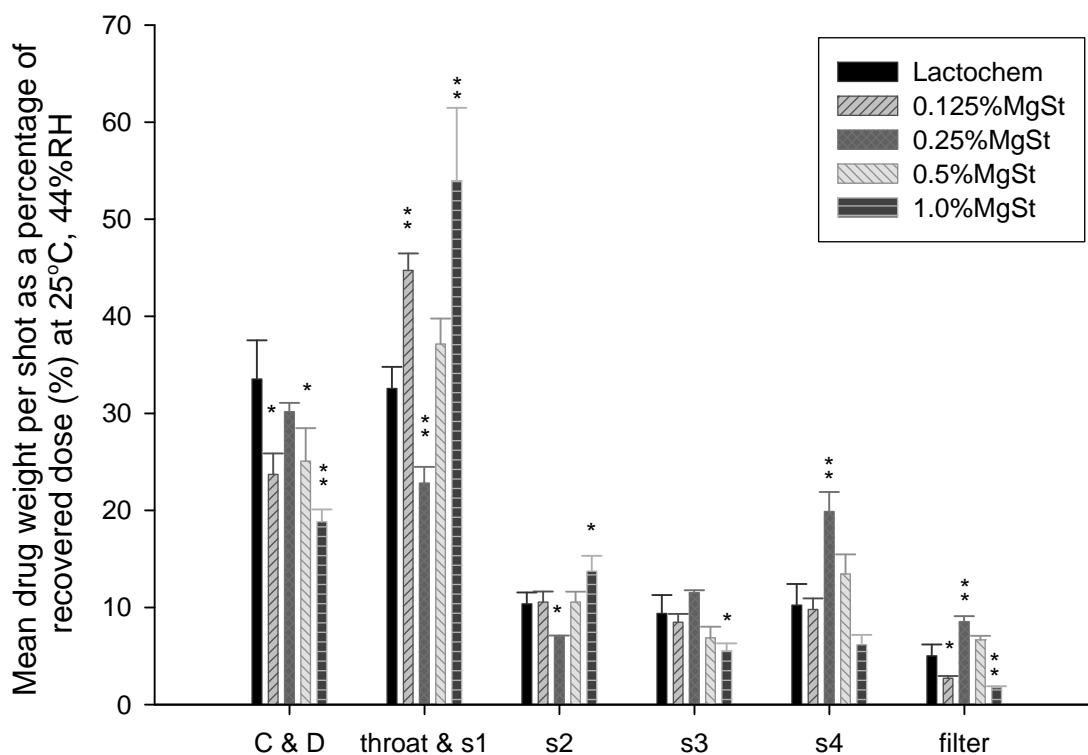


**Figure 3.16** The deposition of budesonide, as a percentage of total recovered dose, for Lactochem and MgSt-Lactochem formulations at 25°C, 44%RH. (Mean  $\pm$  S.D, n=3).

(\*  $P<0.05$ , \*  $P<0.01$ : significant difference compared to Lactochem control formulation by ANOVA one-way. C & D: capsules & device).

**Table 3.11 The deposition of budesonide as mean drug weight per shot (ug) at 25°C, 44% RH in the different stages of the MSLI for the Lactochem formulations and standard deviations (Mean  $\pm$  SD), n=3.**

Blend	(Mean $\pm$ SD) ( $\mu$ g) At 25°C, 44%RH	caps& device	Throat	s1	s2	s3	s4	filter
J	Lactochem+ budesonide	53.9 $\pm$ 8.9	15.8 $\pm$ 0.2	36.7 $\pm$ 4.8	16.8 $\pm$ 3.3	15.2 $\pm$ 5.1	16.6 $\pm$ 6.0	6.3 $\pm$ 3.2
B	0.125% w/w MgSt + Lactochem+budesonide	34.3 $\pm$ 4.0	12.7 $\pm$ 1.9	52.1 $\pm$ 2.2	15.3 $\pm$ 2.3	12.3 $\pm$ 1.9	14.2 $\pm$ 2.3	3.9 $\pm$ 0.6
D	0.25% w/w MgSt + Lactochem+budesonide	70.3 $\pm$ 14.6	11.1 $\pm$ 2.2	43.5 $\pm$ 7.1	14.7 $\pm$ 1.8	25.8 $\pm$ 6.4	46.1 $\pm$ 12.7	20.0 $\pm$ 8.0
F	0.5% w/w MgSt + Lactochem+budesonide	44.0 $\pm$ 8.6	8.8 $\pm$ 2.1	63.3 $\pm$ 14.5	15.4 $\pm$ 6.2	12.3 $\pm$ 4.2	24.0 $\pm$ 7.7	11.8 $\pm$ 1.8
H	1% w/w MgSt + Lactochem+budesonide	33.0 $\pm$ 2.2	17.0 $\pm$ 9.8	77.9 $\pm$ 10.9	24.4 $\pm$ 6.5	9.8 $\pm$ 2.4	10.7 $\pm$ 2.3	3.1 $\pm$ 0.2

As shown in figure 3.16 the largest percentage of drug, as a function of the total recovered dose, remains in the capsule/device and the throat and upper stage of the MSLI. This suggested incomplete device emptying and inadequate removal of the active ingredient from the excipient surface upon aerolisation. The throat stage has been combined with the stage 1 of the MSLI due to the fact that there was no apparent difference in the amount of drug deposited in the throat between formulations and the fact that due to the configuration of the system (i.e. no preseparator) the majority of the excipient particles would fall into stage S1 of the impinger via gravity.

The coating of the lactose with MgSt reduced the device retention of the active ingredient in all the formulations, although the addition of 0.25%w/w MgSt was not significant. This suggested greater removal efficiency of the formulation upon actuation which may relate to a possible modification in the flow and fluidisation behaviour of the formulation upon the introduction of the MgSt<sup>6</sup>.

For the emitted fraction, significant differences in the deaggregation and deposition in the upper stages of the in vitro apparatus was determined. For the throat and the first stage (S1) of the MSLI, the highest percentage of drug deposited was for the 1.0% w/w MgSt-Lactochem (Blend H) formulation. This suggested that an excess of MgSt may have been processed with the lactose in reducing the drug-lactose interaction. As a result, the possible segregation of the active from the lactose surface and the creation of loose agglomerates may lead to an increase in the deposition of the active in the throat and S1 of the MSLI. The significant inter-variation in the throat and S1 deposition of the drug with varying concentrations of MgSt highlights the significant influence of the force control agent on modifying the fine balance of the inter-particulate forces within the formulation and how it may transform a system which was initially dominated by the adhesive drug-lactose forces into a cohesive drug-drug led system. The addition of 1.0% w/w MgSt has lowered the interactions between the drug and excipient to such an extent that it could possibly lead to an unstable formulation, subjected to undesirable segregation. The amount of drug deposited by the 0.125% and 1.0% w/w MgSt formulations were significantly higher (ANOVA  $p < 0.01$ ) compared to the amount of drug deposited by the control formulation



while the 0.25% w/w MgSt formulation was significantly lower (ANOVA  $p < 0.01$ ). From these data, an optimum performance in terms of reducing upper airway deposition was obtained for the addition and processing of 0.25% w/w MgSt with the Lactochem carrier.

In stage 2 of the MSLI, the amount of drug deposited by the 0.25% w/w MgSt (Blend X) formulation was significantly lower (ANOVA  $p < 0.05$ ) than all the other formulations while the 1.0% w/w MgSt formulation was significantly higher (ANOVA  $p < 0.05$ ) than all other formulations. The other MgSt concentrations were not significantly different to the control formulation. The 1.0% w/w MgSt formulation was significantly lower (ANOVA  $p < 0.05$ ) than the control formulation in stage 3 of the MSLI, while the drug deposition for all other concentrations of MgSt were not significantly different. In the critical stage of the MSLI, stage 4, only the amount of drug deposited by the 0.25% w/w MgSt formulation was significantly higher (ANOVA  $p < 0.01$ ) than the control formulation. These data show that the amount of drug delivered in the aerodynamic size range 1.7-2.4  $\mu\text{m}$  for the 0.25%w/w MgSt processed lactose was approximately twice that for the control. All the other MgSt processed formulations were not significantly different to the control formulation.

The stage-by-stage deposition of budesonide for the Nanolac carrier with increasing concentrations of MgSt are shown in Figure 3.17 and summarised in Table 3.12. The deposition profiles of budesonide from Nanolac formulations are different to the Lactochem formulations. In contrast to Figure 3.16, the drug retention within the device and capsule for the Nanolac control formulation was very low ( $< 60\%$ ). This may be either may be a consequence of a change to the fluidisation behaviour of the carrier due to the etching process or more likely a change to the drug-excipient interaction due to the increased surface smoothness of the excipient particles. However, while there is efficient emission of the formulation via the Cyclohaler device, the increased amount of drug emitted is retained in the throat and stage 1 of the in vitro apparatus suggesting that the Nanolac process has produced a highly adhesive interaction of the drug with the excipient.

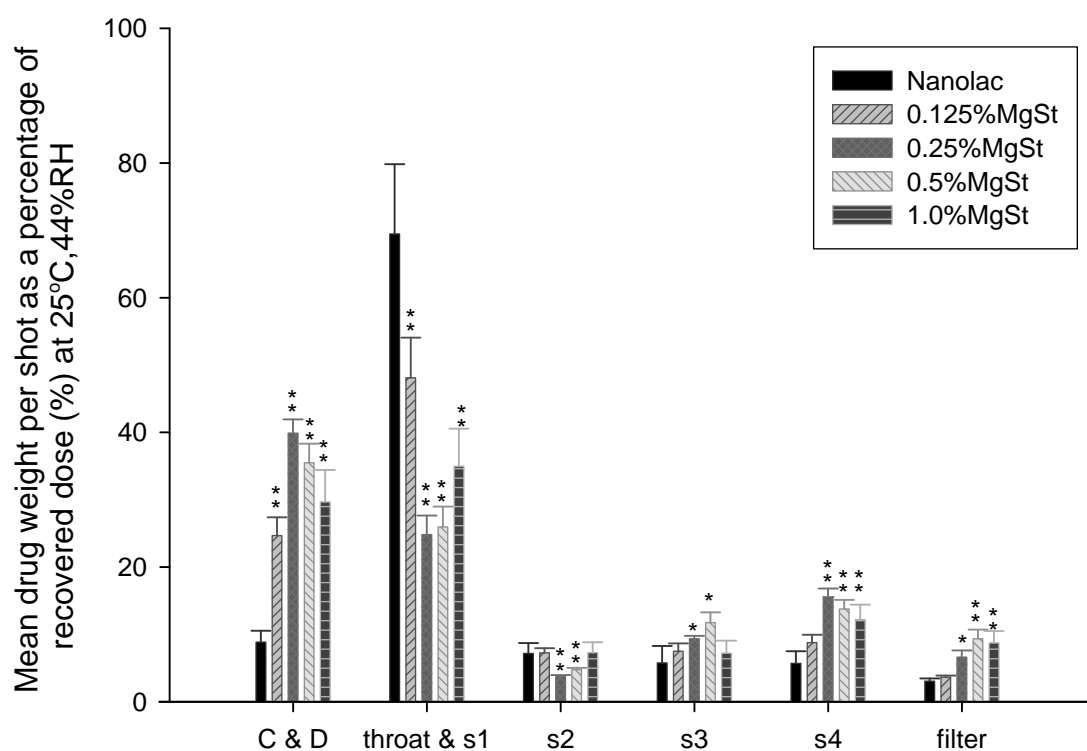


**Figure 3.17** Deposition of budesonide, as a percentage of recovered dose for Nanolac formulations at 25°C, 44%RH. (Mean  $\pm$  S.D, n=3) with increasing concentration of MgSt ( \*  $P<0.05$ , \*  $P<0.01$ : significant difference compared to Nanolac control formulation by ANOVA one-way. C & D: capsules & device)

**Table 3.12 The deposition of budesonide as mean drug weight per shot (ug) at 25°C, 44% RH in the different stages of the MSLI for the Nanolac formulations and standard deviations (Mean  $\pm$  SD), n=3.**

Blend	(Mean $\pm$ SD) ( $\mu$ g) At 25°C, 44%RH	caps& device	throat	s1	s2	s3	s4	filter
I	Nanolac + budesonide	9.1 $\pm$ 2.1	8.8 $\pm$ 5.4	62.5 $\pm$ 3.2	7.3 $\pm$ 1.6	6.0 $\pm$ 2.9	5.8 $\pm$ 1.7	3.2 $\pm$ 0.5
A	0.125% w/w MgSt + Nanolac+budesonide	31.2 $\pm$ 3.7	8.5 $\pm$ 0.1	51.9 $\pm$ 10.0	9.1 $\pm$ 0.7	9.4 $\pm$ 1.6	11.0 $\pm$ 1.5	4.6 $\pm$ 0.1
C	0.25% w/w MgSt + Nanolac+budesonide	72.7 $\pm$ 3.2	7.0 $\pm$ 2.6	38.6 $\pm$ 8.7	6.9 $\pm$ 0.9	18.4 $\pm$ 3.8	28.3 $\pm$ 1.4	12.8 $\pm$ 4.5
E	0.5% w/w MgSt + Nanolac+budesonide	62.8 $\pm$ 7.0	7.5 $\pm$ 1.8	38.8 $\pm$ 9.1	8.5 $\pm$ 0.9	20.8 $\pm$ 4.2	24.5 $\pm$ 5.0	14.6 $\pm$ 3.0
G	1% w/w MgSt + Nanolac+budesonide	24.0 $\pm$ 3.8	4.4 $\pm$ 0.7	23.8 $\pm$ 3.5	5.9 $\pm$ 1.2	5.8 $\pm$ 1.2	9.8 $\pm$ 0.6	7.0 $\pm$ 0.1

As would be expected, the introduction of MgSt may lead to a decrease in this interaction as suggested by an increasing device retention and a lowering in the percentage of the drug retained in the throat and stage 1. For the MgSt-Nanolac formulations, the optimum concentration for minimising upper airway losses is between 0.25%w/w and 0.5% w/w.

The addition of MgSt led to a significantly increase in device retention, whereas in the throat and s1 the amount of drug was significantly lower. In stage 2 of the MSLI, the amount of drug deposited for the addition of 0.25% and 0.5% w/w MgSt formulations were significantly lower (ANOVA  $p < 0.01$ ) than the control formulation. The amount of drug deposited for other concentrations of MgSt were not significantly different. The amount of drug deposited on stage 3 of the MSLI for the addition of 0.25% and 0.5% w/w MgSt formulations were significantly higher (ANOVA  $p < 0.05$ ) compared to the control formulation. Once again, the amount of drug deposited by the other formulations was not significantly different. In stage 4 of the MSLI, the amount of drug deposited by the 0.25%, 0.5% and 1.0% w/w MgSt formulations were significantly higher (ANOVA  $p < 0.01$ ) compared to the control formulation. In the filter stage, the amount of drug deposited for the 0.25% w/w ( $P < 0.05$ ), 0.5% and the 1.0% w/w ( $P < 0.01$ ) MgSt formulation were significantly higher than the control, suggesting that more drug reaches the lower airways of the respiratory tract and that the addition of MgSt to the formulations significantly improved aerosol deposition performance.

These data suggest that the 0.5% w/w MgSt formulation exhibited the optimum aerosolisation performance, since it has the largest amount of drug deposit in stages 3 and 4 which is associated with the deposition profile in the conducting airways of the respiratory tract. It should be noted that processing the Nanolac-MgSt materials with ball bearing will lead to an increase in the surface roughness of the lactose particles. Thus, this roughening process may also contribute towards the lowering of the adhesive interaction leading to the significant changes in the formulation performance with respect to the Nanolac formulations.

**Table 3.13 The deposition of budesonide in the MSLI from the Lactochem formulations at 25°C, 44%RH via a Cyclohaler (Mean ± SD, n=3).**

Blend	(Mean ± SD) At 25°C, 44%RH	Recovered Dose (µg)	Emitted Dose (µg)	Fine particle dose (µg)	FPF <sub>RD</sub> (%)	FPF <sub>ED</sub> (%)
J	Lactochem+ budesonide	161.1±4.3	107.3±13.2	38.0±13.3	23.5±7.8	35.0±9.5
B	0.125% w/w MgSt + Lactochem+budesonide	144.9±3.0	110.6±6.3	30.5±4.0	27.5±2.6	21.0±2.6
D	0.25% w/w MgSt + Lactochem+budesonide	231.6±50.3	161.3±35.7	92.0±25.9	39.4±2.7	56.6±3.7
F	0.5% w/w MgSt + Lactochem+budesonide	179.6±24.7	135.7±32.8	48.1±13.1	26.5±3.6	35.4±3.5
H	1% w/w MgSt + Lactochem+budesonide	175.8±13.6	142.8±13.3	23.5±3.3	13.5±2.3	16.6±3.2

**Table 3.14 The deposition of budesonide in the MSLI from the Nanolac formulations at 25°C, 44%RH via a Cyclohaler**  
**(Mean ± SD, n=3)**

Blend	(Mean ± SD) At 25°C, 44%RH	Recovered Dose (µg)	Emitted Dose (µg)	Fine particle dose (µg)	FPF <sub>RD</sub> (%)	FPF <sub>ED</sub> (%)
I	Nanolac + budesonide	102.7±4.9	93.6±3.0	15.0±1.8	14.5±1.2	16.0±1.4
A	0.125% w/w MgSt + Nanolac +budesonide	125.7±4.6	94.5±7.2	24.9±3.2	26.6±5.1	19.9±2.9
C	0.25% w/w MgSt + Nanolac +budesonide	184.6±17.4	112.0±15.4	59.5±6.7	32.2±2.1	53.3±3.3
E	0.5% w/w MgSt + Nanolac +budesonide	177.4±6.3	114.6±11.8	59.9±7.2	33.8±4.2	52.4±5.4
G	1% w/w MgSt + Nanolac +budesonide	80.5±9.0	56.6±5.6	22.5±1.7	28.1±2.7	40.0±2.8

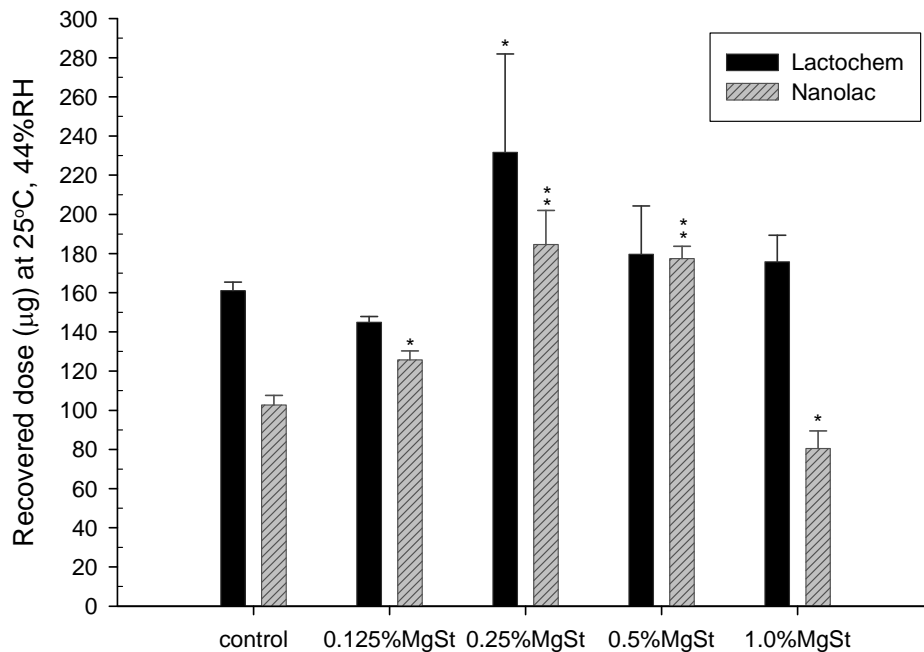


**Figure 3.18** A graph showing the relationship between the recovered dose and the concentration of Magnesium stearate of both types of formulations. (Mean  $\pm$  SD,  $n=3$ )  
( \*  $P<0.05$ , \*  $P<0.01$ : significant difference compared to the control formulations by ANOVA one-way. C & D: capsules & device)

The in vitro deposition data for the addition of increasing concentration of MgSt for the Lactochem and Nanolac formulations are summarised in Tables 3.13 and 3.14, respectively, in terms of the recovered, emitted and fine particle dose together with the fine particle fraction as a function of the recovered and emitted doses. These data are shown graphically in Figures 3(.18, .19, .20 and.21).

Figure 3.18 shows that that the recovered doses of the Nanolac formulations containing MgSt were statistically significant compared to the control formulation which did not contain MgSt. All of them were significantly higher, except the formulation containing 1.0% w/w MgSt which was significantly lower than the control (ANOVA  $p<0.05$ ). The 0.125% w/w MgSt formulation was significantly higher (ANOVA  $p<0.05$ ), as well as the 0.25% and 0.5% w/w MgSt (ANOVA  $p<0.01$ ). The 0.25% w/w MgSt formulations have the

highest recovered doses, both with Nanolac and Lactochem and an increasing trend can be seen from the control until the 0.25% w/w concentration of MgSt, gets to its maximum at 0.25% w/w concentration of MgSt and then starts decreasing. Therefore, it could be suggested that at the optimum concentration of 0.25% w/w MgSt, more drug is leaving the capsule and device and entering the respiratory tract. Consequently the 1.0%w/w MgSt+Nanolac+budesonide formulation has the lowest recovered dose. In the Lactochem formulations, all recovered doses of the formulations containing MgSt were higher than the control one, except the formulation containing 0.125% w/w MgSt which was lower. However, only the 0.25% w/w MgSt formulation was significantly higher compared to the Lactochem control formulation (ANOVA  $p < 0.05$ ). When comparing the Nanolac with the Lactochem formulations, Lactochem formulations have higher recovered doses, possibly suggesting that fines do play a significant role in this particular experiment. Lactochem having a rough surface with clefts and cavities makes the force of adhesion between the drug particles and its surface quite low since their contact area is small and very limited. Therefore only a small amount of energy is required to detach the drug particles from the carrier surface. On the other hand, Nanolac has a smooth surface, and therefore a large contact surface area between the drug particles and the carrier surface and therefore a high force of adhesion. Consequently, a large amount of energy needs to be applied in order to detach the drug particles from the carrier surface.



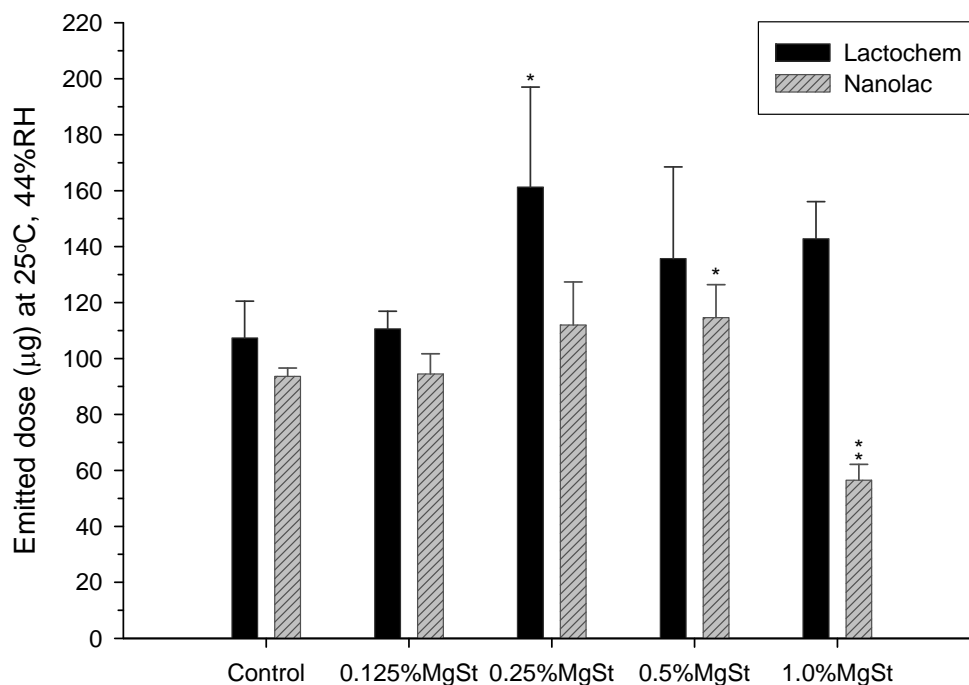


**Figure 3.19** A graph showing the relationship between the emitted dose and the concentration of Magnesium stearate of both types of formulations. (Mean  $\pm$  SD,  $n=3$ ).  
( \*  $P<0.05$ , \*  $P<0.01$ : significant difference compared to the control formulations by ANOVA one-way. C & D: capsules & device)

As shown in figure 3.19, only the emitted dose of the 0.25% w/w MgSt formulation amongst the Lactochem formulations was statistically significant (ANOVA  $p<0.05$ ). The emitted doses of the other formulations were not significantly different, suggesting that the addition of MgSt to the Lactochem formulations did not have a dramatic change in the emitted doses, as well as the recovered doses which was discussed above. Only the addition of 0.25% w/w MgSt to the Lactochem formulation resulted in a significantly higher emitted dose, suggesting that the optimum concentration of MgSt required for the maximum amount of drug to enter the respiratory tract is 0.25% w/w.

Amongst the Nanolac formulations, the emitted dose of the 0.5% w/w MgSt formulation was significantly higher (ANOVA  $p<0.05$ ) compared to the control formulation and the

1.0% w/w MgSt formulations was significantly lower (ANOVA  $p < 0.01$ ). This low amount of drug of the 1.0% w/w MgSt formulation emitted to the respiratory tract could be due to the agglomerates (either MgSt agglomerates and/or drug agglomerates) being formed because of the increased concentration of MgSt which lowers the force of adhesion between the drug particles and the carrier surface therefore falling off the surface and existing as loose agglomerates which are too big and remain in the capsules and the device. The 0.5% w/w MgSt formulation has the largest amount of drug emitted compared to the other Nanolac formulations, therefore more drug is entering the RT. The other Nanolac formulations did not show a significant difference compared to the control formulation, but their recovered doses were significantly different, leading to the assumption that a large amount of the drug in those formulations gets deposited in the capsules and the device rather than entering the respiratory tract.

Once again, the Lactochem formulations have larger emitted doses compared to their equivalent concentrations of Nanolac formulations. As discussed above, this is due to their difference in surface morphology influencing the interparticulate interactions between drug particles and the surface of the carrier.

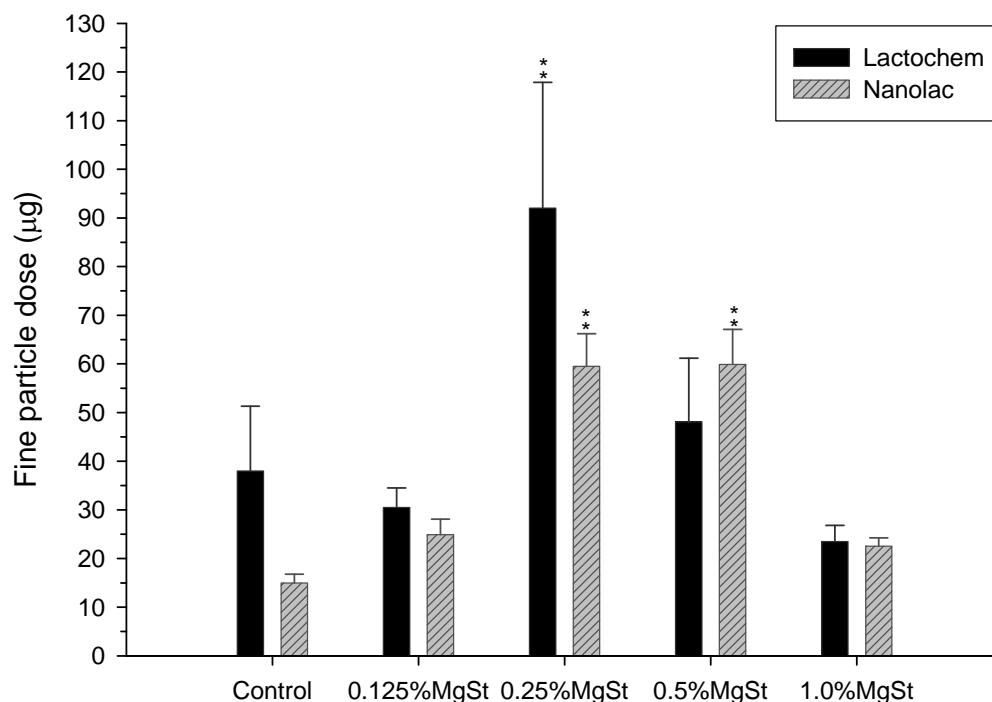


**Figure 3.20** A graph showing the relationship between the fine particle dose and the concentration of Magnesium stearate of both types of formulations. (Mean  $\pm$  SD,  $n=3$ ).

( \*  $P<0.05$ , \*  $P<0.01$ : significant difference compared to the control formulations by ANOVA one-way. C & D: capsules & device)

The fine particle dose (FPD) represents the amount of drug that reaches the lower airways of the RT and is the concentration of drug deposited in stages 3-5 of the MSLI apparatus. Amongst the Lactochem formulations, only the FPD of the 0.25% w/w MgSt formulation was significantly different (ANOVA  $p<0.01$ ) to the control formulation. The FPD of the other Lactochem formulations were not significantly different compared to the control formulation. The addition of 0.25% w/w MgSt to the formulation dramatically increased the FPD value to 3x times the value of the control formulation. The FPD of the 0.5% w/w MgSt formulation was increased but not significantly. The other formulations had a lower FPD compared to the control formulation but the difference was not significant. There is an increasing trend up to 0.25% w/w concentration of MgSt, where it has the greatest FPD and

then it starts decreasing gradually reaching the lowest FPD at the 1.0% w/w MgSt formulation.

Amongst the Nanolac formulations, the fine particle doses of the 0.25% and 0.5% w/w MgSt formulations were significantly higher (ANOVA  $p < 0.01$ ), having values approximately 4x the value of the control formulation. The 0.5% w/w MgSt formulation has the highest FPD but only with a slight difference of  $0.5\mu\text{g}$  to the 0.25% w/w MgSt formulation. The other formulations had higher FPD values than the control formulation but were not significantly higher. These data suggests that the addition of MgSt to the Nanolac formulations increases the FPD and especially the addition of 0.5% w/w MgSt has the greatest FPD. In addition, an increasing trend is observed starting from the control formulation up to the optimum 0.5% w/w MgSt concentration and then a sharp decrease to the 1/3 of the FPD value at the 1.0% w/w MgSt formulation.

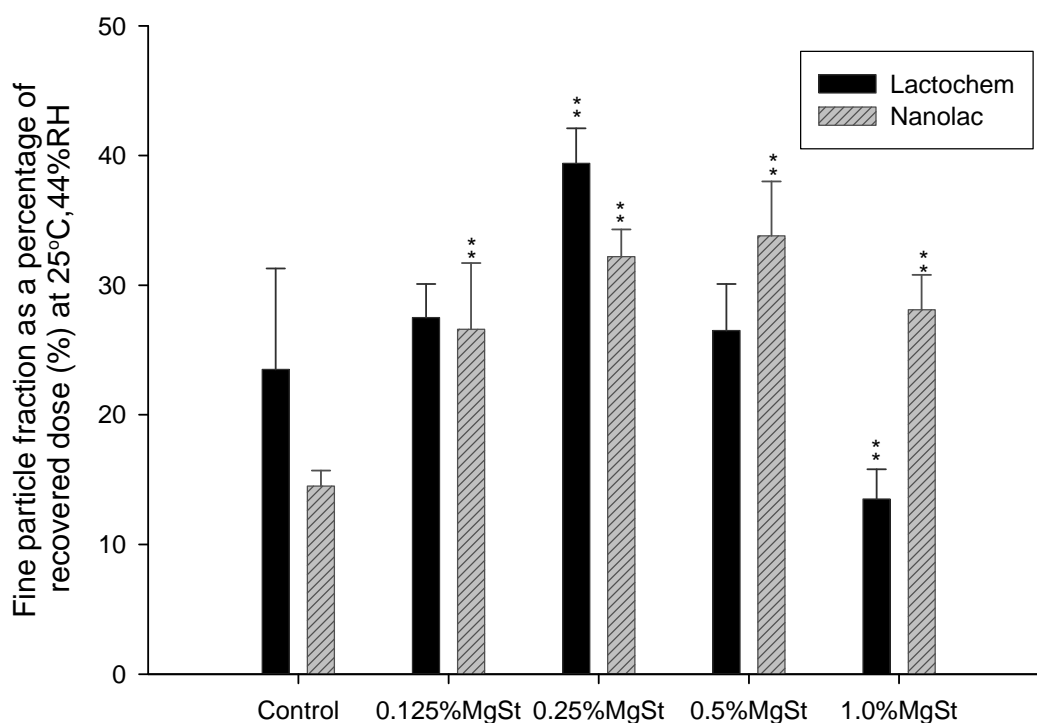


**Figure 3.21** A graph showing the relationship between the fine particle fraction as a percentage of recovered dose and the concentration of Magnesium stearate of both types

*of formulations. (Mean  $\pm$  SD, n=3).(\*  $P<0.05$ , \*  $P<0.01$ : significant difference compared to the control formulations by ANOVA one-way. C & D: capsules & device)*

As shown in figure 3.21 there is an increasing trend in the Lactochem formulations, reaching the optimum concentration of 0.25% w/w MgSt and then a decreasing trend is observed. The highest FPF<sub>RD</sub> in the Lactochem formulations is observed with the addition of 0.25% w/w MgSt, having a significant effect on the aerosol performance (ANOVA  $p<0.01$ ). It could be suggested that for a formulation containing Lactochem and budesonide, the optimum concentration of MgSt that is needed to achieve the most efficient drug delivery is 0.25% w/w. A decrease in the performance can be seen thereafter with the presence of higher concentrations of MgSt, which could be due to the fact that at concentrations higher than 0.25% w/w, MgSt de-stabilizes the ordered powder formulation resulting in powder segregation and agglomeration. The poorest aerosol performance amongst the Lactochem formulations was observed with the formulation of 1.0% w/w MgSt, having a significant decrease in the drug deposition (ANOVA  $p<0.01$ ), with a value of 10% less than that of the control formulation. This may be due to incomplete surface coverage of the lactose carrier by the MgSt upon addition of higher concentrations of MgSt or due to localised coverage of the carrier surface by MgSt. Therefore, instead of MgSt forming a continuous film on the carrier surface it may just form a film at selected areas of the carrier surface or may not even form a film and just agglomerate with the drug particles and/ or fines. When making the powder formulations, the lactose carrier was pre-blended with the MgSt and then this mixture was blended with the drug particles. It could be that during the pre-blending process the MgSt particles occupy the active sites (which are sites with high energy) of the carrier surface and therefore leaving the drug particles to occupy the passive sites of the carrier surface or existing as free or weakly bound fine particles<sup>7</sup>. When having 0.25% w/w MgSt, it could be that only some of the active sites are occupied, enabling some active sites to be occupied by the drug particles and therefore aerosolise upon actuation. However, if all the active sites are occupied by the MgSt particles, then the drug particles would have to exist as free particles or be weakly bound to the carrier surface or even agglomerate between them or with the fines of lactose, therefore not being able to penetrate into the lungs.

Another explanation, could be that the interparticulate interactions at the 0.25% w/w MgSt formulation are balanced, therefore not being too weak which would lead to the falling off the drug particles and forming agglomerates and not too strong which would not enable their detachment from the carrier surface.

The Nanolac formulations were statistically significant compared to the controlled formulation which did not contain any MgSt. However, the best aerosol performance was exerted by the 0.5% w/w MgSt formulation with only 1.6% difference to the 0.25% w/w MgSt and both were approximately double the value of the control formulation. Therefore, an increasing trend can be seen starting from the controlled formulation, reaching the optimum concentration of 0.5% w/w MgSt which modifies adhesion and then decreasing at 1.0% w/w MgSt, but still being higher by 13.6% to the control formulation. The difference between the Nanolac and Lactochem formulations could be attributed to the difference in surface topography and therefore the interparticulate forces. As can be seen from the data, Lactochem formulations have higher aerosol performance until they reach the optimum concentration and then Nanolac formulations have higher aerosol performance.

Previous studies have reported that the presence of fines increases the fine particle fraction through the formation of agglomerates or multiplets. Recent studies by Louey et al (2003)<sup>1</sup> suggest that increased lactose fines result in an agglomerated based system, resulting from the reduction of the free carrier space. Consequently, the fine particle fraction would eventually plateau and decrease due to multilayer or aggregate formation and formulation segregation. Therefore, looking at the data it could be that concentrations of MgSt higher than 0.25% w/w, the intrinsic lactose fines start to agglomerate and segregate and therefore decrease the fine particle fraction.

Several studies have focussed on the surface roughness of carrier particles on the in vitro deposition pattern of the drug<sup>8,9,10</sup>. It was shown by Heng et al (2000)<sup>11</sup> that an optimum lactose surface roughness was required for an increased fine particle fraction of salbutamol

sulfate. All these studies demonstrated that the different surface roughness of the lactose carrier resulted in different adhesion forces between the drug and the carrier, which was reflected in the in vitro deposition results.

During inhalation, the adhesive forces that exist between drug and carrier particles have to be overcome in order to aerosolise primary drug particles. The magnitude of the separation forces during inhalation relative to the adhesive forces in the mixture determines the obtained fine particle fraction. Consequently, optimising a dry powder inhalation system with respect to delivered fine particle dose requires careful balancing between both types of forces. This balance between the forces could possibly be reached upon the addition of 0.25% w/w MgSt to the Lactochem formulations and 0.5% w/w MgSt to the Nanolac formulations and therefore a greater fine particle fraction is observed. The attachment forces have to be strong enough to maintain satisfactory blend homogeneity during handling and storage but weak enough to yield a high drug release from the carrier particles during inhalation.

The addition of MgSt to the budesonide-Lactochem/Nanolac dry powder formulations was performed to investigate any effect it would have on their aerosolization performance and also to investigate any difference between the Nanolac and Lactochem formulations. This was considered to be related to the potential of lowering the adhesive interactions between the drug and the carrier, therefore increasing the detachment efficiency of the drug particles from the carrier upon aerosolization and thus improve the aerosol performance of DPI formulations.

Magnesium stearate as suggested by other studies, should form weaker drug-lactose interactions within the blends by significantly modifying the adhesive and cohesive interactions. Within a controlled blend containing drug and lactose, it is perceived that a large amount of energy would be required to overcome the adhesive interaction for the dispersion of the drug from the lactose surface, due to the fact that there is a strong affinity between them compared to their cohesive forces. This should be significantly modified by the introduction of MgSt to the DPI formulation.

In the beginning of the blending process, MgSt should form a molecular film which on further blending would gradually build up a particulate film. The formation of a monomolecular film of MgSt over the excipient is due to the strong adhesive interactions and decreased cohesive forces between the excipient particles<sup>3</sup>. The difference in the amount of drug deposited in the different stages of the MSLI between the Lactochem and Nanolac formulations can be attributed to a number of parameters including the difference in surface morphology and the presence of lactose fines.

As mentioned above, Lactochem having a heterogeneous surface roughness enables a range of weak and strong adhesive interaction between the drug particles and the carrier surface. Thus, particle deaggregation may occur over a wide range of energies. However, in the case of the Nanolac formulations, having a smooth surface enables strong interparticulate interactions and adhesion due to the large contact area between the drug particles and the carrier surface and thus a large amount of energy is required to detach them. The addition of MgSt, facilitates the detachment in both types of formulations via a significant reduction in interfacial interactions as a result of the low surface energy of the MgSt. It has been previously suggested that drug particles are lifted vertically off the carrier surface in dry powder formulations when exposed to a turbulent air flow<sup>12</sup>. Further investigations are now being made into whether this is actually the true mechanism<sup>13</sup>. Vainshtein et al. (1997)<sup>14</sup> and Ziskind et al. (1997)<sup>15</sup> were some of the first groups to research the kinetic movement of particles removed from a surface by drag force. Transfer of turbulent energy onto a drug particle occurs when it is exposed to a turbulent air stream. The drug particle can be removed from its carrier surface when it accumulates enough energy to overcome the adhesion force. Vainshtein et al.<sup>14</sup> found that particles underwent non-linear oscillations on the carrier surface and the pull-off force was determined by this. In turbulent air flow the drag forces are greater than the lift forces and so the removal rate of the drug particles caused by the drag force is significantly larger than that of the lift forces. Drag forces cause a particle to pivot. The easiest way for a particle to be removed is for it to pivot on two of its contact points and to lift off the third. Once in motion the particle rolls easily off its pivot points. Nanolac has a smooth surface. Budesonide particles may pivot and roll off the Nanolac surface more easily than the Lactochem surface as Lactochem does not have as



smooth a surface. Lactochem particles have active sites and passive sites. Particles adhere more strongly to active sites such as clefts or troughs. Budesonide particles adhered to the Lactochem in a cleft will be hard to remove from the surface. Air cannot flow so well in these areas and so not enough energy is created to remove the particle. However, overall, budesonide particles adhere less strongly to the Lactochem surface than the Nanolac surface. Adhesion force is proportional to the true area of contact between particle and surface<sup>16</sup>.

When MgSt is used in formulations, it coats the carrier surface and evens out peaks and troughs to create a smoother surface. It also decreases the adhesion forces as mentioned previously. Adding MgSt to a formulation may therefore increase the number of budesonide particles removed from the lactose carrier as less energy is required to remove them and they are freer to roll off the smoother surface. Moreover, the findings of this work were in accordance with the findings of the study performed by Lord et al (1996)<sup>17</sup> who found that the inclusion of lactose fines in carrier-based formulations resulted in decreasing adhesion between the drug particles and carrier surface, therefore requiring a small amount of energy to detach the drug particles leading to an increased aerosol deposition performance. As the data from this study suggest the Lactochem formulations which contained intrinsic lactose fines had a higher aerosol deposition performance from the control up to the 0.25% w/w MgSt formulation. This could be explained by reference to the work of Hersey (1975)<sup>7</sup> on the interactions between coarse and fine particles in the formation of ordered mixtures which proposed that fine particles preferentially bind to areas of high energy (active sites) on the surface of the carrier, leading the drug particles to bind to areas with lower energy. Once aerosolised, the drug particles are more easily detached from the surface of the carrier, increasing the proportion of drug available for inhalation. Therefore, carriers containing greater proportions of intrinsic lactose fines give better aerosol deposition performance, which can be decreased by their removal. However, the optimum concentration of fines for the greatest aerosol performance is unclear and further studies need to be conducted.

In addition, studies have shown that the addition of fine particles to binary mixtures of drug and lactose resulted in an increase in the fine particle fraction of the drug<sup>10,18,19</sup>. One of the reasons for the increase in fine particle fraction was the formation of multiplets of drug and the fine force and thus easier detachment of drug from the surface of the fine particles<sup>20</sup>. This could be the main reason for the best aerosolisation efficiency observed with the addition of 0.25% MgSt in the Lactochem formulations.

In a dry powder inhaler formulation, an ideal carrier should have a suitable surface topography; a surface on which the adhesion forces between carrier and drug is strong enough for drug particles to be attached and emitted from the inhaler, yet such that a large proportion of the emitted dose can subsequently detach from the carrier upon inhalation<sup>20</sup>. Addition of fine lactose to the powder formulations may result in the formation of mono- or multi-layers of the fine lactose adhered to the coarse lactose, filling of surface crevices and saturation of the strong binding sites on the coarse lactose. Therefore, fine particles of lactose would be expected to reduce the interparticulate forces between the drug and the coarse carrier and consequently enhance the detachment of the drug from the carrier thereby improving the FPF of the drug<sup>21</sup>.

The addition of MgSt to the formulations in theory produced a layer over the carrier and drug particles, as previously mentioned. When the amount of MgSt is sufficient, the coverage of the carrier surface with this layer is complete, therefore further reducing the adhesive force between the drug particles and carrier surface, increasing their detachment and deposition to the lungs.

From the discussion above, it is clear that the interparticulate interactions between the various types of particles present in a carrier-based DPI formulation are critical in determining the overall aerosol performance. In addition, the presence of intrinsic fines in the carrier surface of the Lactochem played a significant role in the aerosolisation performance. This is explained by the 'active site' theory as mentioned above. This hypothesis is in accordance with the data by which a larger drug deposit is observed with the Lactochem formulations compared to the Nanolac formulations.

Therefore, it could be suggested that by the addition of 0.25% w/w MgSt in the Lactochem formulations the interparticulate forces are balanced resulting in an optimised dry powder inhalation system with respect to delivered fine particle dose. However, in the Nanolac formulations the addition of 0.5% w/w MgSt results in balanced interparticulate forces. The relationship between the concentration of MgSt and aerosolisation efficiency can be attributed to the balance of interparticulate forces acting between the individual particulates.

### **3.5 Conclusion**

The influence of different concentrations of MgSt on the aerosol deposition performance of two types of carrier based formulations was investigated. The addition of MgSt to the formulations has improved the aerosol deposition performance of all the formulations except the 1.0% w/w MgSt formulation with Lactochem which had a decreased aerosol deposition performance. As mentioned previously, MgSt reduces the adhesion forces between the drug particles and the carrier surface, facilitating their detachment and entry into the respiratory tract.

However, excessive MgSt will decrease the adhesion forces to such an extent that there is virtually no interaction between the drug particles and the carrier surface and drug particles exist as loose agglomerates falling off the surface of the excipient and being captured at the early stages of the MSLI. Among the Lactochem formulations the optimum concentration of MgSt for the best aerosol deposition performance is 0.25% w/w since it greatly increased the fine particle fraction. It could be that this specific concentration of MgSt is the optimal for the application of a continuous thin film of MgSt around the surface, exerting an efficient delivery of drugs to the lungs.

Among the Nanolac formulations, the 0.5% w/w MgSt formulation exerted the best aerosol deposition performance. This difference between Nanolac and Lactochem formulations could be attributed to their surface morphology. Nanolac has stronger adhesion forces between the drug particles and the carrier surface due to the large contact area and therefore

a larger amount of MgSt is required to achieve the same reduction of adhesion forces as with the lactochem formulations.

Several recent patents have been registered on using MgSt in dry powder formulations such as by Staniforth (2002)<sup>22</sup>. This concept is being researched and developed. Chan et al. (2003)<sup>23</sup> reviewed all of the current techniques being applied to improve dry powder aerosol delivery. They found that the use of MgSt did improve dry powder formulations. The results from this study are highly significant and should be investigated further so that in the near future there may be a licensed dry powder inhaler formulation available which delivers a much higher fine particle fraction of active drug to the patient. This may mean that a lower dose of drug with a narrow therapeutic index will be needed to elicit a response in the patient than is currently used, which would mean fewer side effects for the patient. Dry powder inhalation formulations may be developed for systemic diseases if a high fine particle fraction is achieved leading to novel clinical treatments for many difficult to treat diseases.

### 3.6 References

1. Louey M.D, Razia S, Stewart P.J, “Influence of physico-chemical carrier properties on the in vitro aerosol deposition from interactive mixtures”, *International Journal of Pharmaceutics* 2003;252:87-98.
2. Begat P, Price R, Harris H, Morton D.A.V, Staniforth J.N, “The influence of force control agents on the cohesive-adhesive balance in dry powder inhaler formulations”, *KONA* 2005;23:109-119.
3. Staniforth J.N, “Powders comprising anti-adherent materials for use in dry powder inhalers”, Vectura Ltd, 2002.
4. El-Sabawi D, Price R, Edge S, Young P.M, “Novel temperature controlled surface dissolution of excipient particles for carrier based dry powder inhaler formulation”, *Drug Development and Industrial Pharmacy* 2006;32:243-251.
5. Copley scientific catalogue [Online] available at <http://www.copleyscientific.co.uk/copleycatalogue.asp>
6. Taylor K.M.G, Pancholi K, Wong D.Y.T, “In-vitro evaluation of dry powder inhaler formulations of micronized and milled nedocromil sodium”, *Pharm Pharmacol Commun* 1999;5:255-257.
7. Hersey J.A, “Ordered mixing: a new concept in powder mixing practice”, *Powder Technology* 1975;11:41-44.
8. Ganderton D, “The generation of respirable clouds from coarse powder aggregates”, *Journal of Biopharmaceutical Sciences* 1992;3:101-105.
9. Kawashima Y, Serigano T, Hino T, Yamamoto H, Takeuchi H, “Effect of surface morphology of carrier lactose on dry powder inhalation property of pranlukast hydrate”, *International Journal of Pharmaceutics* 1998;172:179-188.
10. Zeng X.M, Martin G.P, Marriott C, Pritchard J, “Lactose as a carrier in dry powder formulations: The influence of surface characteristics on drug delivery”, *Journal of Pharmaceutical Sciences* 2001;90:1424-1434.
11. Heng P.W.S, Chan L.W, Lim L.T, “Quantification of the surface morphologies of lactose carriers and their effect on the in vitro deposition of salbutamol sulfate”, *Chemical Pharmaceutical Bulletin* 2000;48:393-398.

12. Reeks M.W, Reed J.R, Hall D, "The resuspension of small particles by a turbulent flow", *Journal of Physics* 1988;D21:574-589.
13. Reeks M.W, Hall D, "Kinetic models for particles resuspension in turbulent flows: theory and measurement", *Journal of Aerosol Science* 2001;32:1-31.
14. Vainshtein P, Ziskind G, Fichman M, Gutfinger C, "Kinetic model of particle resuspension by drag force", *Physical Review Letters*, The American Physical Society 1997;78:551.
15. Ziskind G, Fichman M, Gutfinder C, "Adhesion moment model for estimating particle detachment from a surface", *Journal of Aerosol Science* 1997;28:623-634.
16. Podzeck F, "The relationship between physical properties of lactose monohydrate and the aerodynamic behaviour of adhered drug particles", *International Journal of Pharmaceutics* 1998;160:119-130.
17. Lord J.D, Staniforth J.N, "Particle size effects on packing and dispersion of powders", In *Respiratory Drug Delivery V*, 1996, (Dalby R.N, Byron P.R, Farr S.J eds), p.75-84, Interpharm Press Inc.
18. Zeng X.M, Martin G.P, Tee S.K, Ghoush A.A, Marriott C, "Effects of particle size and adding sequence of fine lactose on the deposition of salbutamol sulfate from a dry powder formulation", *International Journal of Pharmaceutics* 1999;182:133-144.
19. Lucas P, Anderson K, Staniforth J.N, "Protein deposition from dry powder inhalers: fine particle multiplets as performance modifiers", *Pharmaceutical Research* 1998;15:562-569.
20. Chan L.W, Lim L.T, Heng P.W.S, "Immobilization of fine particles on lactose carrier by precision coating and its effect on the performance of dry powder formulations", *Journal of Pharmaceutical Sciences* 2003;92:975-984.
21. Zeng X.M, Martin G.P, Tee S.K, Marriott C, "The role of fine particle lactose on the dispersion and deaggregation of salbutamol sulphate in an air stream in vitro", *International Journal of Pharmaceutics* 1998;176:99-110.
22. Staniforth J.N, Harris H, Morton D.A.V, Bannister, R, "Pharmaceutical compositions for inhalation containing magnesium stearate", WO World 2002 IPO 0243702 A2.
23. Chan H.K, Chew N.Y.K, "Novel alternative methods for the delivery of drugs for the treatment of asthma", *Advanced Drug Delivery Reviews* 2003;55:793-805.

24. Islam N, Stewart P, Larson I, Hartley P, “Lactose surface modification by decantation: are drug-fine lactose ratios the key to better dispersion of salmeterol xinafoate from lactose-interactive mixtures?”, *Pharmaceutical Research* 2004;21:492-499.
25. Lambregts D, Gruben K, De Boer A.H, “Importance of the choice of lactose in combination with dry powder inhalers”, In *Drug Delivery to the Lungs* 15, 2004, London, p.157-160, The Aerosol Society.

# Chapter 4

## Effects of environmental conditions on the aerosol deposition performance of DPI formulations containing different concentrations of MgSt

### 4.1 Introduction

The primary adhesion forces acting between a particle with a carrier surface in a dry environment i.e low relative humidity, consist of van der Waals and electrostatic forces. In humid environments, the condensation of water vapour leads to the introduction of a surface tensional force at relatively low humidity conditions leading to a meniscus type, capillary force at high relative humidity.<sup>1</sup> This dynamic force has been shown to predominate for a number of hydrophilic and hydrophobic drug particles with a lactose carrier surface and significantly increasing particle adhesion<sup>3,4</sup>.

Moisture uptake can directly affect the flowability of the powders and the force to detach the micronized particles from the carrier surface. Hence, the fine particle dose responsible for the pharmacological effect may be directly affected since the de-agglomeration properties of the powder blend will change upon storage due to moisture uptake.

A number of investigations have focused on the influence of environmental conditions on the interparticulate interactions and subsequently on the aerosolisation performance of inhalation systems. Young *et al.* (2003)<sup>1</sup> investigated the influence of humidity on the aerosolisation of three micronized drugs: disodium cromoglycate (DSCG), salbutamol sulphate and triamcinolone acetonide (TAA); which were stored for 12 hours at 15, 30, 45, 60 and 75% RH. A decrease in the fine particle fraction (FPF) for both DSCG and salbutamol sulphate was observed with increasing humidity, suggesting that the adhesion properties for both drugs are predominately influenced by capillary interactions. However,



the FPF of TAA significantly increased as the humidity increased over the range 15% to 75%RH, suggesting that tribology induced electrostatic forces predominated interparticulate interactions<sup>5</sup>. Young *et al.*, (2004)<sup>2</sup> also reported the effect of storage humidity on the aerosolisation efficiency of salbutamol sulphate produced *via* micronization and supercritical fluid (SEDS) particle engineering. It was shown that storage humidity had a significant effect on the aerosolisation efficiency of formulations comprised of both micronised and SEDS salbutamol sulphate suggesting again that capillary interactions play an important factor in DPI formulation performance. Jashnani *et al.*, (1995)<sup>6</sup> have also investigated the dry powder aerosol performance of salbutamol base and salbutamol sulphate under different temperatures and relative humidities (20, 30 and 45°C; 30-95% RH). The FPF for both salbutamol base and salbutamol sulphate decreased with increasing relative humidity at any given temperature with more profound changes observed at higher temperatures. Increasing temperature also resulted in diminished aerosol performance.

With the introduction of a hydrophobic force control agent (e.g MgSt) to a carrier based DPI formulation, its role as a protectant from storage conditions particularly as a function of variations in relative humidity is a key. In addition, there is a need to define specific ranges of temperature and humidity for the testing of DPI formulations as well as for the proper storage of medication to prevent instability and degradation of the formulation.

In this study, the formulations prepared in Chapter 3, with different concentrations of MgSt blended under shear, were tested with a MSLI upon being stored for 3 months at pre-defined temperature and humidity, to investigate the specific role of MgSt as a hydrophobic agent and its concentration on aerosol deposition. The formulations were tested at three different environmental conditions; firstly at 25°C, 44% RH tested immediately after their preparation (as described in Chapter 2), and then after 3 months stored at 25°C, 75% RH and 40°C, 75% RH to examine how these environmental factors and time affect the aerosol deposition performance of the DPI formulations.

## **4.2 Materials**

$\alpha$ -Lactose monohydrate (Lactochem<sup>®</sup>) was supplied by Friesland Foods (Borculo, Netherlands). The lactose was vibrated through a nest of sieves to obtain 63-90  $\mu$ m sieve fraction, which was used throughout the study. Micronised budesonide was supplied by Sicor (Batch no. 6157/M1, Santhia, Italy). Ten percent etched lactose (Nanolac) was produced according to the procedure described in Chapter 3, Section 3.3.3 outlined by El-Sabawi et al. (2006)<sup>7</sup>. Magnesium stearate was supplied by Fisher chemicals (Batch no. 9880836, Loughborough, UK). The acetonitrile and methanol were of HPLC grade and were obtained from Fisher Scientific (Loughborough, UK). Water was purified by reverse osmosis (MilliQ, Millipore, Molsheim, France). Hydroxypropyl methylcellulose (HPMC) capsules (size 3) were supplied by Qualicaps (Batch no. EO404632, Shiongi Qualicaps, Madrid, Spain). Potassium carbonate anhydrous was supplied by Acros Organics (Batch no. A018189301, New Jersey, USA) for use as a humidifier. Ceramic balls of 10mm diameter were used.

## **4.3 Methods**

### **4.3.1 Scanning electron microscopy**

SEM was used to image the powder blends after storage, using the method described in Section 2.2.1.

### **4.3.2 Particle size analysis of aerosol cloud**

The particle size distribution of the aerosol cloud emitted from a Cyclohaler<sup>®</sup> by each of the formulations described in Chapter 3 following storage for 3 months at 25°C, 75%RH and 40°C, 75% RH were determined using a HELOS laser diffraction sensor and INHALER adapter (both from Sympatec GmbH, Clausthal-Zellerfeld, Germany). The flow rate through the INHALER module was set at 60 L/min and the mouthpiece of the Cyclohaler<sup>®</sup> was fitted directly into the measuring chamber, to enable measurement of the particle size

distribution of the aerosol cloud immediately after emission. For each measurement, a size 3 HPMC capsule filled with  $25 \pm 1$  mg of the test formulation was inserted in to the Cyclohaler<sup>®</sup>, opened by piercing the capsule and its contents aerosolised through the laser of the diffraction sensor for 10 seconds. Particle size analysis was carried out using WINDOX 4.0 software (Sympatec GmbH, Clausthal-Zellerfeld, Germany). Particles size distributions and values presented are the average of 5 determinations.

#### **4.3.3 *In vitro* aerosolisation studies**

HPMC capsules, size 3, were filled with  $25 \pm 3$  mg of the powder blends prepared as described in section 3.4.4. Ninety capsules were filled for each concentration of the blends from the same powder blend. A series of both long term and accelerated stability studies were performed. Ninety capsules of each formulation were stored in a sealed container at a relative humidity of 75% RH (prepared using saturated solution of sodium chloride<sup>7</sup>) at 40°C and of 75% RH at 25°C respectively, within temperature controlled ovens for 3 months.

The *in vitro* inhalation performance of budesonide from each blend was assessed using a MSLI (Copley Instruments Ltd, Nottingham, UK) as discussed in chapter 2, Section 2.2.3.

#### **4.3.4 Analysis of budesonide**

The budesonide was analysed using high performance liquid chromatography (HPLC), as discussed in Chapter 2, Section 2.2.5.1.

#### **4.3.5 Optical imaging of powder samples**

Digital optical images of samples of powder samples were taken using a digital camera (Samsung, China) after being stored for three months at the various environmental conditions (25°C/44%RH, 25°C/75%RH, 40°C/75%RH) investigated throughout the study.

#### **4.3.6 Statistical analysis**

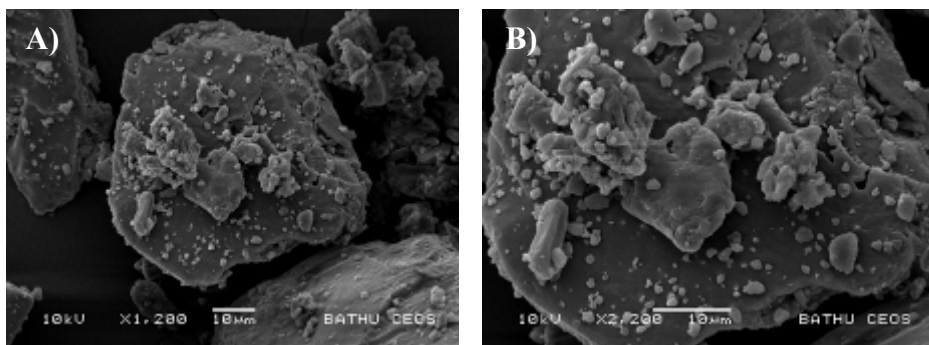
Statistical analysis of the data was carried out using Minitab for Windows. One-way ANOVA (analysis of variance) was used to determine the variance of data. Fisher's pair-wise analysis was carried out to determine where those differences were. Statistical significance was defined as either  $P < 0.05$  or  $P < 0.01$ . The levels of significance obtained are indicated in the key on individual graphs.

### **4.4 Results and Discussion**

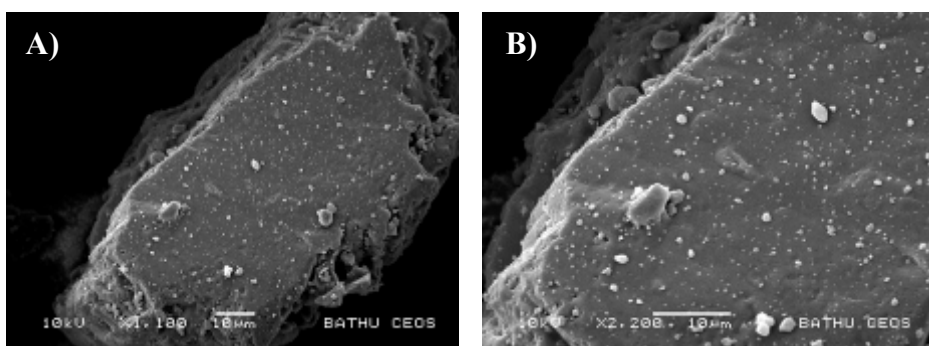
#### **4.4.1 Scanning electron microscopy**

Scanning electron microscopy images of the various blends upon storage at elevated temperature and/or relative humidity are shown in figures 4.1-4.8. The SEMs showed a considerable degree of powder clustering and agglomeration at high humidities with significant agglomeration at the highest humidity used in this study (40°C, 75%RH). The Lactochem formulations showed a more pronounced agglomerations than the Nanolac formulations. Such physical interaction and agglomeration may be an indication of a considerable increase in inter-particle adhesion arising from the condensation of water vapour at high RH levels, as a consequence promoting the formation of a capillary meniscus around the contact points of contiguous surfaces. A similar behaviour was observed at 25°C, 75%RH, although the degree of agglomeration may have been less.

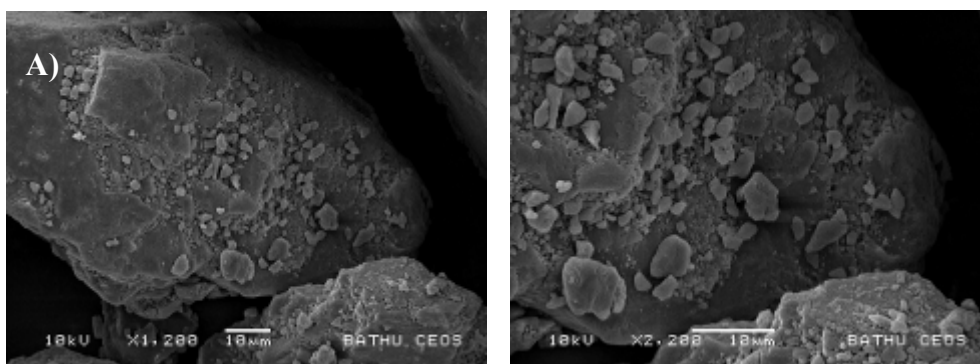
The agglomeration was more profound for the Lactochem formulations than the Nanolac formulations when stored at 25°C, 75%RH. However, both types of formulations exhibited a high degree of agglomeration when stored at 40°C, 75%RH. The SEMs of the Lactochem formulations at 40°C, 75%RH show respirable sized drug particles adhering to a larger, excipient particles whereas the Nanolac formulations show a number of agglomerates of respirable sized particles.

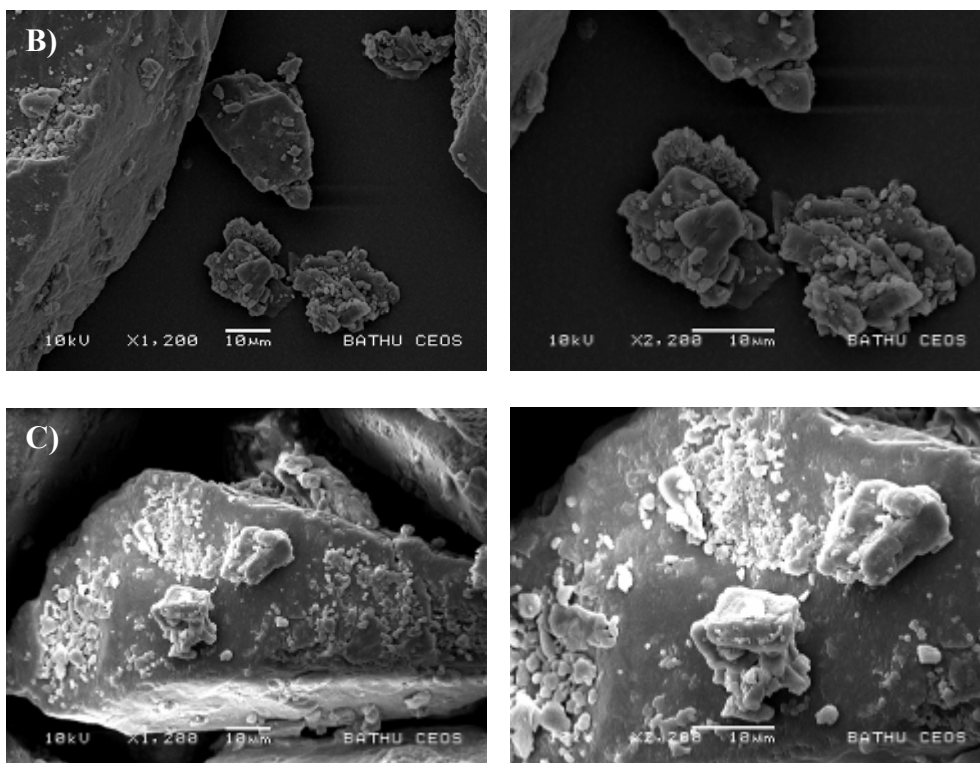


*Figure 4.1 Representative scanning electron micrographs showing the control formulation at 25°C, 75%RH containing Lactochem and budesonide at A) x1200 and B) x2200 magnifications.*

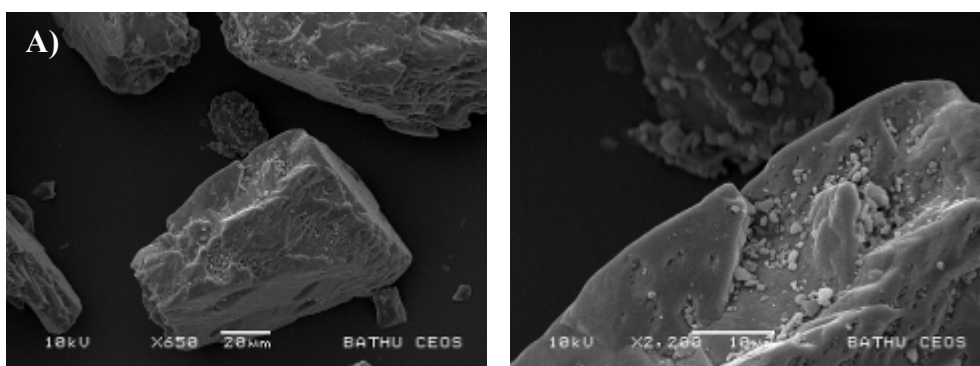


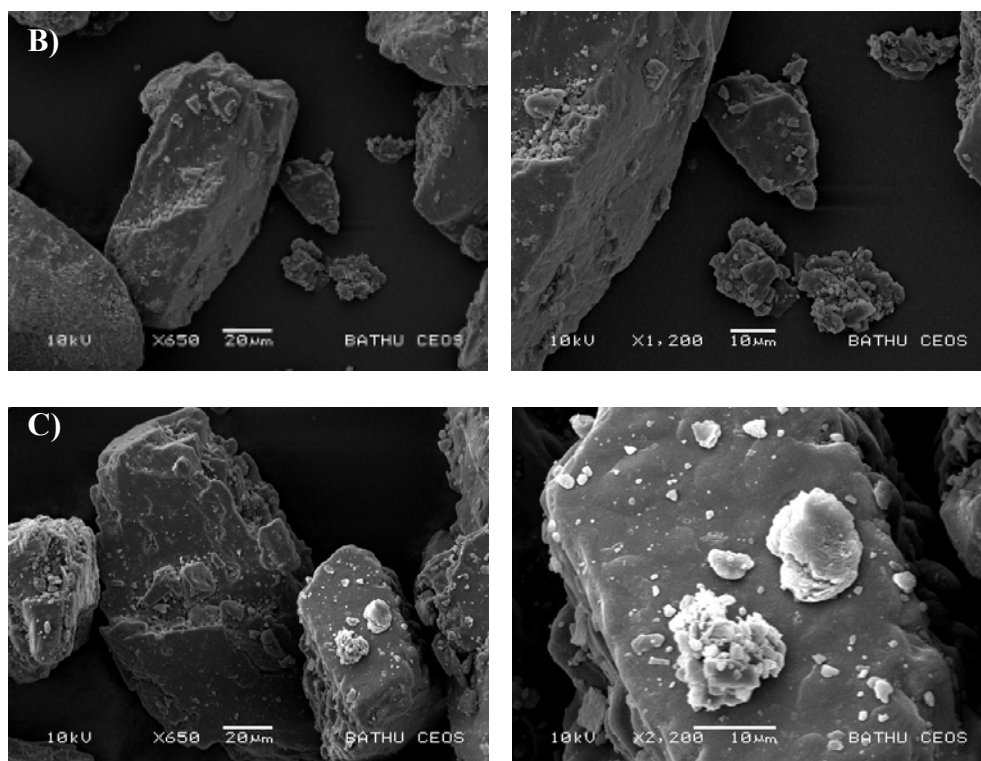
*Figure 4.2 Representative scanning electron micrographs showing the control formulation at 25°C, 75%RH containing Nanolac and budesonide at A) x1200 and B) x2200 magnifications.*



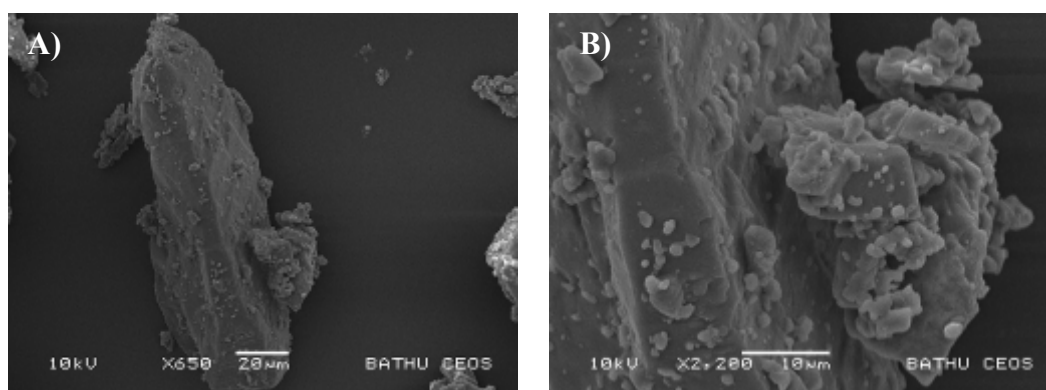


***Figure 4.3 Representative scanning electron micrographs of the formulations containing Lactochem and budesonide pre-conditioned with A) 0.25%, B) 0.5% and C) 1.0% w/w MgSt at 25°C, 75%RH.***

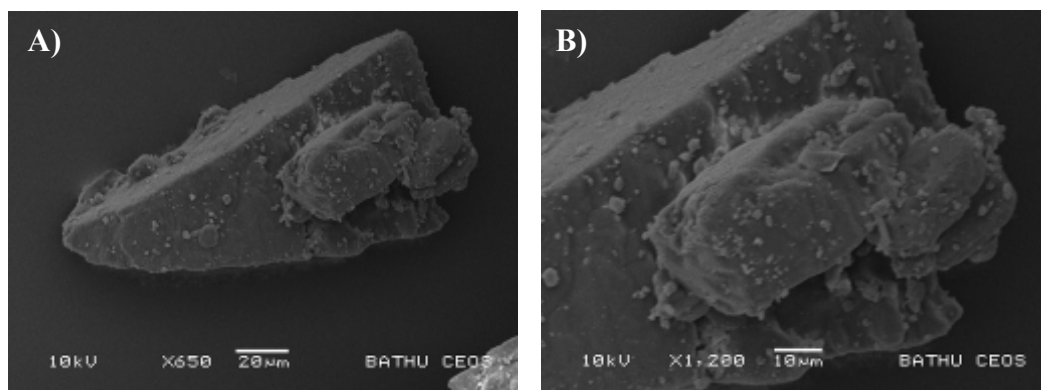




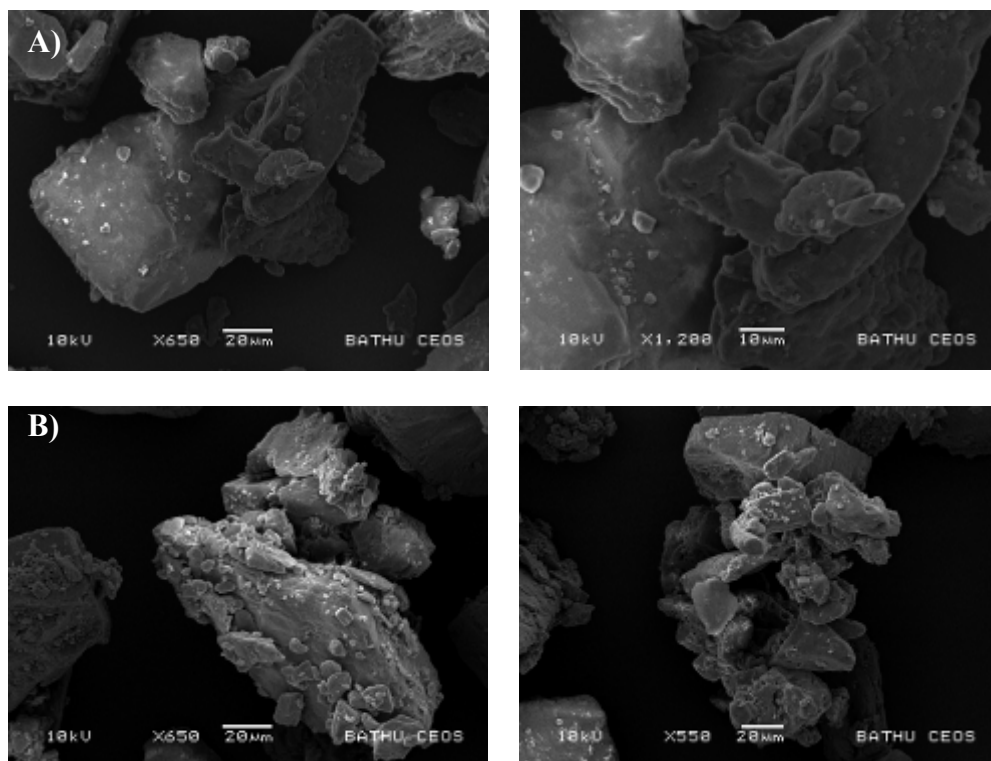
**Figure 4.4** Representative scanning electron micrographs of the formulations containing Nanolac and budesonide pre-conditioned with A) 0.25%, B) 0.5% and C) 1.0% w/w MgSt at 25°C, 75%RH.



**Figure 4.5** Representative scanning electron micrographs showing the control formulation at 40°C, 75%RH containing Lactochem and budesonide at A) x650 and B) x2200 magnifications.



*Figure 4.6 Representative scanning electron micrographs showing the control formulation at 40°C, 75%RH containing Nanolac and budesonide at A) x650 and B) x1200 magnifications.*





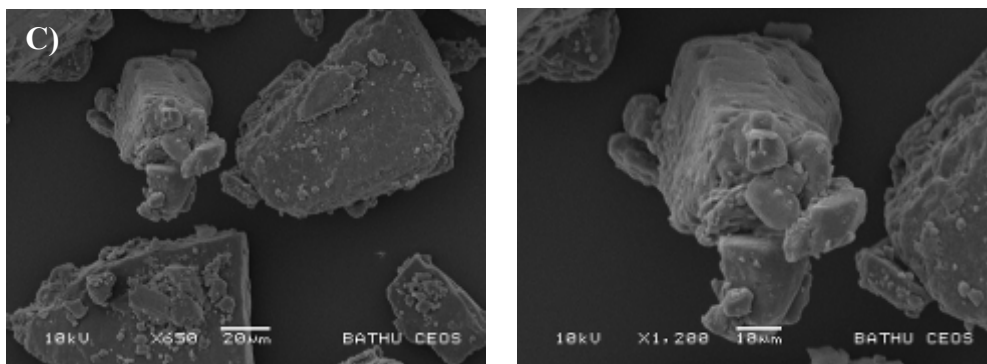


**Figure 4.7** Representative scanning electron micrographs of the formulations containing Lactochem and budesonide pre-conditioned with A) 0.25%, B) 0.5%, C) 1.0% w/w MgSt at 40°C, 75%RH.

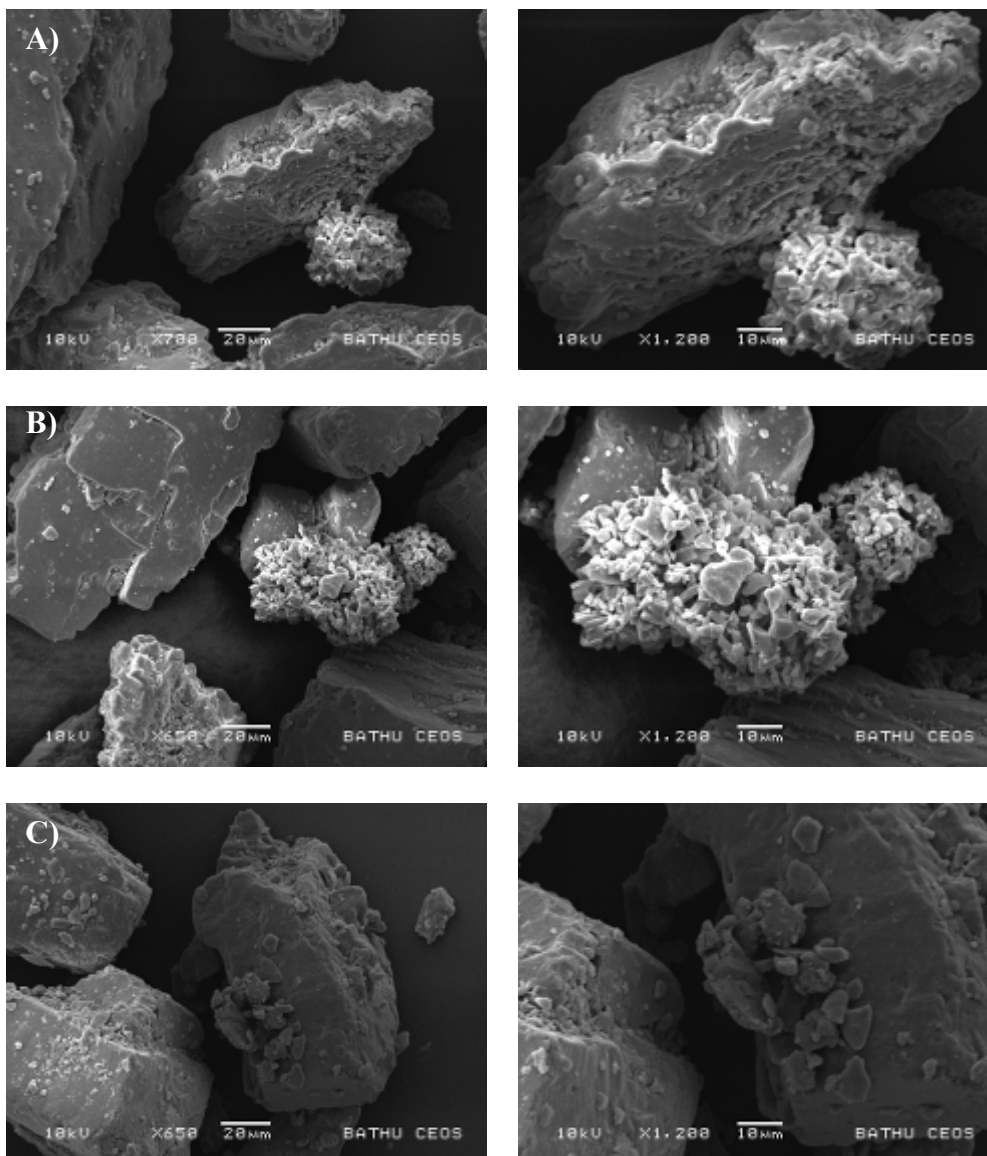


***Figure 4.8 Representative scanning electron micrographs of the formulations containing Nanolac and budesonide pre-conditioned with A) 0.25%, B) 0.5%, C) 1.0% w/w MgSt at 40°C, 75%RH.***

#### **4.4.2 Particle size analysis**

The particle size distribution of the Lactochem and Nanolac formulations upon storage at 25C, 75% RH are shown in tables 4.1 and 4.2 respectively. As shown in the tables below, no significant difference in the coarse particle size measurements  $d_{50}$  and  $d_{90}$  can be seen with storage. However, these data suggest that there is an influence on the smaller particle size measurements ( $d_{10}$ ) as upon introducing 0.25% w/w MgSt to the Lactochem and Nanolac formulations there was a decrease of 50% of the fines. In addition, the number of particles with a diameter of  $< 5 \mu\text{m}$  were doubled upon introducing the 0.25% w/w MgSt, while the number of particles with a diameter  $< 10 \mu\text{m}$  was also increased. While for the 0.5 % and 1.0% MgSt and Lactochem formulations the  $d_{10}$  values and particles  $< 5 \mu\text{m}$  were almost the same as the control formulations, with the Nanolac formulations the  $d_{10}$  values for all the concentrations of MgSt were significantly lower than the control Nanolac formulation and the particles  $< 5 \mu\text{m}$  were significantly higher than the control formulation. It is also interesting to note in table 4.2, that with the Nanolac formulation upon increasing the concentration of MgSt, the  $d_{10}$  particles are decreased while the particles  $< 5 \mu\text{m}$  are increased. The data could suggest that by using the Nanolac lactose, more fines with a smaller particle size are being added to the formulation.

**Table 4.1 Particle size distribution statistics summary of the Lactochem formulations at 25°C, 75%RH.**

<b>Materials At 25°C, 75%RH</b>	<b>d10 (µm ± SD)</b>	<b>d50 (µm ± SD)</b>	<b>d90 (µm ± SD)</b>	<b>% &lt; 10 µm (µm ± SD)</b>	<b>% &lt; 5 µm (µm ± SD)</b>
Lactochem+budesonide	7.81±1.01	58.88±9.14	116.11±7.49	13.51±1.98	6.06±0.78
0.25% MgSt +Lactochem+budesonide	4.77±1.63	62.63±9.05	122.83±2.63	19.58±7.12	12.05±4.34
0.5% MgSt + Lactochem+budesonide	8.05±1.61	69.38±9.36	117.31±8.70	12.49±1.91	6.47±1.17
1.0% MgSt + Lactochem+budesonide	8.25±2.60	63.48±5.30	120.08±5.41	13.37±2.81	5.68±1.12

**Table 4.2 Particle size distribution statistics summary of the Nanolac formulations at 25°C, 75%RH.**

<b>Materials At 25°C, 75%RH</b>	<b>d10 (µm ± SD)</b>	<b>d50 (µm ± SD)</b>	<b>d90 (µm ± SD)</b>	<b>% &lt; 10 µm (µm ± SD)</b>	<b>% &lt; 5 µm (µm ± SD)</b>
Nanolac+budesonide	45.43±4.26	89.92±1.84	130.14±3.44	5.46±0.79	3.91±0.53
0.25% MgSt + Nanolac +budesonide	28.05±8.77	89.48±1.41	130.42±2.38	8.49±1.92	6.54±1.77
0.5% MgSt + Nanolac +budesonide	27.09±3.59	89.18±1.41	127.60±2.97	9.42±1.70	7.02±1.30
1.0% MgSt + Nanolac +budesonide	30.40±12.41	92.53±2.15	136.30±2.92	8.49±2.85	6.31±1.90

The particle size distribution of the Lactochem and Nanolac formulations upon storage at 40°C, 75%RH, have similar findings as with the formulations stored at 25°C, 75%RH. As can be seen in table 4.3, the addition of 0.25% w/w MgSt to the Lactochem formulation, decreases the value of d<sub>10</sub> and significantly increases the particles < 5 µm. However, a different effect was observed for the Nanolac formulations upon storage at 40°C, 75%RH (Table 4.4). Upon addition of 0.25% MgSt, no change was observed on the d<sub>10</sub> but gets to the lowest value upon addition of 0.5% MgSt, which then slightly increases at 1.0% MgSt. The particles < 5 µm are slightly increased upon addition of 0.25% MgSt, reaching the highest value at 0.5% MgSt and then decreases again upon addition of 1.0% MgSt.

**Table 4.3 Particle size distribution statistics summary of the Lactochem formulations at 40°C, 75%RH.**

<b>Materials At 40°C, 75%RH</b>	<b>d<sub>10</sub> (µm ± SD)</b>	<b>d<sub>50</sub> (µm ± SD)</b>	<b>d<sub>90</sub> (µm ± SD)</b>	<b>% &lt; 10 µm (µm ± SD)</b>	<b>% &lt; 5 µm (µm ± SD)</b>
Lactochem+budesonide	13.15±1.78	63.12±7.10	145.06±5.21	7.42±0.87	2.88±0.32
0.25%MgSt+Lactochem +budesonide	9.91±3.92	58.42±9.87	111.34±5.74	11.61±1.43	8.80±1.31
0.5% MgSt +Lactochem +budesonide	12.52±1.82	86.00±5.69	141.87±7.52	8.73±1.44	4.35±0.77
1.0% MgSt +Lactochem +budesonide	9.79±2.66	70.02±5.61	128.79±9.65	10.88±2.12	4.75±0.84

**Table 4.4 Particle size distribution statistics summary of the Nanolac formulations at 40°C, 75%RH.**

<b>Materials At 40°C, 75%RH</b>	<b>d<sub>10</sub> (µm ± SD)</b>	<b>d<sub>50</sub> (µm ± SD)</b>	<b>d<sub>90</sub> (µm ± SD)</b>	<b>% &lt; 10 µm (µm ± SD)</b>	<b>% &lt; 5 µm (µm ± SD)</b>
Nanolac+budesonide	51.55±2.83	91.23±2.66	140.67±2.88	1.89±0.63	1.31±0.48
0.25% MgSt + Nanolac +budesonide	51.14±2.20	90.65±2.17	141.16±2.01	2.80±0.89	1.90±0.61
0.5% MgSt + Nanolac +budesonide	34.03±3.39	91.65±1.32	137.64±1.19	7.71±1.42	5.70±1.09
1.0% MgSt + Nanolac +budesonide	46.07±4.13	88.19±2.15	144.29±2.28	4.07±0.93	2.62±0.55

#### **4.4.3 In vitro aerosolisation studies**

##### **4.4.3.1 The influence of storage conditions on the in vitro aerolisation performance of Lactochem and Nanolac formulations.**

As shown in Figure 4.9a of the stage-by-stage deposition within the MSLI there is an increase in the capsules/device retention and upper stages of the impinger upon storage, indicating a relative decrease in amount of the dose actually entering the lower stages of the MSLI. The retention of drug in the capsules and device and upper stages of the MSLI may be due to the increased cohesiveness and adhesiveness of the drug upon storage at elevated temperature and humidity, reducing the detachment of the drug particles from the carrier surface. This increase in interparticulate interaction could be due to the increase in capillary forces which arises from the condensation of the increasingly adsorbed water vapour layers onto the surface at high RH levels and promoting the formation of a capillary meniscus around the contact points of contiguous surfaces<sup>2</sup>. Another possible explanation could be the re-crystallization of amorphous domains at conditions of elevated RH levels leading to irreversible aggregation through solid bridge formation which can affect aerosol generation and lung deposition performance<sup>8,9</sup>. There was no significant statistical difference between the amount of drug deposited at the capsules and device stage between the different environmental conditions. However, there was a significant increase (ANOVA  $p < 0.05$ ) in the amount of drug deposited at the throat and stage 1 upon storage at 25°C, 75%RH compared to the formulation stored at 25°C, 44%RH, with a larger significant increase (ANOVA  $p < 0.01$ ) upon storage of the formulation at 40°C, 75%RH. No significant difference was observed on the amount of drug deposited at stages 2 and 3 of the MSLI apparatus between the different environmental conditions. However, there was a significant reduction (ANOVA  $p < 0.05$ ) of the drug deposition at stage 4 upon storage at 25°C, 75%RH compared to the amount of drug deposited by the formulation stored at 25°C, 44%RH. The significant decrease (ANOVA  $p < 0.01$ ) in the amount of drug deposited in stage 4 upon storage at 40°C, 75%RH was half the value of the amount of drug deposited by the formulation stored at 25°C, 44%RH. This was due to the fact that most of the drug was captured at

the initial stages of the MSLI apparatus with huge losses in the capsules and device stage and throat and s1 stage. The formulations at both environmental conditions (25°C, 75%RH and 40°C, 75%RH) exerted a significant decrease (ANOVA  $p<0.01$ ) in the drug deposition in the filter stage of the MSLI compared to the formulation stored at the ambient conditions. The drug deposition was remarkably reduced to the 1/5<sup>th</sup> of the amount of drug deposited by the formulation stored at ambient conditions. Therefore, the data suggests that the environmental conditions have greatly influenced the aerosol deposition performance of the Lactochem control formulation.

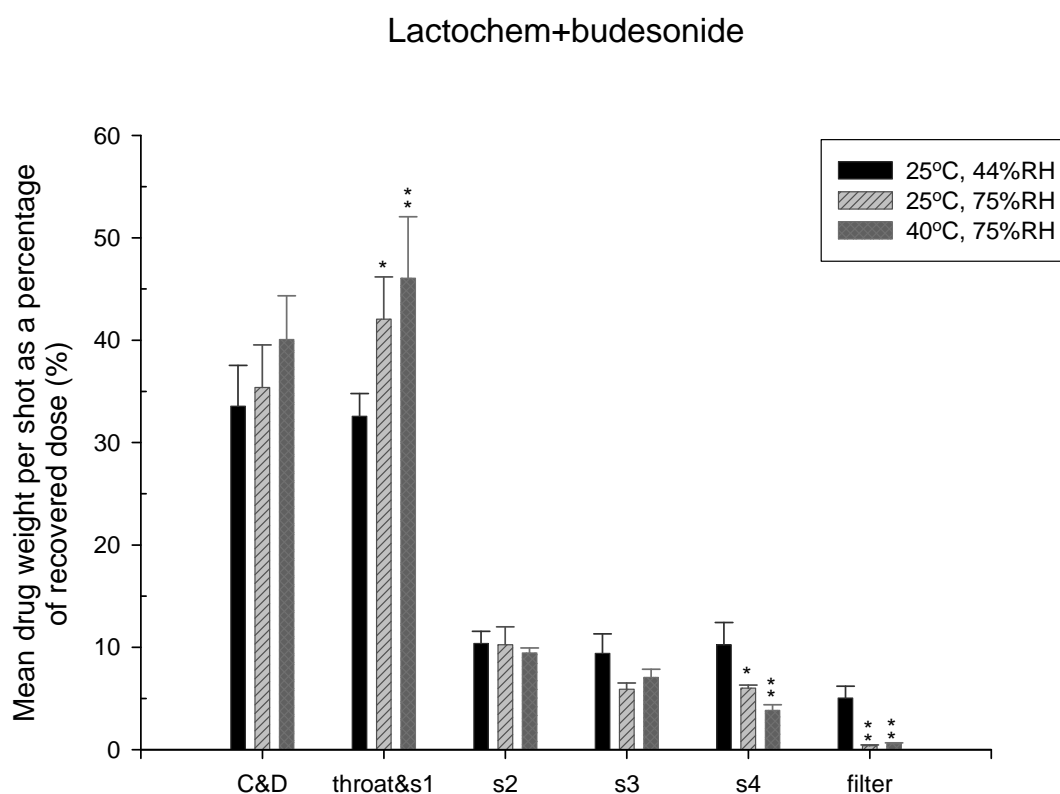


**Figure 4.9a** The deposition of budesonide, as a percentage of recovered dose throughout the MSLI for the Lactochem control formulations at the different environmental conditions.

(Mean  $\pm$  S.D,  $n=3$ , \*  $P<0.05$ , \*  $P<0.01$ : significant difference compared to the ambient conditions by ANOVA one-way. C & D: capsules & device)

## Nanolac+budesonide

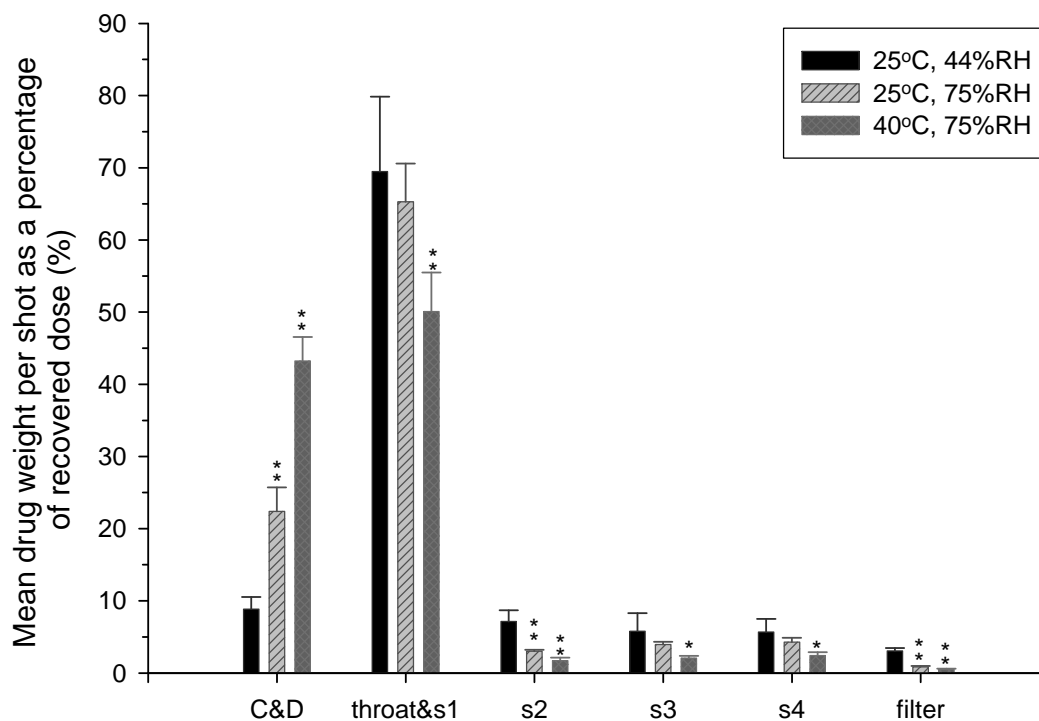


**Figure 4.9b** The deposition of budesonide, as a percentage of recovered dose, throughout the MSLI for the Nanolac control formulation at the different environmental conditions. (Mean  $\pm$  S.D,  $n=3$ , \*  $P<0.05$ , \*  $P<0.01$ : significant difference compared to the ambient conditions by ANOVA one-way. C & D: capsules & device)

Figures 4.9a and 4.9b show the stage-by stage deposition profile of the Lactochem and Nanolac formulations respectively upon storage. The drug retention in the capsule/device upon storage at both elevated environmental conditions was significantly higher (ANOVA  $p<0.01$ ) than the control, with a 15% and 35% increase in the drug deposited, respectively, compared to the drug deposited by the formulation stored at 25°C, 44%RH. These data suggested that the environmental conditions significantly affected the drug deposition in the capsules and device. The increase in drug deposition in the capsules and device stage

may subsequently lead to a small drug deposition in the following stages of the MSLI. Interestingly, upon storage of the formulation at 40°C, 75%RH the amount of drug deposited in the throat and stage 1 was significantly reduced (ANOVA  $p < 0.01$ ), compared to the amount of drug deposited by the formulation stored at the ambient conditions, while no significant difference was observed upon storage of the formulation at 25°C, 75%RH. The amount of drug deposited in stage 2 upon storage of the formulations at the elevated conditions was significantly reduced (ANOVA  $p < 0.01$ ) to half the value of that of the formulation stored at the ambient conditions. In stage 3 and stage 4, only the storage of the formulation at 40°C, 75%RH resulted in a significantly lower drug deposition (ANOVA  $p < 0.05$ ). Upon storage of the formulations at both elevated conditions, the amount of drug deposited in the filter stage was significantly lower (ANOVA  $p < 0.01$ ).

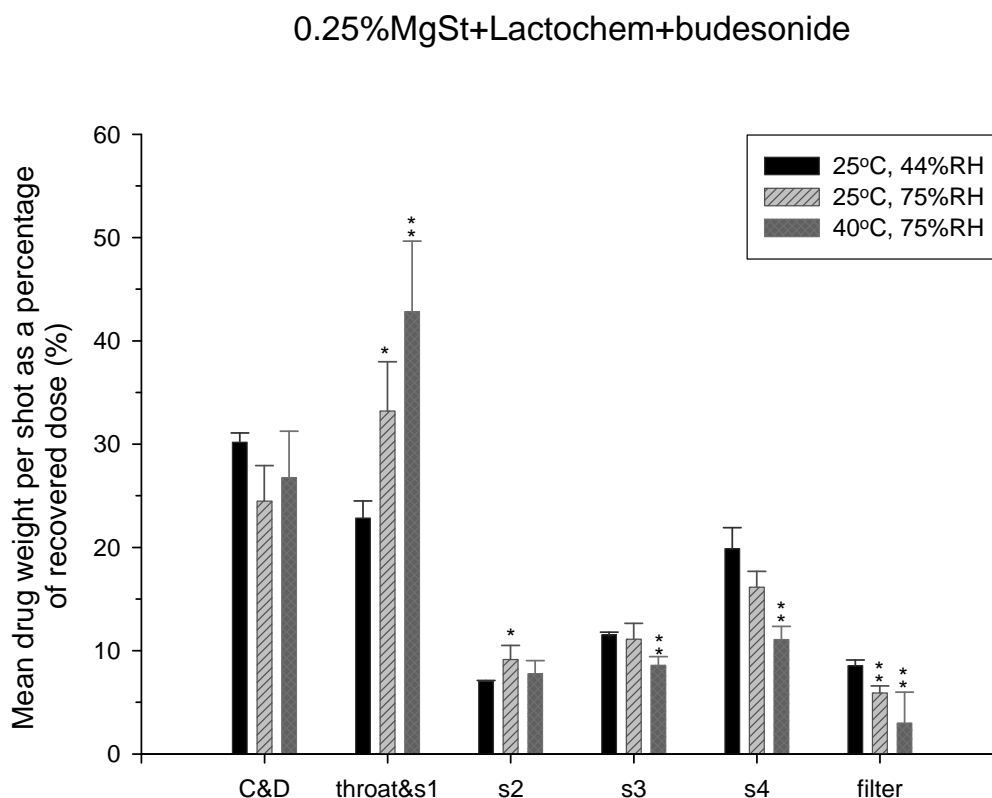


**Figure 4.10a** The deposition of budesonide, as a percentage of recovered dose, throughout the MSLI for the 0.25% w/w MgSt+Lactochem+budesonide formulation



at the different environmental conditions. (Mean  $\pm$  S.D, n=3, \*  $P<0.05$ , \*  $P<0.01$ : significant difference compared to the ambient conditions by ANOVA one-way. C & D: capsules & device)

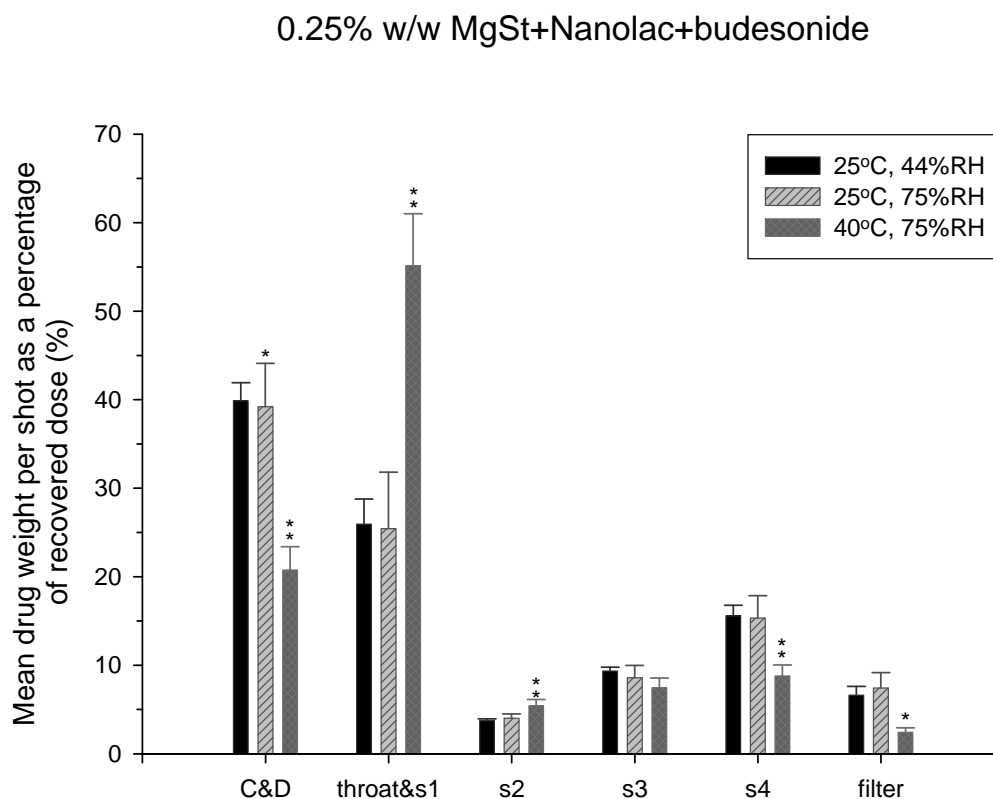


**Figure 4.10b** The deposition of budesonide, as a percentage of recovered dose, throughout the MSLI for the 0.25% w/w MgSt+Nanolac +budesonide formulation at the different environmental conditions. (Mean  $\pm$  S.D, n=3, \*  $P<0.05$ , \*  $P<0.01$ : significant difference compared to the ambient conditions by ANOVA one-way. C & D: capsules & device)

#### **4.4.3.2 The influence of storage conditions on the in vitro aerolisation performance of 0.25% w/w MgSt formulations**

The addition of 0.25% w/w MgSt to the Lactochem and budesonide formulation, the amount of drug deposited in the capsules and device stage was reduced upon storage at 25°C, 75%RH and 40°C, 75%RH compared to the same formulation stored at 25°C, 44%RH. However, the reduction of the amount of drug deposited was not statistically significant. In addition, a smaller amount of drug remains in the capsule and device compared to the Lactochem control formulation, indicating that a higher emitted dose of the drug via the addition of MgSt. A significant increase (ANOVA  $p < 0.05$ ) in the amount of drug deposited in the throat and stage 1 upon storage of the formulation at 25°C, 75%RH was measured to with respect to the storage of the 0.25% MgSt formulation at 25°C, 44%RH. A further significant increase (ANOVA  $p < 0.01$ ) in the amount deposited that the upper stage was observed upon storage of the formulation at 40°C, 75%RH. A significant increase (ANOVA  $p < 0.05$ ) in the amount of drug deposited in stage 2 was also determined for the storage at 25°C, 75%RH compared to the formulation stored at 25°C, 44%RH. There was no significant difference upon storage of the formulation at 40°C, 75%RH. Upon storage of the formulation at 40°C, 75%RH, the amount of drug deposited in stages 3 and 4 of the MSLI was significantly reduced (ANOVA  $p < 0.01$ ), while the amount of drug deposited by the formulation stored at 25°C, 75%RH exhibited no significant difference. The amount of drug deposited in the filter stage of the MSLI from the formulations stored at elevated environmental conditions was significantly reduced (ANOVA  $p < 0.01$ ) compared to the amount of drug deposited in the filter stage by the formulation stored at 25°C, 44%RH.

As shown in figures 4.10a and 4.10b for the stage-by-stage deposition of the addition of 0.25%w/w MgSt to nanolac and budesonide, the amount of drug deposited in the capsules and device stage upon storage of the formulation at 25°C, 75%RH was significantly lower (ANOVA  $p < 0.05$ ), compared to the formulation stored at 25°C, 44%RH, (tables 4.5-4.6) which was further significantly reduced (ANOVA  $p < 0.01$ ) upon storage at 40°C, 75%RH to half the value of the formulation upon storage at

25°C, 44%RH. These data suggest that upon storage of the formulations at the elevated environmental conditions more drug is leaving the capsules and device and entering the MSLI apparatus. While no significant difference was observed in the drug deposited in the throat and stage 1 upon storage at 25°C, 75%RH, a significant increase (ANOVA  $p<0.01$ ) was observed upon storage at 40°C, 75%RH, (tables 4.7-4.8) to a value twice that of the formulation stored at the ambient conditions. Hence, at 40°C, 75%RH there is a significant retention of drug particles to the carrier particles and thus suggesting either a considerable adhesion or the formation of solid bridges to the carrier surface at elevated temperature. Considering the significant difference between the retention on the upper stages of the MSLI for the 25°C, 75%RH and 44°C, 75%RH formulations, these data suggest that temperature may have a key influence on its variability. Upon storage of the formulation at 40°C, 75%RH, the amount of drug deposited in stage 2 of the MSLI was significantly higher (ANOVA  $p<0.01$ ) to the amount of drug deposited by the formulation stored at ambient conditions, while upon storage at 25°C, 75%RH no significant difference was observed. No significant differences were observed in the amount of drug deposited in stage 3 of the MSLI between the formulations at the different environmental conditions. In stage 4, the amount of drug deposited by the formulation stored at 40°C, 75%RH was significantly lower (ANOVA  $p<0.01$ ) compared to the amount of drug deposited by the formulation stored at 25°C, 44%RH, while there was no significant difference with the formulation stored at 25°C, 75%RH. This was expected, as the drug retention in the upper stages was greater for the formulation stored at 40°C, 75%RH. Upon storage of the formulation at 40°C, 75%RH, the amount of drug deposited in the filter stage was significantly reduced (ANOVA  $p<0.01$ ) to the amount of drug deposited by the formulation stored at the ambient conditions. There was no significant difference between the formulation stored at ambient conditions and at 25°C, 75%RH. The set conditions of 25°C, 75%RH did not have an influence on the aerosolisation performance of this formulation since the amount of drug deposited in each of the MSLI stages was not significantly different to the amount of drug deposited by the formulation stored at ambient conditions. However, upon storage of this formulation at 40°C, 75 % RH resulted in a significant decrease in aerosolisation performance.

#### **4.4.3.3 The influence of storage conditions on the in vitro aerolisation performance of 0.5% w/w MgSt formulations**

As shown in figure 4.11a, upon storage of the 0.5% w/w MgSt Lactochem formulation at 40°C, 75%RH the amount of drug deposited in the capsules and device stage was significantly reduced (ANOVA  $p < 0.05$ ), while no significant difference was observed in the drug deposition of the formulation stored at 25°C, 75%RH. In this case, the storage of the formulation at 40°C, 75%RH resulted in less drug remaining in the capsules and device and more drug entering the following stages of the MSLI. Therefore the increased humidity and temperature had a positive influence on drug retention in the capsules and device stage of this formulation. One possible cause may be due to the formation of agglomerates caused by considerable increase in inter-particle adhesion due to capillary interaction. Upon storage of the formulation at 25°C, 75%RH, the amount of drug deposited in the throat and stage 1 of the MSLI was significantly reduced (ANOVA  $p < 0.05$ ), while the amount of drug deposited by the formulation stored at 40°C, 75%RH was not significantly different to the amount of drug deposited by the formulation stored at the ambient conditions. No significant difference in the amount of drug deposited in stage 2 was observed upon storage of the formulations at the elevated environmental conditions. Furthermore, the amount of drug deposited in stage 3 of the MSLI upon storage at elevated conditions was significantly higher (ANOVA  $p < 0.05$ ) than the amount of drug deposited upon storage at 25°C, 44%RH, resulting in a larger amount of drug reaching the lower stages of the MSLI and therefore the lower airways in the RT. The amount of drug deposited in stage 4 of the MSLI upon storage of the formulations at the elevated conditions was not significantly different to the amount of drug deposited by the formulation stored at 25°C, 44%RH. Upon storage of the formulation at 25°C, 75%RH, the amount of drug deposited in the filter stage was significantly lower (ANOVA  $p < 0.05$ ) than the amount of drug deposited by the formulation stored at the ambient conditions, while the amount of drug deposited by the formulation stored at 40°C, 75%RH was not significantly different. These data suggest that the addition of 0.5% w/w MgSt to the

formulation has provided stability to the formulation over the elevated environmental conditions.

As shown in figure 4.11b for the addition of 0.5%w/w MgSt-Nanolac formulation the amount of drug deposited in the capsule and device stage upon storage at both elevated environmental conditions was not significantly different to the amount of drug deposited by the formulation stored at the ambient conditions. Upon storage of the formulation at 40°C, 75%RH the amount of drug deposited in the throat and stage 1 of the MSLI was significantly increased (ANOVA  $p<0.05$ ) compared to the amount of drug deposited by the formulation stored at 25°C, 44%RH. The amount of drug in the upper stages upon storage at 25°C, 75%RH was not significantly different to the amount of drug deposited by the formulation stored at the ambient conditions. The amount of drug deposited in stage 2 and stage 3 of the MSLI upon storage at both elevated environmental conditions was not significantly different to the amount of drug deposited by the formulation stored at the ambient conditions. The amount of drug deposited in stage 4 of the MSLI for the 25°C, 75%RH was significantly higher (ANOVA  $p<0.05$ ) than the amount of drug deposited by the formulation stored at 25°C, 44%RH, while the formulation stored at 40°C, 75%RH showed no significant difference. In the filter stage, no significant difference was observed in the amount of drug deposited between the formulations stored at the different environmental conditions. These data suggested that environmental conditions do not affect the aerosolisation performance of the 0.5% w/w MgSt formulation. The reason could be the formation of the hydrophobic layer of MgSt over the whole surface of the carrier, providing an interfacial barrier and thereby limiting the influence of elevated conditions of relative humidity. The same results were observed with the Lactochem formulations as discussed previously; the addition of 0.5% w/w MgSt provided stability to the formulation.

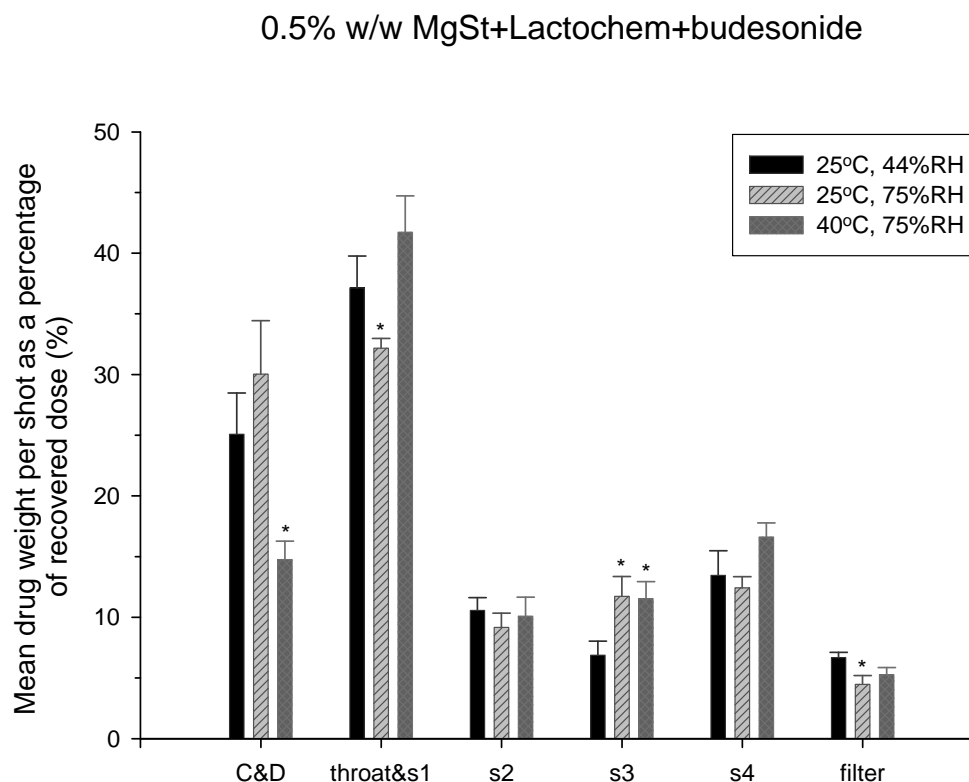


**Figure 4.11a** The deposition of budesonide, as a percentage of recovered dose, throughout the MSLI for the 0.5% w/w MgSt+Lactochem+budesonide formulation at the different environmental conditions. (Mean  $\pm$  S.D,  $n=3$ , \*  $P<0.05$ , \*  $P<0.01$ : significant difference compared to the ambient conditions by ANOVA one-way. C & D: capsules & device)

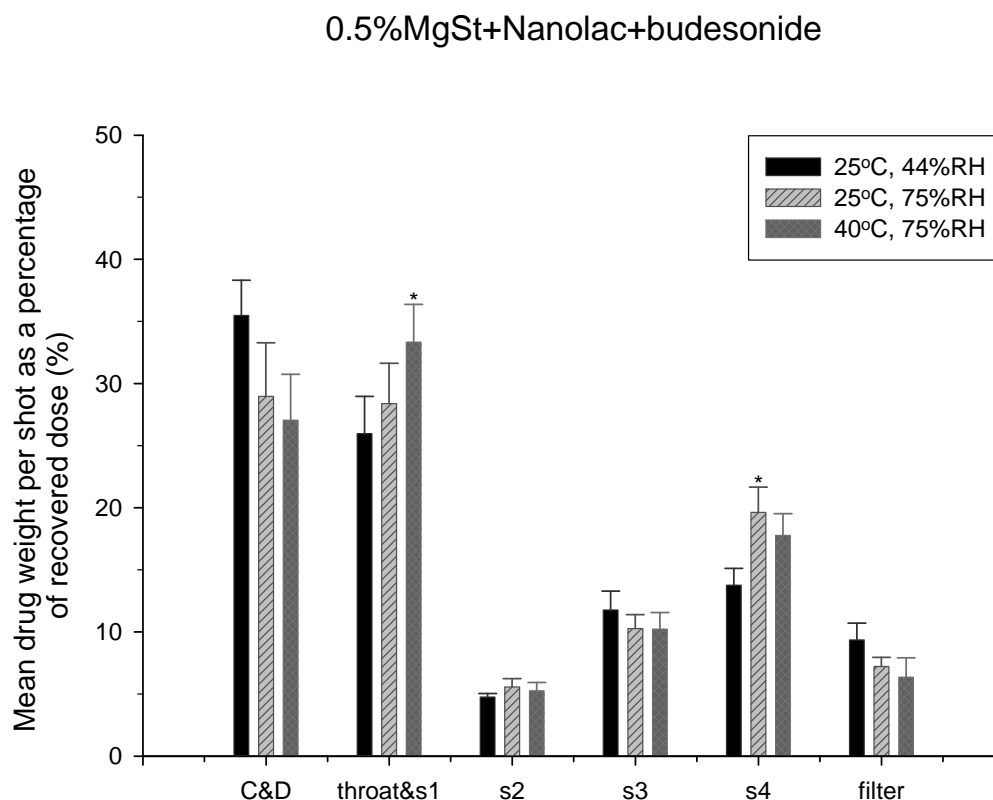


**Figure 4.11b** The deposition of budesonide, as a percentage of recovered dose, throughout the MSLI for the 0.5% w/w MgSt+Nanolac +budesonide formulation at the different environmental conditions. (Mean  $\pm$  S.D, n=3, \*  $P<0.05$ , \*  $P<0.01$ : significant difference compared to the ambient conditions by ANOVA one-way. C & D: capsules & device)

#### 4.4.3.4 The influence of storage conditions on the in vitro aerosolisation performance of 1.0% w/w MgSt formulations

The drug deposition of the 1.0% w/w MgSt-Lactochem formulation in the capsules and device stage varied at the different environmental conditions as shown in figure 4.12a. Upon storage at 25°C, 75%RH there was no significant difference in the amount of drug deposited in the capsules and device compared to the drug deposited by the formulation stored at the ambient conditions. However upon storage at 40°C, 75%RH,

the drug retention was significantly higher (ANOVA  $p < 0.01$ ). The retention was approximately double that of the formulation stored at ambient conditions. Interestingly, the drug retention in the capsules and device was not influenced by the storing at 25°C, 75%RH. The direct influence of temperature further suggests the possible formation of solid crystal bridges at these elevated conditions. There was no significant difference in the drug deposited in the throat and stage1 of the MSLI apparatus between the formulations stored at the different environmental conditions. The drug deposited in stage 2 of the MSLI, was significantly lower (ANOVA  $p < 0.05$ ) upon storage of the formulation at 40° C, 75%RH, while no significant difference was observed with the formulation stored at 25°C, 75%RH compared to the formulation stored at ambient conditions.

Storage of the formulations at different environmental conditions had no significant influence on the amount of drug deposited on stage 3 of the MSLI apparatus. There was a significant decrease of 50% in the drug deposited in stage 4 (ANOVA  $p < 0.01$ ) upon storage at 40° C, 75%RH, while no significant difference was observed with the formulation stored at 25°C, 75%RH. The drug deposition in the filter stage of the MSLI apparatus of the formulations stored at both elevated conditions were significantly reduced (ANOVA  $p < 0.01$ ), resulting in very poor aerosol performance.



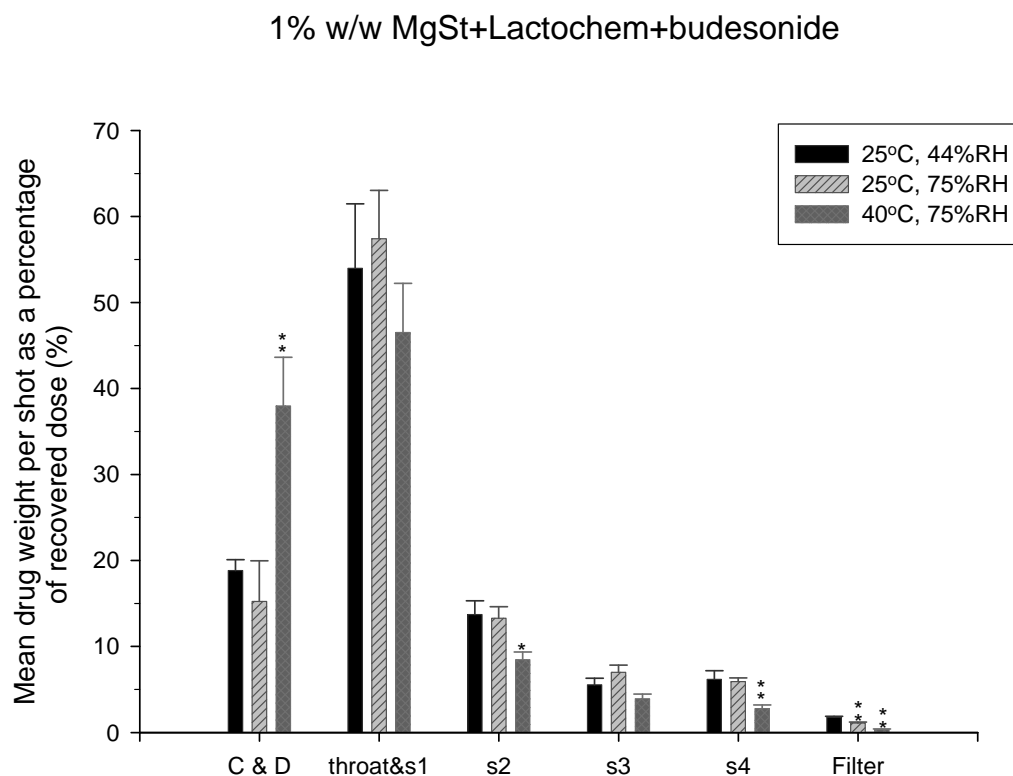


**Figure 4.12a** The deposition of budesonide, as a percentage of recovered dose, throughout the MSLI for the 1.0% w/w MgSt+Lactochem+budesonide formulation at the different environmental conditions. (Mean  $\pm$  S.D, n=3, \*  $P<0.05$ , \*  $P<0.01$ : significant difference compared to the ambient conditions by ANOVA one-way. C & D: capsules & device)

### 1% w/w MgSt+Nanolac+budesonide

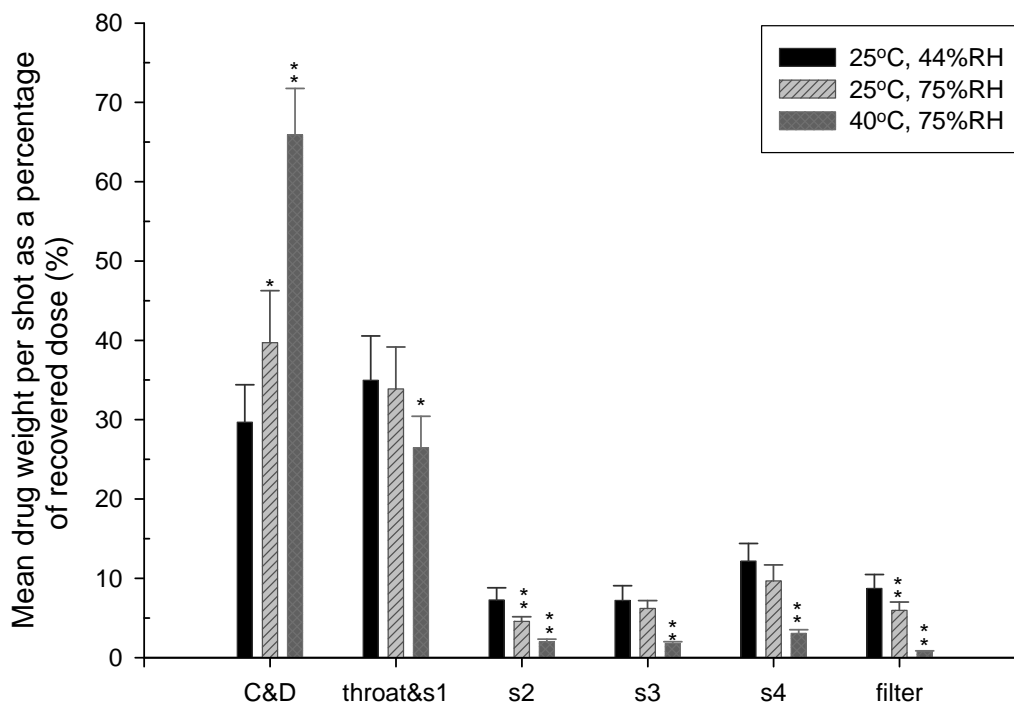


**Figure 4.12b** The deposition of budesonide, as a percentage of recovered dose, throughout the MSLI for the 1.0% w/w MgSt+Nanolac +budesonide formulation at the different environmental conditions. (Mean  $\pm$  S.D, n=3, \*  $P<0.05$ , \*\*  $P<0.01$ : significant difference compared to the ambient conditions by ANOVA one-way. C & D: capsules & device)

As shown in figure 4.12b, the amount of drug deposited in the capsules and device stage upon storage of the formulation at 25°C, 75%RH was significantly higher (ANOVA  $p<0.05$ ) than the control formulation stored at 25°C, 44%RH. An even greater significant increase (ANOVA  $p<0.01$ ) in the amount of drug deposited was observed upon storage of the formulation at 40°C, 75%RH having a value double that of the formulation stored at ambient conditions. Upon storage of the formulation at 40°C, 75%RH the amount of drug deposited in the throat and stage 1 was significantly lower (ANOVA  $p<0.05$ ) compared to the amount of drug deposited by the formulation stored at 25°C, 44%RH, while no significant difference was observed upon storage at

25°C, 75%RH. The amount of drug deposited in stage 2 of the MSLI was significantly lower (ANOVA  $p < 0.01$ ) upon storage of the formulations at both elevated environmental conditions compared to the amount of drug deposited upon storage at ambient conditions. Upon storage of the formulation at 40°C, 75%RH the amount of drug deposited in stages 3 and 4 of the MSLI was significantly lower (ANOVA  $p < 0.01$ ) to a value approximately a third of the formulation stored at ambient conditions, while there was no significant difference upon storage at 25°C, 75%RH. The amount of drug deposited in the filter stage of the MSLI was significantly lower (ANOVA  $p < 0.01$ ) for the formulations stored at the elevated environmental conditions, than the formulation stored at ambient conditions. Thus, storage of the formulation at 40°C, 75%RH led to a dramatic decrease in aerolisation performance and indicating the significant influence environmental conditions have on the aerosol performance.

**Table 4.5 The deposition of budesonide as mean drug weight per shot ( $\mu\text{g}$ ) at 25°C, 75%RH in the different stages of the MSLI for the Lactochem formulations and standard deviations (Mean  $\pm$  SD), n=3.**

(Mean $\pm$ SD) ( $\mu\text{g}$ ) At 25°C, 75%RH	caps& device	throat	s1	s2	s3	s4	filter
Lactochem+ budesonide	53.0 $\pm$ 10.8	13.1 $\pm$ 1.9	49.7 $\pm$ 7.2	15.2 $\pm$ 3.1	8.8 $\pm$ 1.3	9.0 $\pm$ 0.1	0.6 $\pm$ 0.2
0.25% w/w MgSt + Lactochem+budesonide	29.3 $\pm$ 6.6	7.3 $\pm$ 0.9	31.8 $\pm$ 2.0	10.9 $\pm$ 1.9	13.2 $\pm$ 2.3	19.2 $\pm$ 2.5	7.1 $\pm$ 1.3
0.5% w/w MgSt + Lactochem+budesonide	45.2 $\pm$ 10.7	8.7 $\pm$ 0.3	37.0 $\pm$ 4.4	13.7 $\pm$ 2.3	17.6 $\pm$ 3.7	18.6 $\pm$ 1.9	6.7 $\pm$ 1.4
1% w/w MgSt + Lactochem+budesonide	21.3 $\pm$ 8.7	12.9 $\pm$ 1.5	67.5 $\pm$ 7.7	18.7 $\pm$ 3.6	9.9 $\pm$ 2.3	8.3 $\pm$ 0.9	1.5 $\pm$ 0.3

**Table 4.6 The deposition of budesonide as mean drug weight per shot ( $\mu\text{g}$ ) at 25°C, 75%RH in the different stages of the MSLI for the Nanolac formulations and standard deviations (Mean  $\pm$  SD), n=3.**

(Mean $\pm$ SD) ( $\mu\text{g}$ ) At 25°C, 75%RH	caps& device	throat	s1	s2	s3	s4	filter
Nanolac + budesonide	31.8 $\pm$ 8.7	5.0 $\pm$ 1.3	86.6 $\pm$ 3.3	4.2 $\pm$ 0.2	5.5 $\pm$ 0.9	6.0 $\pm$ 1.2	1.2 $\pm$ 0.3
0.25% w/w MgSt + Nanolac+budesonide	52.6 $\pm$ 5.4	5.1 $\pm$ 1.1	30.1 $\pm$ 12.9	5.4 $\pm$ 0.8	11.4 $\pm$ 0.5	20.4 $\pm$ 1.0	10.1 $\pm$ 3.4
0.5% w/w MgSt + Nanolac+budesonide	42.0 $\pm$ 8.4	5.3 $\pm$ 0.7	35.7 $\pm$ 3.54	8.1 $\pm$ 1.7	15.2 $\pm$ 3.0	28.7 $\pm$ 5.5	10.5 $\pm$ 2.2
1% w/w MgSt + Nanolac+budesonide	44.9 $\pm$ 5.2	3.0 $\pm$ 1.0	35.5 $\pm$ 5.9	5.2 $\pm$ 1.0	7.1 $\pm$ 1.9	11.2 $\pm$ 3.7	6.8 $\pm$ 1.2

**Table 4.7 The deposition of budesonide as mean drug weight per shot ( $\mu\text{g}$ ) at 40°C, 75%RH in the different stages of the MSLI for the Lactochem formulations and standard deviations (Mean  $\pm$  SD),n=3.**

(Mean $\pm$ SD) ( $\mu\text{g}$ ) At 40°C, 75%RH	caps& device	throat	s1	s2	s3	s4	filter
Lactochem+ budesonide	52.9 $\pm$ 6.1	15.4 $\pm$ 2.5	45.7 $\pm$ 9.3	12.5 $\pm$ 0.7	9.3 $\pm$ 0.6	5.1 $\pm$ 0.9	0.7 $\pm$ 0.2
0.25% w/w MgSt + Lactochem+budesonide	28.3 $\pm$ 2.0	6.2 $\pm$ 0.3	39.8 $\pm$ 9.3	8.3 $\pm$ 1.8	9.2 $\pm$ 1.2	11.8 $\pm$ 0.4	3.1 $\pm$ 0.6
0.5% w/w MgSt + Lactochem+budesonide	21.7 $\pm$ 2.3	11.5 $\pm$ 1.9	50.2 $\pm$ 4.1	15.1 $\pm$ 4.2	17.0 $\pm$ 2.7	24.6 $\pm$ 2.4	7.8 $\pm$ 1.2
1% w/w MgSt + Lactochem+budesonide	57.9 $\pm$ 12.8	8.5 $\pm$ 1.1	62.5 $\pm$ 12.6	12.9 $\pm$ 2.2	6.0 $\pm$ 1.3	4.2 $\pm$ 1.1	0.6 $\pm$ 0.1

**Table 4.8 The deposition of budesonide as mean drug weight per shot ( $\mu\text{g}$ ) at 40 °C, 75%RH in the different stages of the MSLI for the Nanolac formulations and standard deviations (Mean  $\pm$  SD),n=3.**

(Mean $\pm$ SD) ( $\mu\text{g}$ ) At 40°C, 75%RH	caps& device	throat	s1	s2	s3	s4	filter
Nanolac + budesonide	54.9 $\pm$ 3.1	3.0 $\pm$ 0.7	60.8 $\pm$ 10.0	2.2 $\pm$ 0.6	2.6 $\pm$ 0.4	3.1 $\pm$ 0.6	0.6 $\pm$ 0.1
0.25% w/w MgSt + Nanolac+budesonide	27.9 $\pm$ 2.0	3.4 $\pm$ 0.4	71.6 $\pm$ 14.3	7.3 $\pm$ 1.3	10.1 $\pm$ 1.9	11.8 $\pm$ 0.3	3.3 $\pm$ 0.7
0.5% w/w MgSt + Nanolac+budesonide	38.9 $\pm$ 5.2	4.9 $\pm$ 0.6	43.2 $\pm$ 5.2	7.6 $\pm$ 0.8	14.8 $\pm$ 3.3	25.8 $\pm$ 4.7	9.4 $\pm$ 4.3
1% w/w MgSt + Nanolac+budesonide	94.7 $\pm$ 4.5	1.3 $\pm$ 0.1	37.3 $\pm$ 10.7	2.9 $\pm$ 0.9	2.6 $\pm$ 0.5	4.4 $\pm$ 0.9	1.1 $\pm$ 0.3

#### 4.4.4 Summary of deposition performance of the formulations upon storage at different conditions

**Table 4.9 Table 4.10 The deposition of budesonide in the MSLI from the Lactochem formulations at 25°C, 75%RH via a Cyclohaler (Mean  $\pm$  S.D, n=3).**

(Mean $\pm$ SD)	Recovered Dose ( $\mu$ g)	Emitted Dose ( $\mu$ g)	Fine particle dose ( $\mu$ g)	FPF <sub>RD</sub> (%)	FPF <sub>ED</sub> (%)
At 25°C, 75%RH					
Lactochem+ budesonide	149.2 $\pm$ 8.2	96.3 $\pm$ 7.7	18.3 $\pm$ 1.3	12.3 $\pm$ 0.9	19.1 $\pm$ 0.4
0.25% w/w MgSt + Lactochem+budesonide	118.7 $\pm$ 13.2	89.4 $\pm$ 7.3	39.5 $\pm$ 5.8	33.2 $\pm$ 1.8	44.0 $\pm$ 3.0
0.5% w/w MgSt + Lactochem+budesonide	147.5 $\pm$ 4.2	102.3 $\pm$ 13.0	42.9 $\pm$ 6.2	29.1 $\pm$ 3.6	41.9 $\pm$ 1.0
1% w/w MgSt + Lactochem+budesonide	140.2 $\pm$ 12.0	118.9 $\pm$ 14.1	19.7 $\pm$ 3.2	14.0 $\pm$ 1.0	16.6 $\pm$ 1.7

**Table 4.10 The deposition of budesonide in the MSLI from the Nanolac formulations at 25°C, 75%RH via a Cyclohaler (Mean  $\pm$  S.D, n=3).**

(Mean $\pm$ SD)	Recovered Dose ( $\mu$ g)	Emitted Dose ( $\mu$ g)	Fine particle dose ( $\mu$ g)	FPF <sub>RD</sub> (%)	FPF <sub>ED</sub> (%)
At 25°C, 75%RH					
Nanolac + budesonide	140.3 $\pm$ 12.0	108.6 $\pm$ 3.9	12.7 $\pm$ 2.1	9.1 $\pm$ 1.3	11.7 $\pm$ 1.6
0.25% w/w MgSt + Nanolac+budesonide	135.2 $\pm$ 18.1	82.5 $\pm$ 15.1	41.9 $\pm$ 2.0	31.4 $\pm$ 4.1	51.9 $\pm$ 9.3
0.5% w/w MgSt + Nanolac+budesonide	145.5 $\pm$ 10.0	103.5 $\pm$ 11.9	54.4 $\pm$ 10.3	37.2 $\pm$ 4.8	52.3 $\pm$ 4.6
1% w/w MgSt + Nanolac+budesonide	113.8 $\pm$ 15.0	68.9 $\pm$ 13.5	25.1 $\pm$ 6.3	21.9 $\pm$ 2.5	36.3 $\pm$ 2.9

**Table 4.11 The deposition of budesonide in the MSLI from the Lactochem formulations at 40°C, 75%RH via a Cyclohaler (Mean  $\pm$  S.D, n=3).**

(Mean $\pm$ SD) At 40°C, 75%RH	Recovered Dose ( $\mu$ g)	Emitted dose ( $\mu$ g)	Fine particle dose ( $\mu$ g)	FPF <sub>RD</sub> (%)	FPF <sub>ED</sub> (%)
Lactochem+ budesonide	141.6 $\pm$ 7.9	88.7 $\pm$ 9.7	15.1 $\pm$ 1.0	10.7 $\pm$ 1.1	17.2 $\pm$ 2.8
0.25% w/w MgSt + Lactochem+budesonide	106.9 $\pm$ 10.1	78.54 $\pm$ 11.4	24.1 $\pm$ 1.1	22.7 $\pm$ 1.4	31.1 $\pm$ 3.7
0.5% w/w MgSt + Lactochem+budesonide	147.7 $\pm$ 14.9	126.0 $\pm$ 14.4	50.1 $\pm$ 12.1	34.4 $\pm$ 4.4	47.0 $\pm$ 3.4
1% w/w MgSt + Lactochem+budesonide	144.3 $\pm$ 15.4	50.0 $\pm$ 11.8	8.1 $\pm$ 1.6	5.6 $\pm$ 1.0	16.8 $\pm$ 4.1

**Table 4.12 The deposition of budesonide in the MSLI from the Nanolac formulations at 40°C, 75%RH via a Cyclohaler (Mean  $\pm$  SD, n=3)**

(Mean $\pm$ SD) At 40°C, 75%RH	Recovered Dose ( $\mu$ g)	Emitted Dose ( $\mu$ g)	Fine particle dose ( $\mu$ g)	FPF <sub>RD</sub> (%)	FPF <sub>ED</sub> (%)
Nanolac + budesonide	127.2 $\pm$ 7.9	72.3 $\pm$ 8.0	6.3 $\pm$ 1.2	5.0 $\pm$ 1.1	8.9 $\pm$ 2.4
0.25% w/w MgSt + Nanolac+budesonide	106.9 $\pm$ 10.1	78.5 $\pm$ 11.4	24.1 $\pm$ 1.1	22.7 $\pm$ 1.4	31.1 $\pm$ 3.7
0.5% w/w MgSt + Nanolac+budesonide	147.7 $\pm$ 14.8	126.0 $\pm$ 14.1	49.3 $\pm$ 5.6	33.4 $\pm$ 2.7	39.2 $\pm$ 2.6
1% w/w MgSt + Nanolac+budesonide	152.6 $\pm$ 1.2	94.7 $\pm$ 13.8	10.8 $\pm$ 1.5	7.0 $\pm$ 0.9	11.5 $\pm$ 2.5

The environmental conditions under which the formulations were stored significantly affected the recovered dose of the Lactochem formulations as shown in figure 4.13a. This could be due to the formation of agglomerates as suggested by the SEMs and the optical images. Upon storage of the Lactochem control formulation at 25°C, 75%RH there was a slight decrease in recovered dose but not significantly different compared to the formulation stored at 25°C, 44%RH. A significant 12.5% decrease (ANOVA  $p<0.05$ ) in recovered dose was observed upon storage of the formulation at 40°C, 75%RH. The 0.25% w/w MgSt formulation exhibited a significant reduction upon storage at both elevated conditions of temperature and humidity, with the dose recovery being half that of the formulation at ambient conditions (ANOVA  $p<0.01$ ). Upon storage of the 0.5% w/w MgSt formulation at elevated environmental conditions, there was only a slight decrease in recovered dose compared to the formulation stored at ambient conditions, indicating that the environmental conditions did not affect the recovered dose of this formulation. The 1.0% w/w MgSt formulation stored at 25°C, 75%RH showed a significant reduction (ANOVA  $p<0.01$ ) in recovered dose compared to the formulation stored at 25°C, 44%RH. Upon its storage at 40°C, 75%RH the recovered dose was again significantly reduced (ANOVA  $p<0.05$ ) but to a lesser amount than the formulation stored at 25°C, 75%RH.

The recovered doses of the Nanolac formulations with and without MgSt are shown in Figure 4.13b. It is evident that the recovered dose of the Nanolac control formulation upon storage at elevated environmental conditions significantly increased, whereas the Lactochem control formulations were significantly decreased. This difference could be attributed to possible difference in surface morphology and the degree of processed induced disorder. Upon storage of the Nanolac control formulation at 25°C, 75%RH the recovered dose was significantly increased by 30% (ANOVA  $p<0.01$ ) while the recovered dose of the formulation upon storage at 40°C, 75%RH was significantly increased by 19% (ANOVA  $p<0.05$ ). However, upon the addition of 0.25% w/w MgSt there was a significant decrease of 29% in recovered dose (ANOVA  $p<0.05$ ) at both elevated conditions compared to the recovered dose of the formulation stored at the ambient conditions. Furthermore a significant decrease (ANOVA  $p<0.05$ ) in recovered dose was also observed upon storage of the 0.5% w/w MgSt formulation at both elevated conditions. The recovered dose of the 1.0% w/w



MgSt formulation upon storage at 25°C, 75%RH significantly increased (ANOVA  $p < 0.05$ ) with a further increase in recovered dose observed upon storage of the formulation at 40°C, 75%RH (ANOVA  $p < 0.01$ ).

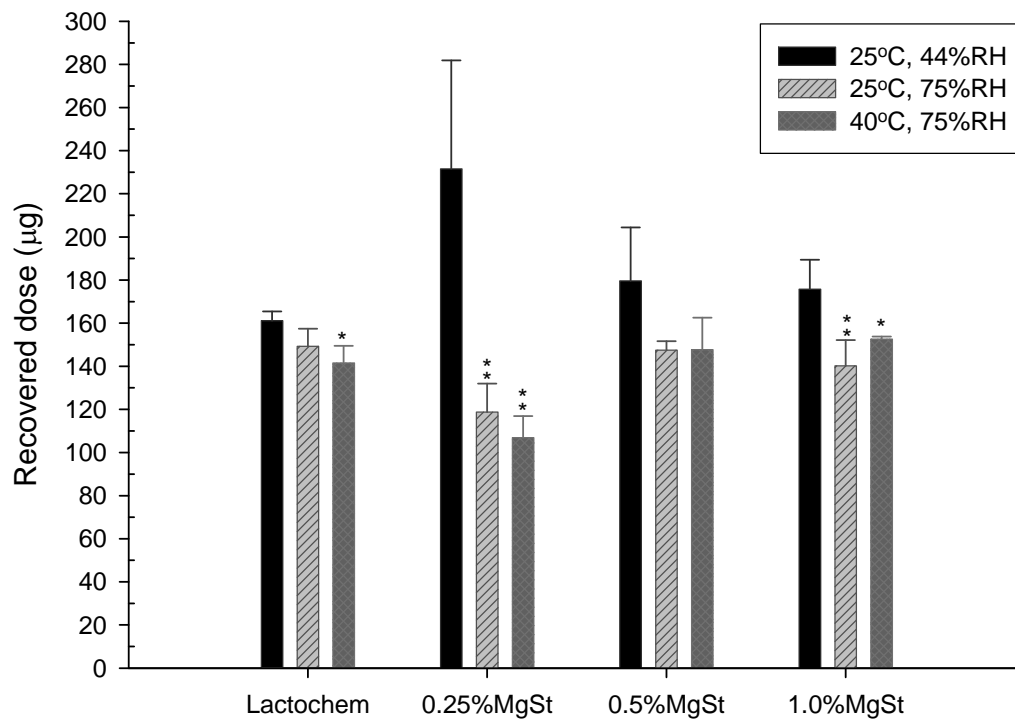


**Figure 4.13a** A graph showing the relationship between the recovered dose and the Lactochem formulations at the different environmental conditions. (Mean  $\pm$  SD,  $n=3$ ) ( \*  $P < 0.05$ , \*  $P < 0.01$ : significant difference compared to the formulations at the ambient conditions by ANOVA one-way. C & D: capsules & device)

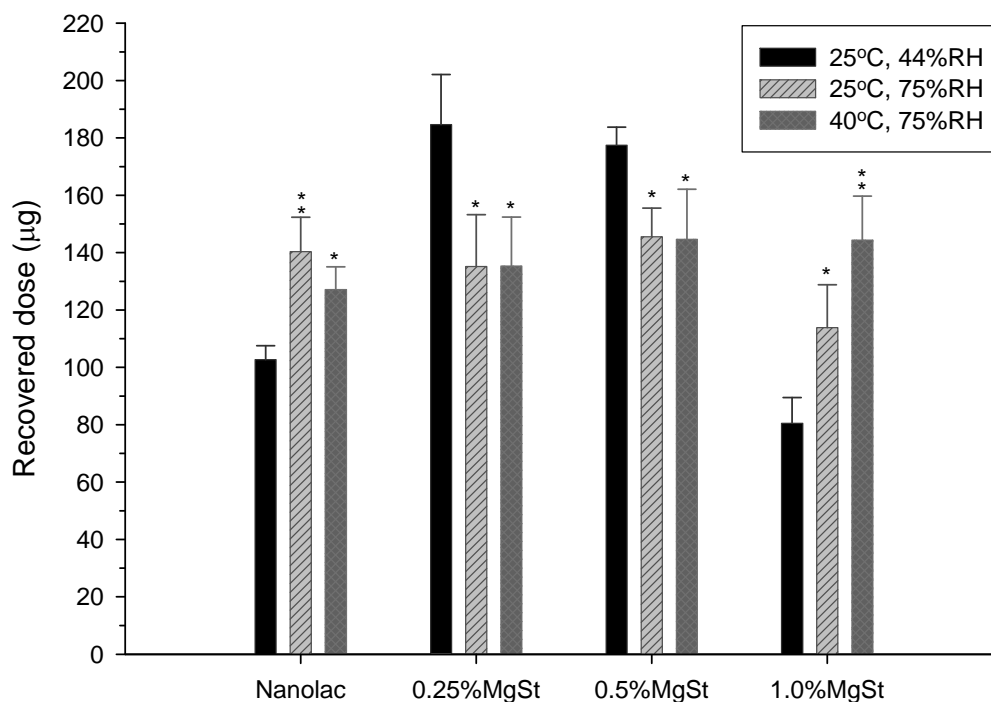


**Figure 4.13b** A graph showing the relationship between the recovered dose and the Nanolac formulations at the different environmental conditions. (Mean  $\pm$  SD,  $n=3$ )

\*  $P<0.05$ , \*  $P<0.01$ : significant difference compared to the formulations at the ambient conditions by ANOVA one-way. C & D: capsules & device)

As shown in Figure 4.14a the environmental conditions did not significantly affect the emitted dose of the Lactochem control formulations. Upon storage of the 0.25% w/w MgSt formulation at both elevated conditions their emitted doses were significantly reduced (ANOVA  $p<0.01$ ) compared to the same formulation stored at 25°C, 44%RH. The decrease is in accordance with the decrease in the recovered dose of the formulation. The storage of the 0.5% w/w MgSt formulation at both elevated conditions did not alter their emitted dose significantly, compared to the same formulation stored at the ambient conditions. The emitted dose of the 1.0% w/w MgSt formulation upon storage at 40°C, 75%RH was significantly reduced (ANOVA  $p<0.01$ ) compared to the emitted dose of the same formulation stored at ambient conditions. However, upon storage of the formulation at 25°C,

75%RH no significant difference in the emitted dose compared to the emitted dose of the formulation stored at the ambient conditions was observed. These data suggest that only the 40°C, 75%RH conditions affects the emitted dose of the 1.0% MgSt formulation and that at 25°C, 75%RH the emitted dose is not affected.

Interestingly, the emitted doses of the all the formulations of Nanolac containing MgSt shown in Figure 4.14b, were not significantly affected upon storage at elevated environmental conditions when compared to the formulations stored at ambient conditions. Interestingly, the emitted dose of the Nanolac control formulation upon storage at 40°C, 75%RH was significantly lower (ANOVA  $p < 0.01$ ) than the emitted dose of the formulation stored at ambient conditions, while the emitted dose of the formulation stored at 25°C, 75%RH was not significantly different.

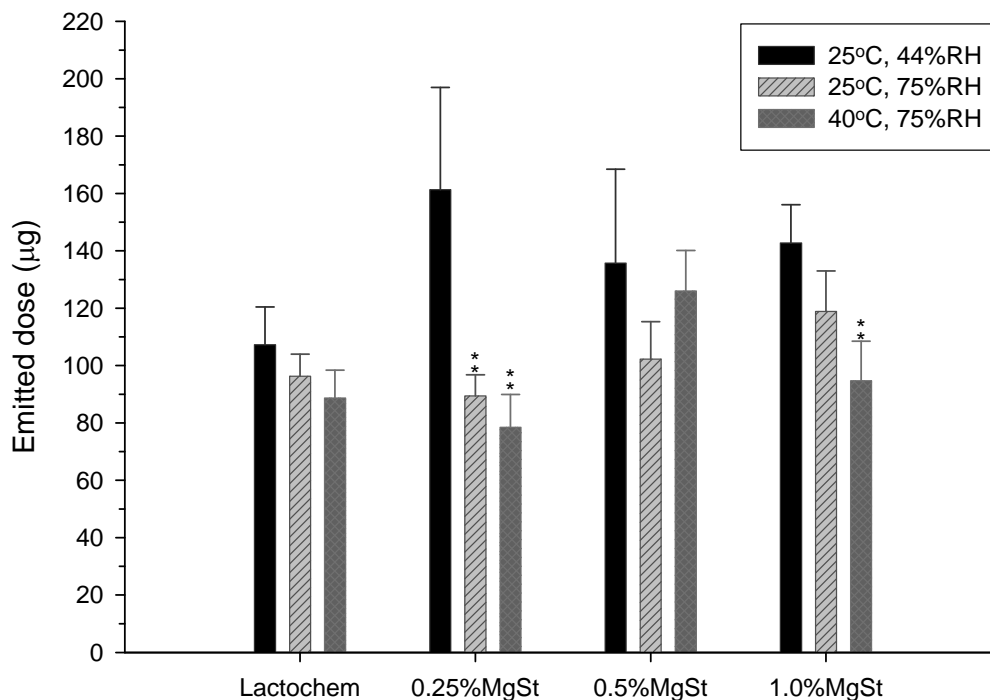


**Figure 4.14a** A graph showing the relationship between the emitted dose and the Lactochem formulations at the different environmental conditions. (Mean  $\pm$  SD,  $n=3$ ) ( \*  $P < 0.05$ , \*  $P < 0.01$ : significant difference compared to the formulations at the ambient conditions by ANOVA one-way. C & D: capsules & device)

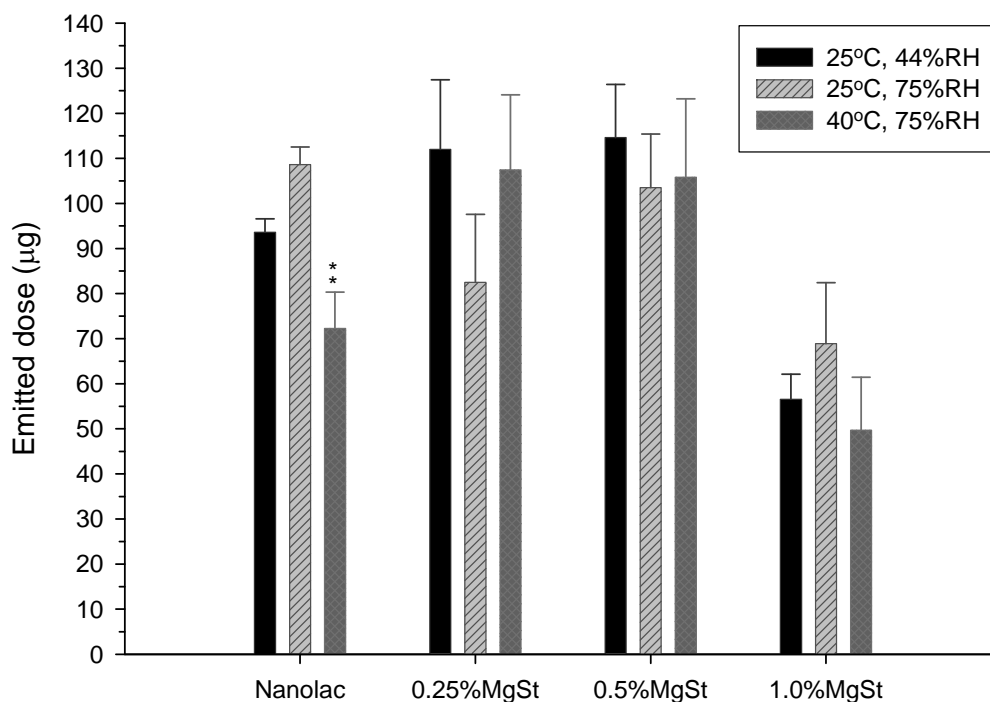


**Figure 4.14b** A graph showing the relationship between the emitted dose and the Nanolac formulations at the different environmental conditions. (Mean  $\pm$  SD,  $n=3$ , \*  $P<0.05$ , \*  $P<0.01$ : significant difference compared to the formulations at the ambient conditions by ANOVA one-way. C & D: capsules & device)

Upon storage of the Lactochem control formulations at elevated environmental conditions the fine particle dose was significantly reduced (ANOVA  $p<0.05$ ) to approximately half the value of the formulation stored at the ambient conditions as shown in figure 4.15a. A similar decrease was observed upon storage of the formulation at 25°C, 75%RH, which was further decreased by 15% upon storage of the formulation at 40°C, 75%RH. The FPD at both elevated conditions was significantly reduced (ANOVA  $p<0.01$ ) indicating the major influence the environmental conditions has on the stability performance of the formulation. The FPD of the 0.25% w/w MgSt formulations stored at 25°C, 75%RH and 40°C, 75%RH were significantly reduced by 26% and 59% respectively (ANOVA  $p<0.01$ ), indicating the instability of the formulation at elevated conditions of temperature and

humidity. However, storage of the 0.5% w/w MgSt formulation at both elevated conditions, did not significantly affect the aerosolisation performance. Furthermore, upon storage of the 1.0% w/w MgSt formulation at 25°C, 75%RH no significant difference in FPD was observed. However, upon storage at 40°C, 75%RH, the FPD was significantly reduced (ANOVA  $p<0.01$ ) indicating that its instability is dependant on the conditions of storage.

As shown in Figure 4.15b for the Nanolac formulations, the addition of 0.5% w/w MgSt showed the optimum stability in the fine particle dose delivery. The FPD of the 0.25% w/w MgSt formulations stored at 25°C, 75%RH and 40°C, 75%RH were significantly reduced by 26% and 59% respectively (ANOVA  $p<0.01$ ). While storage of the 1.0% w/w MgSt formulation at 25°C, 75%RH did not significantly affect performance, storage of the formulation at 40°C, 75%RH resulted in the FPD being significantly reduced by 65% (ANOVA  $p<0.01$ ).

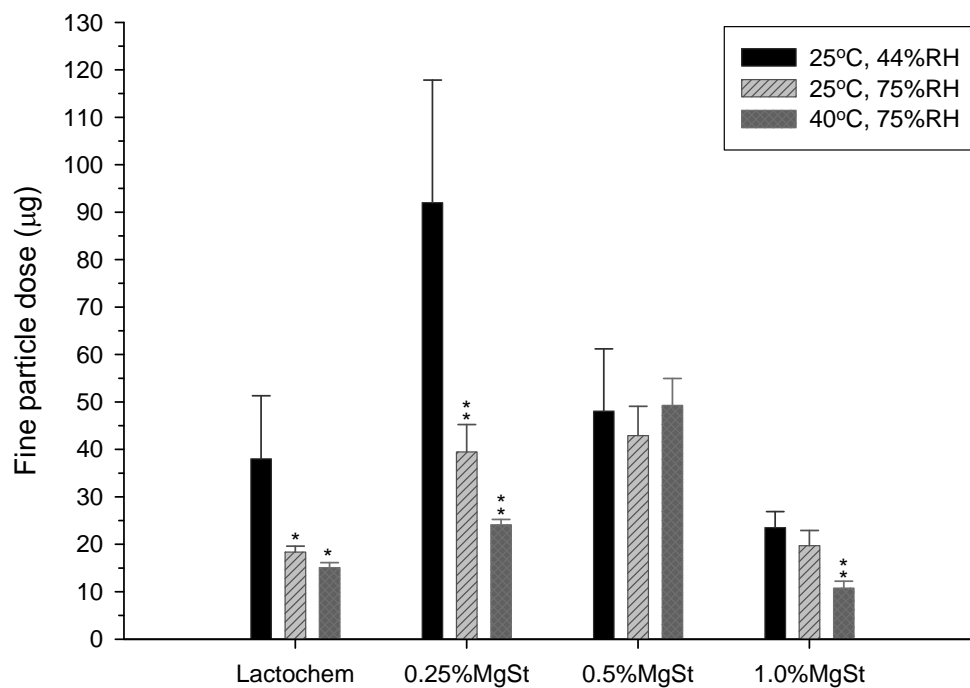


**Figure 4.15a** A graph showing the relationship between the fine particle dose and the Lactochem formulations at the different environmental conditions. (Mean  $\pm$  SD,  $n=3$ ) ( \*  $P<0.05$ , \*  $P<0.01$ : significant difference compared to the formulations at the ambient conditions by ANOVA one-way. C & D: capsules & device)

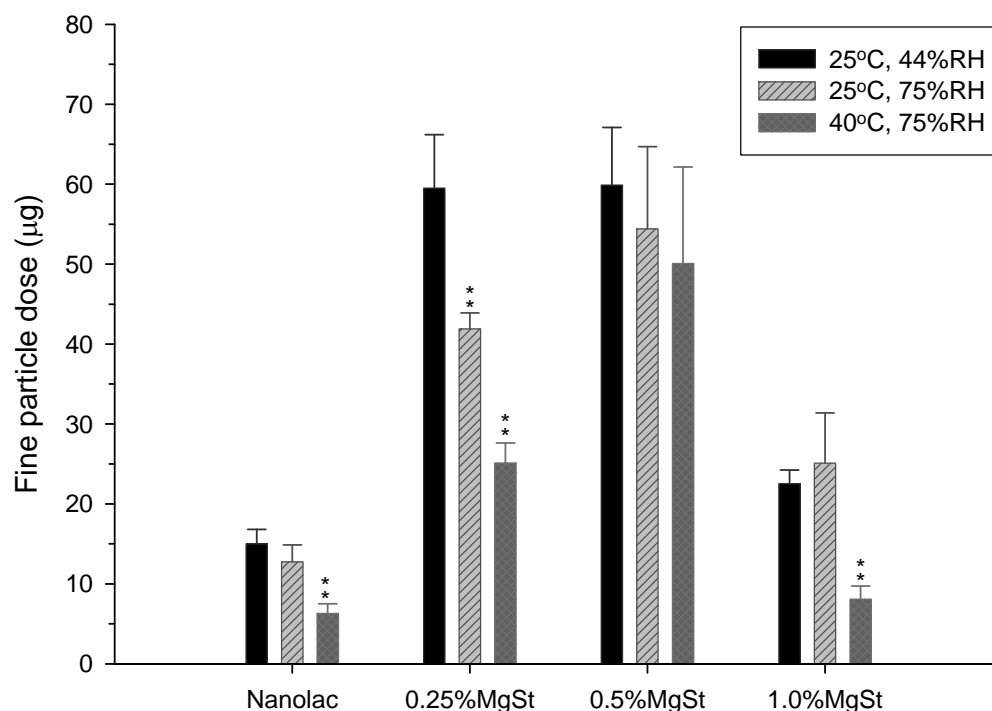


**Figure 4.15b** A graph showing the relationship between the fine particle dose and the Nanolac formulations at the different environmental conditions. (Mean  $\pm$  SD,  $n=3$ )  
 (\*  $P<0.05$ , \*  $P<0.01$ : significant difference compared to the formulations at the ambient conditions by ANOVA one-way. C & D: capsules & device)

As shown in Figure 4.16a all the formulations except the 0.5% w/w MgSt formulation showed a decreased aerosolisation performance upon storage for 3 months at elevated environmental conditions. A considerable 11.2% decrease in FPF was observed with the control formulation upon storage at 25°C, 75%RH and 40°C, 75%RH, which was further reduced by 1.6% upon storage at 40°C, 75%RH. The FPF values of the control formulations which were stored at high humidity were significantly lower (ANOVA  $p<0.05$ ) compared to the control formulation stored at 25°C, 44%RH. Furthermore, a 6.2% decrease in the FPF was observed with the 0.25% w/w MgSt formulation upon storage at 25°C, 75%RH, having a significantly lower FPF value (ANOVA  $p<0.05$ ) than the same formulation stored at 25°C, 44%RH. A significant reduction of 16.7% was observed with the same formulation being stored at 40°C, 75%RH (ANOVA  $p<0.01$ ). This concentration

of MgSt gave the best aerosolisation performance but failed to protect the formulation upon storage at elevated environmental conditions.

However, the addition of 0.5% w/w MgSt formulation showed a 2.6% increase in the FPF upon storage at 25°C, 75%RH, with a further 5.3% increase in the FPF upon storage at 40°C, 75%RH, with the later formulation being significantly higher (ANOVA  $p < 0.05$ ) than the formulation stored at 25°C, 44%RH. It could be suggested that by the addition of 0.5% w/w of MgSt to the formulation, resulted in providing stability to the formulation, thus being the optimum concentration. The reason could be the sufficient build up of a hydrophobic layer of MgSt over the excipient surface of the excipient, protecting it from moisture. While the storage of a 1.0% w/w MgSt formulation at 25°C, 75%RH increased the FPF, a significant decrease was observed upon storage of the formulation at 40°C, 75%RH (ANOVA  $p < 0.01$ ).

As shown in Figure 4.16b the fine particle fractions of all the Nanolac based formulations except the 0.5% w/w MgSt formulation were reduced upon storage at the elevated environmental conditions. These data supported the findings for Lactochem formulations. In the control formulation there was a significant decrease upon storage (ANOVA  $p < 0.01$ ) at both conditions (25°C, 75%RH and 40°C, 75%RH) compared to the initial conditions (25°C, 44%RH).

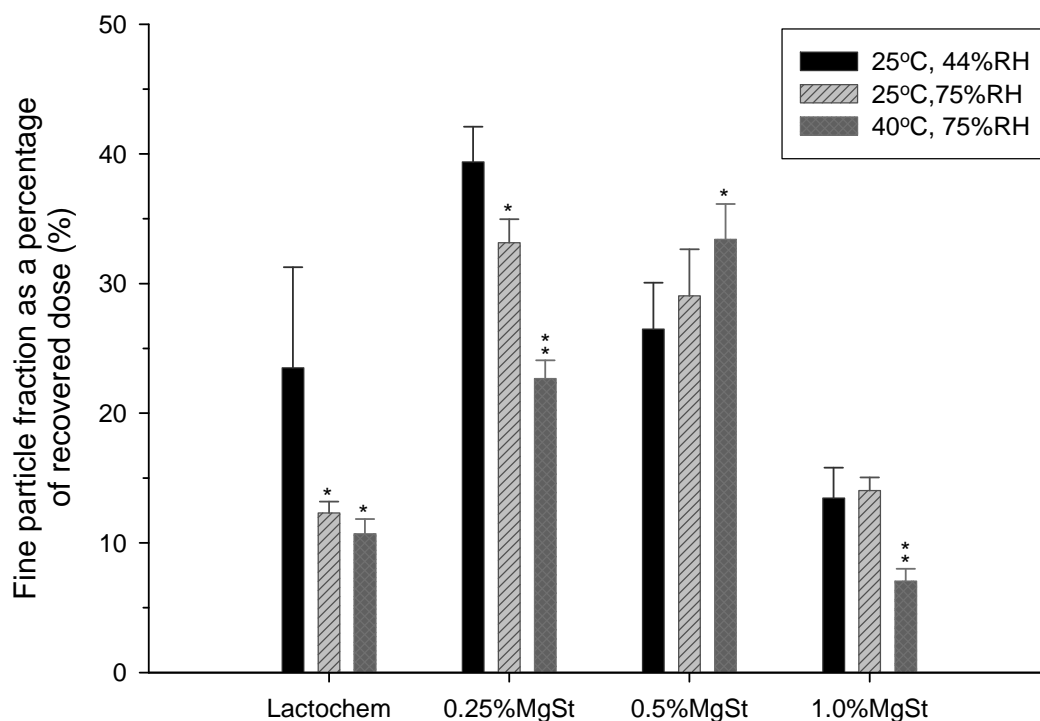


**Figure 4.16a** A graph showing the relationship between the fine particle fraction of recovered dose and the Lactochem formulations at the different environmental conditions. (Mean  $\pm$  SD,  $n=3$ , \*  $P<0.05$ , \*  $P<0.01$ : significant difference compared to the formulations at the ambient conditions by ANOVA one-way. C & D: capsules & device)



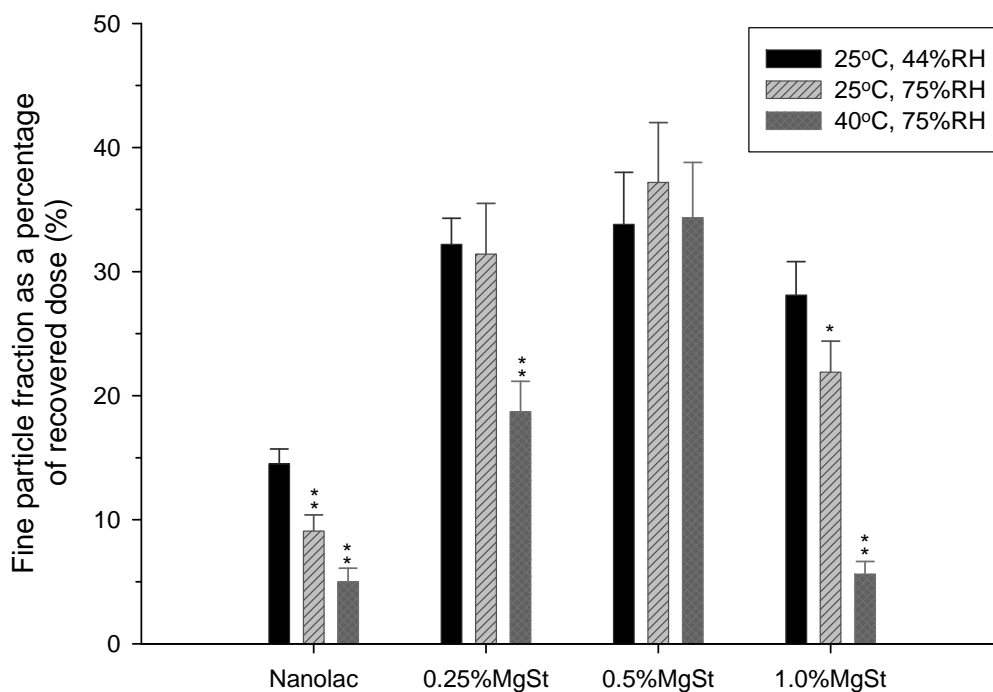


**Figure 4.16b** A graph showing the relationship between the fine particle fraction of recovered dose and the Nanolac formulations at the different environmental conditions. (Mean  $\pm$  SD,  $n=3$ , \*  $P<0.05$ , \*  $P<0.01$ : significant difference compared to the formulations at the ambient conditions by ANOVA one-way. C & D: capsules & device)

These data suggest that RH and temperature play a dominant role on the adhesion properties between the drug and excipient in carrier-based DPI formulations<sup>11</sup>. For a DPI formulation, the drop in FPD may relate to the need for a higher deaggregation energy to detach drug particles from the carrier surfaces and thus reflects the increase in adhesion force acting between attached particles<sup>12</sup>. Furthermore, the FPD responsible for the pharmacological effect might decline because de-agglomeration properties of the powder blend will change upon storage due to moisture uptake. Moisture uptake can affect the flowability of the powders and the force to detach micronized particles from the carrier surface<sup>6</sup>. The relationship between increased humidity and decreased aerosolization performance of budesonide is most likely due to the condensation of water vapour between

the contacting surfaces at a specific humidity until it forms an equilibrium with the surrounding environment<sup>13</sup>. The presence of the water leads to the possible formation of a meniscus contact leading to a capillary force, thereby increasing the interparticulate forces while decreasing the aerosolisation efficiency<sup>13</sup>. The SEMs and optical images suggest a high degree of powder agglomeration. This considerable degree of powder clustering (agglomeration) observed for both types of formulations may be an indication of a considerable increase in inter-particle adhesion due to capillary interaction, arising from the condensation of the increasingly adsorbed water vapour layers onto the surface at high RH levels, promoting the formation of a capillary based meniscus around the contact points of contiguous surfaces<sup>14</sup>. The condensation of water vapour on the particles is mainly due to the high surface energy of fine particles. If enough water condensation occurs, a liquid bridge may form between neighbouring particles, which may greatly increase the attractive forces between particles.

The negative Laplace pressure acting across the meniscus and the surface tensional force at the liquid/air interface induces an attractive force between the contiguous surfaces<sup>14</sup>. Bonding due to adsorbed layer interaction will increasingly occur as the humidity increases, until at the critical humidity liquid bridge bonding becomes dominant<sup>13</sup>. Furthermore, surface roughness strongly affects bonding due to adsorbed layers. Some attraction between adsorbed layers may occur at the peaks of roughness in the Lactochem formulations, but the true area of contact is so small that such attractive forces will be negligible<sup>13</sup>. Particle agglomeration in a dry pharmaceutical system occurs when attractive interparticle bonding forces are sufficient between individual particles to regroup them<sup>15</sup>. Fine cohesive particles adhere to each other under the influence of electrostatic, van der Waals or capillary forces, to form agglomerates that are responsible for their asymmetric distribution in the mixture<sup>16,17</sup>. Dry powder agglomeration mechanisms for multi-component mixtures are not well understood and only a few studies have been conducted describing this phenomenon<sup>15</sup>. Kaye has stated that the more the powder is tumbled around with a stearate, the larger are the spontaneously formed agglomerates<sup>17</sup>. Studies have shown that agglomerates are more easily detached from a carrier surface than single drug particles<sup>18</sup>. This hypothesis could possibly correlate with the behaviour of the 0.5 w/w MgSt

formulations which had the greatest aerosol performance. It has been shown by several studies that larger particles (up to a certain limit) are more easily detached from a surface than smaller ones because whilst adhesion forces increase proportional to particle diameter, the drag and lift forces exerted by an air stream increase proportional to particle diameter squared. Therefore, upon aerosolisation the agglomerates are detached from the carrier surface and remain in the capsules or device due to their large size<sup>4</sup>. The size of the agglomerates and their weight growth are stabilized when a critical size is reached where agglomerates start to break up because the attracting forces become equal to or weaker than gravitational and inertial forces acting on them<sup>15</sup>.

Another possible explanation for the instability of the formulations could be the presence of amorphous domains on the surface of a micronized powder which are liable to undergo re-crystallisation at conditions of elevated RH levels, due to mobility of these domains (plasticization) resulting in solid crystal bridging as previously discussed and potential particle fusion<sup>9,10,20,21</sup>. As changes in the crystalline nature of a solid result in different physical properties, the sluggish transformation during storage can cause unexpected problems in processability of the powder<sup>22</sup>. Moisture is present as liquid bridges at high humidities. Therefore, increasing the relative humidity leads to increased force of adhesion between the drug particles and carrier surface, forming agglomerates in some cases which remain in the capsule and device upon aerosolisation due to the high energy required to detach them. These results indicate that interparticulate interactions increased during storage at elevated environmental conditions. Thus, water sorption on the particle surface may increase the attractive forces between particles through capillary forces<sup>14,23,1,24</sup>. The decrease in the fine particle fraction was more profound in the Lactochem formulations. This could be due to the presence of lactose fines which may exacerbate the instability of carrier based formulations when subjected to environmental conditions of elevated temperature and relative humidity. The reason for this phenomenon could be the potential increase in the overall surface area available for water vapour adsorption. In addition, as a result of the high energy processing of the fine carrier particulates, they are also more likely to show evidence of crystalline disorder, demonstrating a proportion of amorphous

regions that would further enhance solid crystal bridging due to re-crystallisation at conditions of elevated temperature and relative humidity<sup>2</sup>.

Treatment of particle surfaces by hydrophobic compounds such as MgSt helps to make the powder less sensitive to ambient moisture<sup>12</sup>. The effect of coating was demonstrated by Hickey et al (1990)<sup>25</sup> who used fatty acids to get an effective coating that was able to inhibit hygroscopic particle growth of a model drug powder. This coating modifies particle surfaces to make them less sensitive against high RH.

As can be seen by the data, environmental relative humidity is an important factor governing particle-particle and particle-surface interactions. Relative humidity affects the interparticulate forces by reducing the electrostatic forces and inducing capillary forces. At low RH, the water vapour condensation on the particles is negligible and therefore by increasing the RH results in a reduction of the interparticulate forces by decreasing electrostatic forces, as a result of improving electrical charge decay<sup>5</sup>. However at high RH, the water uptake by the particle is substantial and therefore by increasing the RH would increase interparticulate forces as a result of capillary forces<sup>5</sup>.

Looking at the data from this Chapter, it could be suggested that under the elevated environmental conditions, the interparticulate forces between the drug particles are increased due to capillary forces, resulting in poorer entrainment of the particles into an inhaled air stream and leading to a decreased emitted dose from the inhaler. After entrainment, the drag forces of the inhaled air stream were probably not sufficient to deaggregate the particle agglomerates and hence the fine particle fraction was reduced. In addition, due to the fact that the water vapour was allowed to condense on particle surfaces for a prolonged period of time, and especially at elevated temperatures, it could be that it did not only increase the interparticulate forces but also induced growth of drug particles due to migration of adsorbed water molecules into those particles. Both effects will reduce the delivery efficiency of the drug as explained by Jashnani et al (1995)<sup>6</sup>. The addition of MgSt was expected to reduce the rate of increase in RH inside the capsule by providing a protective barrier to external water vapour condensing on the powder formulation. This was

only achieved by the addition of 0.5% w/w MgSt which may be sufficient to form a sufficient hydrophobic layer over the excipient surface and thus protecting it from destabilising and also preventing the development of stronger binding between the particles therefore facilitating their detachment.

#### **4.4.5 Optical imaging of powder samples**

To further probe the potential explanation for the decrease in the performance upon storage at conditions of elevated temperature and relative humidity, the potential for caking and agglomeration of the formulations was examined via optical imaging. Optical images of the blends released from the capsules stored for three months at 25°C, 75%RH and 40°C, 75%RH are shown in figures 4.10 to 4.11. The optical images may verify the possible mechanism of failure of the carrier based formulation upon exposure to accelerated stability conditions, previously suggested with the electron micrographs. The images of formulations carefully released from the capsules showed that under high relative humidity and temperature, the formulations underwent a considerable degree of powder clustering and agglomeration. Agglomeration was observed for both the Nanolac and Lactochem formulations. However, the images indicated that there was a greater degree of powder agglomeration with the Lactochem formulations and in some cases all the powder blend formed a single pellet, as shown in figure 4.10, Image D. The tendency for powder caking may be associated with the instability of intrinsic fine lactose material, particularly when subjected to high temperature and relative humidity. Moreover, this could possibly be occurring due to the potential increase in the overall surface area available for water vapour adsorption. Therefore, due to their high energy processing of fine carrier particulates, they are more likely to show evidence of crystalline disorder, demonstrating a proportion of amorphous regions that would further enhance solid crystal bridging due to recrystallisation at elevated environmental conditions.

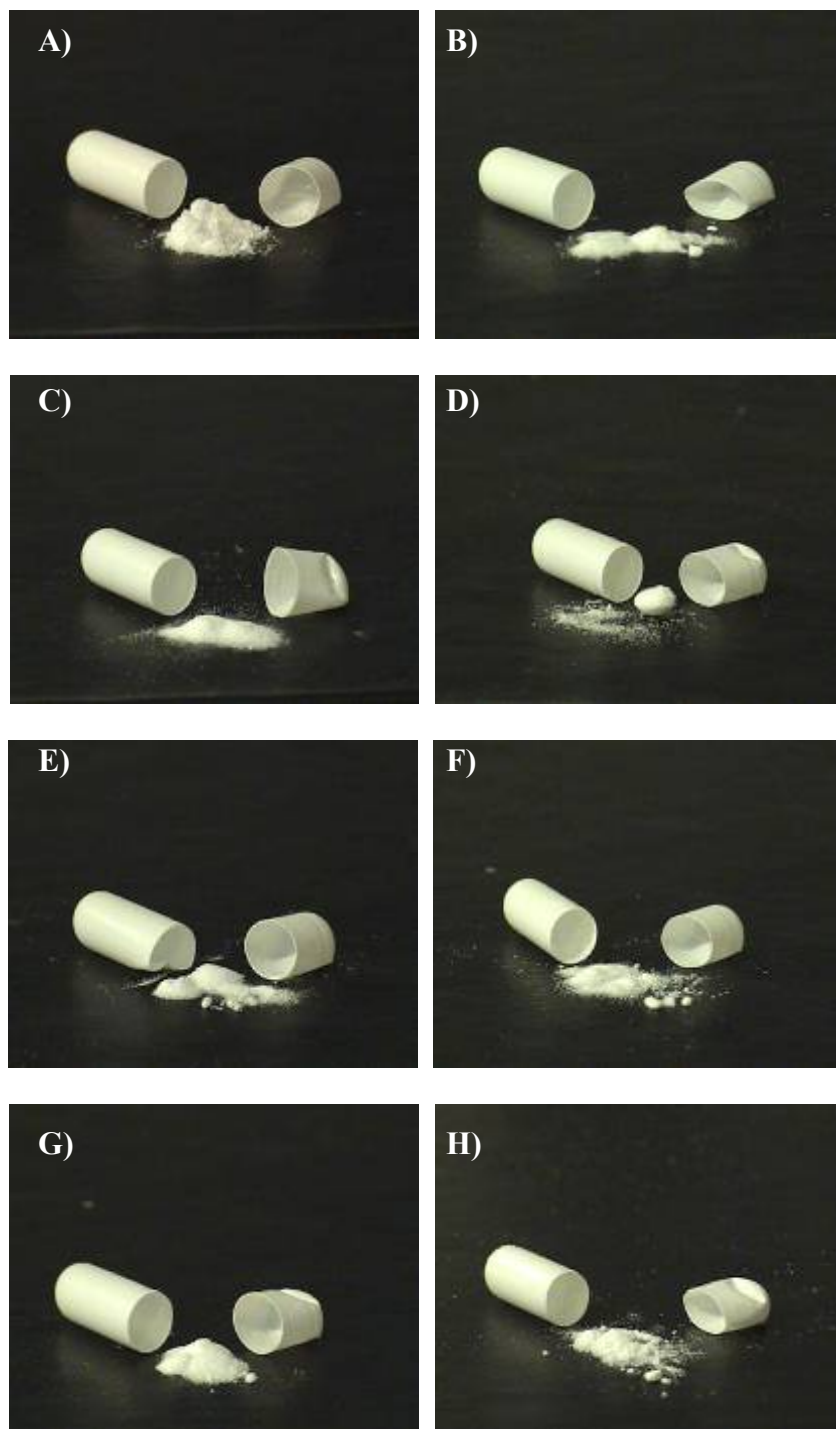


**Figure 4.17** Optical images of A) Lactochem and budesonide at 25°C, 75%RH and B) at 40°C, 75%RH, C) 0.25%w/w MgSt+Lactochem+budesonide at 25°C, 75%RH and D) at 40°C, 75%RH, E) 0.5%w/w MgSt+Lactochem+budesonide at 25°C, 75%RH and F) at 40°C, 75%RH, G) 1.0%w/w MgSt+Lactochem+budesonide at 25°C, 75%RH and H) at 40°C, 75%RH.

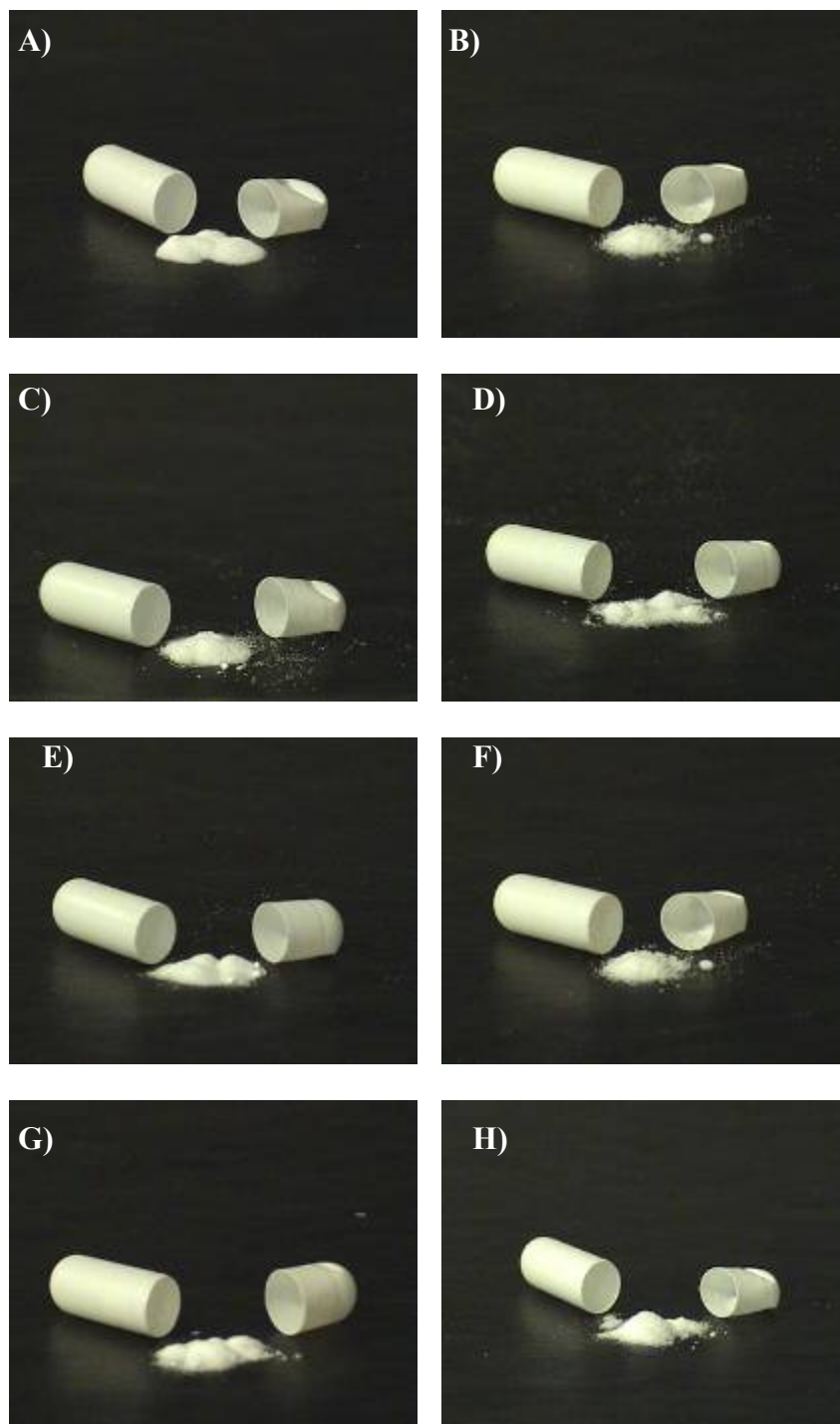


**Figure 4.18** Optical images of A) Nanolac and budesonide at 25°C, 75%RH and B) at 40°C, 75%RH, C) 0.25%w/w MgSt+Nanolac +budesonide at 25°C,75%RH and D) at 40°C,75%RH, E) 0.5%w/w MgSt+Nanolac +budesonide at 25°C,75%RH and F) at 40°C,75%RH, G) 1.0%w/w MgSt+Nanolac +budesonide at 25°C,75%RH and H) at 40°C,75%RH.

## 4.5 Conclusions

The variation in temperature and relative humidity levels of the environment of a typical carrier based DPI formulation was found to influence the aerosol delivery performance. This study suggested that capillary interactions influence DPI performance. As humidity increases, capillary forces become a dominating factor because of the multilayer sorption of water onto crystal surfaces. Ultimately, this increase in energy will influence the aerosolisation performance of the DPI formulation. Furthermore significant differences in aerosolisation efficiency at elevated humidities may be attributed to variations in surface stability. The relationship between humidity and aerosolisation performance can be attributed to the balance of interparticulate forces acting between the individual particulates, the proportion of each being related to the physical and chemical properties of the material. The addition of 0.5% w/w MgSt to both types of formulations provided a protective coating which kept it stable under the high RH and temperature which it was subjected and even increased its aerosolisation performance suggesting that 0.5% w/w of MgSt is the optimum concentration for maintaining a formulation stable at elevated humidity and temperature. Insufficient detachment and deaggregation of drug particles on inhalation is a major reason for the ineffective delivery of drugs to the lungs. These factors have to be carefully balanced so as to ensure dose uniformity and delivery efficiency of drugs from dry powder inhaler formulations.

This study has clearly emphasized the need to understand long term stability issues in order to achieve and maintain aerosolisation performance. Clearly, since an increase in adhesion energy will reduce the dispersion and deaggregation properties of a DPI formulation, the environmental conditions during processing, packaging and storage will ultimately influence the aerosolisation efficiency and therapeutic efficacy of the respirable drugs to the respiratory tract.



## 4.6 References

1. Young P.M, Price R, Tobyn M.J, Buttrum M, Dey F, “Investigation into the effect of humidity on drug-drug interactions using the atomic force microscope”, *Journal of Pharmaceutical Sciences* 2003b;92:815-822.
2. Young P.M, Price R, “The influence of humidity on the aerosolisation of micronised and SEDS produced salbutamol sulphate”, *European Journal of Pharmaceutical Sciences* 2004;22:235-240.
3. Bérard V, Lesniewska E, Andrès C, Pertuy D, Laroche C, Pourcelot Y, “Dry powder inhaler: influence of humidity on topology and adhesion studied by AFM”, *International Journal of Pharmaceutics* 2002;232:213-224.
4. Finot E, Lesniewska E, Mutin J.C, Hosain S.I, Goudonnet J.P, “Contact force dependence on relative humidity: investigations using atomic force microscopy”, *Scanning Microscopy* 1996;10:697-708.
5. Young P.M, Price R, Tobyn M.J, Buttrum M, Dey F, “Effect of humidity on aerosolization of micronized drugs”, *Drug development and industrial pharmacy* 2003a;29:959-966.
6. Jashnani R.N, Byron P.R, Dalby R.N, “Testing of dry powder aerosol formulations in different environmental conditions”, *International Journal of Pharmaceutics* 1995;113:123-30.
7. El-Sabawi D, Price R, Edge S, Young P.M, “Novel temperature controlled surface dissolution of excipient particles for carrier based dry powder inhaler formulation”, *Drug Development and Industrial Pharmacy* 2006;32:243-251.
8. O’Brien F.E.M, “The control of humidity by saturated salt solutions”, *Journal of Scientific Instruments* 1948;25:73-76.
9. Briggner L-E, Buckton G, Bystrom K, Darcy P, “The use of isothermal microcalorimetry in the study of changes in crystallinity induced during the processing of powders”, *International Journal of Pharmaceutics* 1994;105:125-135.
10. Buckton G, Darcy P, “The use of gravimetric studies to assess the degree of crystallinity of predominantly crystalline powders”, *International Journal of Pharmaceutics* 1995;123:265-271.

11. Coelho M.C, Harnby N, "The effect of humidity on the form of water retention in a powder", *Powder Technology* 1978;20:197-200.
12. Müller-Walz R, Keller M, "Improved fine particle fraction of carrier-based salbutamol dry powders for inhalation", *Drug delivery to the lungs IX* 1998, p.80-83.
13. Coelho M.C, Harnby N, "Moisture Bonding in Powders", *Powder Technology* 1978;20:201-205.
14. Price R, Young P.M, Edge S, Staniforth J,N, "The influence of relative humidity on particulate interactions in carrier-based dry powder inhalers formulations", *International Journal of Pharmaceutics* 2002;246:47-59.
15. Lachiver E.D, Abatzoglou N, Cartilier L, Simard J.S, "Agglomeration tendency in dry pharmaceutical granular systems", *European Journal of Pharmaceutics and Biopharmaceutics* 2006;64:193-199.
16. Orr N.A, Sallam E.A, "Content uniformity of potent drugs in tablets", *Journal of Pharmacy and Pharmacology* 1978;30:741-747.
17. Kaye B.H, "Powder mixing", Chapman & Hall, London, 1997, p.263.
18. Podczek F, "The influence of particle size distribution and surface roughness of carrier particles on the in-vitro properties of dry powder inhalations", *Aerosol Science and Technology* 1999;31:301-321.
19. Finot E, Lesniewska E, Mutin J.C, Hosain S.I, Goudonnet J.P, "Contact force dependence on relative humidity: investigations using atomic force microscopy", *Scanning Microscopy* 1996;10:697-708.
20. Telko M.J, Hickey A.J, "Dry powder inhaler formulation", *Respiratory Care* 2005;50:1209-1227.
21. Ward G.H, Schultz R.K, "Process-induced crystallinity changes in albuterol sulphate and its effect on powder physical stability", *Pharmaceutical Research* 1995;12:773-779.
22. Lehto P, Laine E, "Kinetic study on crystallization of an amorphous lubricant", *Pharmaceutical Research* 1997;14:899-903.
23. Zeng X.M, Martin G.P, Mariott C, "Particulate Interactions in Dry Powder Formulations for Inhalation", 2001, London: Taylor & Francis.

24. Harjunen P, Lankinen T, Salonen H, Lehto V.-P, Järvinen K, “Effects of carriers and storage of formulation on the lung deposition of a hydrophobic and hydrophilic drug from a DPI”, *International Journal of Pharmaceutics* 2003;263:151-163.
25. Hickey A.J, Gonda I, Irwin W.J, Fildes F.J.T, “Effect of hygroscopic coating on the behaviour of a hygroscopic aerosol powder in an environment of controlled temperature and relative humidity”, *Journal of Pharmaceutical Science* 1990;79:1009.

# **Chapter 5**

## **Influence of carrier lactose particles modifications on dry powder inhalers performance directly monitored by in line optical measurements**

### **5.1 Introduction**

#### **5.1.1 Laser diffraction**

Laser diffraction techniques, may become a powerful tool in the rapid development and testing of inhalation devices and their formulations. The technique is fast, reliable and the theories of light diffraction are well described<sup>1</sup>. Particle sizing by laser diffraction works on the principle that small particles in the path of a monochromatic light beam scatter the light in a characteristic, symmetrical pattern onto a Fourier lens, and their intensities measured by a photodetector array. With the use of an inversion algorithm, a particle size distribution is inferred from the collected diffracted light data<sup>2</sup>. This technique is widely used for particle size analysis, and there are several commercial instruments based on the principle of laser light diffraction in determining particle sizes distributions<sup>3</sup>. A schematic diagram of the principles of laser light diffraction is shown in Figure 5.1.

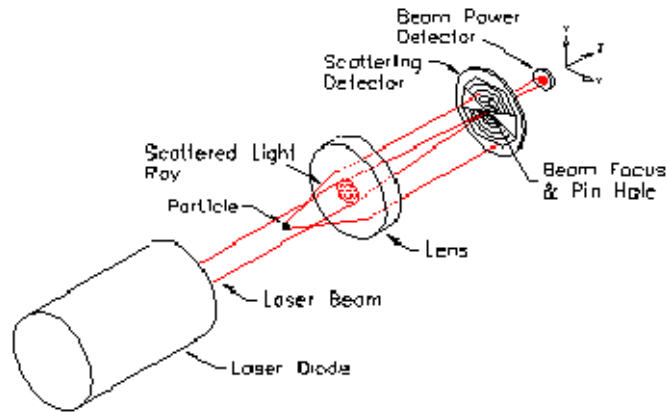


***Figure 5.1 A diagram showing the principle of the laser light diffraction.***

However, laser diffraction does have limitations. It exhibits poor inter-instrument reproducibility, it offers limited resolution and gives information of limited value for submicrometre particles which leads to inaccurate data<sup>4</sup>. The analyser-to-analyser reproducibility is determined by how accurately the laser can be aligned and measurement reproducibility by how consistently the alignment can be maintained. If the laser is not accurately aligned, the light scatter pattern will be observed at the incorrect angle, and hence lead to errors in particle sizing measurements<sup>4</sup>. The resolution is the ability of the system to differentiate between similarly sized particles in order to get measurements of the correct shape and width of the particle size distribution and to determine any tails or shoulders. It is determined by how well the angular scattering pattern is measured. This problem can be addressed by covering a wide angular range with a sufficient number of detectors, so that information from the scattered light is not lost<sup>4</sup>.

A major advantage of the approach is that it can analyse a large number of classes in over a wide size range which is important in lung deposition. Laser diffraction was first introduced for analysing the output of nebulisers in the 1990's<sup>1</sup>. This technique was used for nebulisers because they generate aerosols over a long period of time (5 to 30 minutes). The size distribution for aqueous droplets obtained with laser diffraction were shown not to differ significantly from aerodynamic size distribution<sup>5,6,7,8</sup>. However, the problem in testing

aqueous aerosol particles was what diffraction theory to use (Mie or Fraunhofer) and how to replicate the inspiratory flow rate through the inhaler<sup>9</sup>. The application of in line laser diffraction for carrier based DPI evaluation or development has not been extensively investigated. The major argument is the fact that the aerosol from a DPI is a mixture of primary particles and small agglomerates, for which the dynamic shape factor and density vary from particle to particle and so an aerodynamic size distribution can not be calculated from the laser diffraction result<sup>1</sup>. However, aerodynamic size distribution is only important for predicting lung deposition. The objective of a DPI development is to get the size distribution of the aerosol from the DPI as close as possible to the size distribution of the primary drug particles. This has to be achieved for the highest possible mass fraction of the dose and under inspiratory conditions.

### **5.1.2 VariDose device**

Varidose is a new optical instrument, developed by Loughborough University, which may speed up the measurement of drug inhaler performance, therefore reducing the amount of time the pharmaceutical industry spends in research and development and during quality control measurement of formulations. It utilises custom-designed and state of the art optoelectronics and takes less than 60 seconds to run each test. It could be a potential breakthrough for the pharmaceutical industry as it enables quick and efficient testing of a wide range of drug-device combinations, without relying on standard inhaler testing methods. Images of the varidose system are shown in Fig. 5.2.

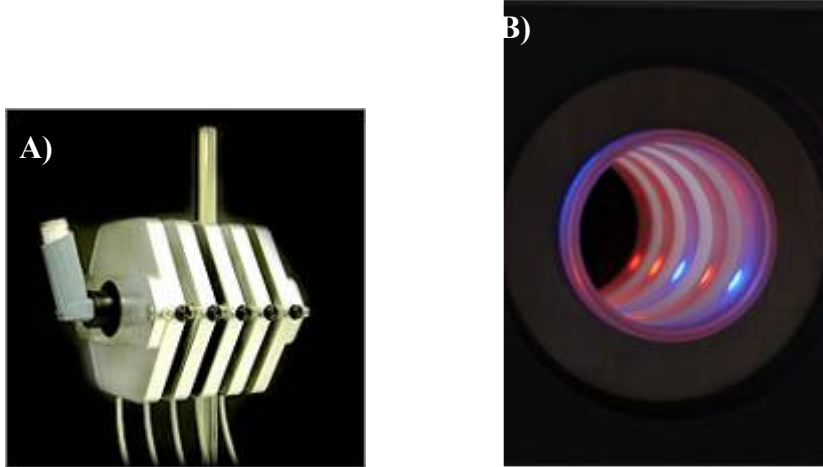


**Figure 5.2 Images of the A) VariDose device with the sensor rings and B) the Varidose tube intersected by co-planar beams of blue and infrared light.**

The varidose measures the characteristic properties of an aerosol cloud from an inhaler as it passes through a tube intersected by co-planar beams of red, blue and infra-red light. As the light passes through, in-built sensors monitor the structure of the evolving cloud. The analysis is then presented on a standard PC. The varidose provides valuable information on the detailed characteristics of the particle or droplet cloud emitted by the inhaler and can also be positioned in-line with other measurement devices or a patient.

The results can be used to investigate essential cloud characteristics related to variability in particle size distribution, fine particle fraction and dose to pin-point how design modifications could improve both drug and device effectiveness<sup>10</sup>. The non-scattered component of a collimated light beam  $I$ , after traversing a homogeneous scattering medium of thickness  $L$ , is estimated by the equation:

$$\text{Equation 5.1} \quad I = I_0 \exp(-\mu_{tr}L)$$

Where  $I_0$  is the intensity of the incident light and  $\mu_{tr} = \mu_a + \mu_s(1-g)$  is the transport attenuation coefficient.

The absorption coefficient  $\mu_a$ , the scattering coefficient  $\mu_s$  and the anisotropy factor  $g$  depend on the optical and geometrical properties of the particles and on the wavelength of the light. The scattering anisotropy  $g$ , is calculated as the mean cosine of the scattering angle. Depending upon the conditions of the medium, this value can vary from  $g = 1$  (forward scattering), through  $g = 0$  (isotropic scattering) to  $g = -1$  (back scattering). An estimate of the reduced scattering coefficient  $\mu_s (1-g)$  for the drug cloud can be made by means of a particle scattering model and this model will dominate the absorption coefficient (in the wavelength of interest: 450-850 nm), hereafter assumed to be zero<sup>10</sup>. Assuming that particles scatter light independently the scattering coefficient of many particles can be calculated via:

Equation 5.2 
$$\mu_s = N\sigma_s$$

Where  $N$  is the number of scattering particles per unit volume and  $\sigma_s$  is the scattering cross-sectional area of a single particle.

For mono-dispersions, the particle number is the ratio of the particle volume concentration  $C_v$  and the single-particle volume (assumed to be spherical):

Equation 5.3 
$$N = \frac{6C_v}{\pi D^3}$$

Where  $D$  is the particle diameter. Using equation 5.3, the transport scattering attenuation coefficient is given by:

Equation 5.4 
$$\mu_{tr} = \frac{6(1-g)C_v\sigma_s}{\pi D^3}$$



The scattering cross-section is sometimes expressed in terms of the product between a geometric cross-section (again assumed spherical) and a scattering efficiency factor  $Q$ , in which case:

Equation 5.5 
$$\mu_{tr} = \frac{3(1-g)C_v Q}{2D}$$

The scattering cross section and the anisotropy factor for spheres were calculated by means of Mie scattering theory.

The varidose is sensitive to the dynamics of the cloud, not only in terms of its density, but also in terms of its homogeneity. In making the hypothesis that the distribution of particles in the drug cloud is not homogeneous, it is also implied that the degree of inhomogeneity will characterise the efficiency of actuation, formulation and device performance. One way in which the cloud might be inhomogeneous is in terms of the spatial distribution of particle size and this might be a consequence of the dissociation and entrainment mechanism of cloud formation<sup>10</sup>. A simultaneous analysis of the delivered dose using light obscuration (Varidose) and a twin stage impinger (TSI) was performed as part of this study.

### **5.1.3 Basic components of a Varidose**

The essential components of the varidose are shown in figure 5.2. The airflow can be provided either by a patient, a breathing simulating machine or a vacuum pump. The airflow actuates an inhaler device creating the aerosol cloud. The cloud then propagates through a glass tube and the sensor module makes measurements at a given distance from the inhaler's mouthpiece. All connections in the flow path are airtight and the tube is screened from the ambient light. The collimated light beam is formed by a SELFOC® fibre collimator Ocean Optics tungsten halogen light source (bulb colour temperature 3,100 °K). The SELFOC® fibre collimator is comprised of a 0.25 pitch GRIN lens and a 200µm fibre with numerical aperture of 0.50 and beam divergence angle of 6.5°. The same fibre

collimator is used for collecting the light passing through the cloud. An Ocean Optics fibre optic variable attenuator FVA-UV controls the illuminating intensity<sup>11</sup>.

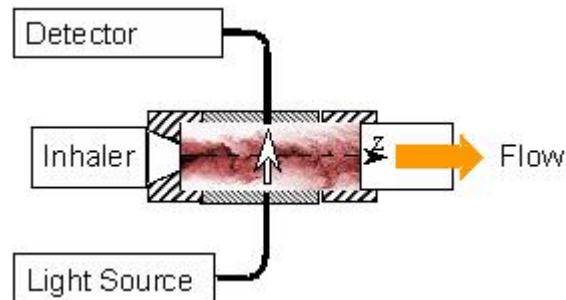


**Figure 5.3 Schematic diagram for optical characterization of the pulmonary drug delivery.**

#### **5.1.4 Sensor position**

The position of the sensor down the stream of propagation produces a profound influence on the aerosol sample that has been actually measured. For instance, if the sensors were adjacent to the mouthpiece of the inhaler the measurement would characterize particles in the immediate vicinity of the inhaler. The sensor records an accumulative effect of temporal and spatial variations in the cloud. The right position for the sensors depends on the individual experiment requirements and the purpose of the measurements. For example, multiple sensors aligned on the cloud path would provide information on the cloud development. For pulmonary delivery, the aim is to characterize the cloud that is emitted from the device. Therefore, in this case the cloud in the middle of the mouth represents a viable sample of the particles which would be available for deep lung deposition<sup>11</sup>.

Particles moving along the glass tube interact with the tube walls resulting in the constant contamination of the tube walls with particle sediment. The wall sediment affects the intensities of the illuminating and collected light<sup>11</sup>. The residue of fine particles can be

taken into account by the data analysis and may even contribute to the aerosol cloud characterization.

#### **5.1.5 Data acquisition**

The varidose measures the light intensity as a function of time. A light detector provides a signal that is proportional to the number of photons accumulated by the detector during the measurement period. The measurement period is a time period and is often referred to as the integration time for the detection system. The detector's readings are streamed to computer memory with the time stamps, using an appropriate integration time. A computer stores the data for further analysis. The light intensity, detector's sensitivity and the integration time are the main variable parameters which control the accuracy and efficacy of the measurement<sup>11</sup>.

#### **5.1.6 Acquisition frequency**

As an aerosol cloud is released from an inhaler device it possesses characteristics such as volume, the start and the end of the cloud release, particle properties and the propagation velocity. The cloud volume and geometric dimensions of the passage define the cloud length, which can be expressed in units of time or length. A single optical sensor records the light intensity as a function of time; therefore each actuation is characterized by a temporal profile of light intensity.

#### **5.1.7 Data analysis**

The analysis of the varidose measurements relate the aerosol content and the light obscuration at a given wavelength. Varidose provides a spectrum of transmitted light intensity for every 5 milliseconds. The profile can be characterized by the position of the maximum (the peak position), the maximal value (the peak value) and the full width of the half maximum<sup>11</sup> (FWHM).

## **5.2 Aims of the study**

The in-vitro deposition characteristics of aerosol based formulations requires significant amount of resources, in terms of personnel and analytical equipment. Furthermore, due to its limitation in automation it is a highly time consuming exercise. There is therefore an ever increasing need to develop a high-throughput aerodynamic classifier which can rapidly test the performance and predict the variability in the delivery characteristics of both nasal and inhalation based formulations.

This study will investigate the use of a novel in-line optical sensing technology for actuation-by-actuation assessment and to utilise the system to investigate the physicochemical properties which govern the aerosol delivery of inhalation systems. The ultimate aim of this study is to develop a system which can lead to an effective and efficient system for testing aerosol based systems for design, cycling, manufacturing and therapeutic management.

More precisely, this study was performed in order to evaluate the use of the Varidose device as a potential screening tool. The pharmaceutical devices currently available for the characterisation of drug formulations like the NGI, TSI, MSLI are labour intensive, therefore costing a lot of money and time to pharmaceutical companies<sup>12</sup>. A device which would characterise the drug formulations and give the information required in a shorter period of time, would be of benefit to pharmaceutical companies. The Varidose could potentially meet up to these requirements but further tests need to be carried out.

## **5.3 Methods**

General methods of each technique or apparatus used in this study are described in detail in Chapter 2.

### **5.3.1 Preparation of Magnesium stearate-lactose blend**

Blends of  $\alpha$ -lactose monohydrate (particle size 63-90 $\mu$ m) with 1% w/w concentration of magnesium stearate were prepared under high shear. Half the amount of lactose required for the blend was accurately weighed and then the amount of magnesium stearate which was accurately weighed was placed in the lactose. The other half remaining amount of lactose was subsequently weighed so as to have the total mass required and sandwiched between the magnesium stearate layer. The blend was mixed in the high shear mixer, KSM2 (Brown, Kronberg, Germany) for 1 minute. Approximately 3.9416g of the magnesium stearate – lactose blend was accurately weighed.

Budesonide was subsequently blended geometrically with the MgSt-lactose blend in a plastic vial. An amount of the blend (~0.12g), equivalent to about twice the total mass of budesonide being used for the blend was put in the plastic vial and then the amount of budesonide was added (0.0584g). This was then mixed for 1 minute using a Whirlimixer (Fisons Scientific Apparatus, Loughborough, UK) and more lactose was added in geometric quantities, followed by mixing with the Whirlimixer for 1 minute after each addition. This was done until all the lactose (3.9416g) was added to the vial. The blend was then mixed in a turbula mixer (Turbula, Glen Creston Ltd, Stanmore, UK) at 46 revolutions per minute for thirty minutes. The formulation was then placed in a jar that was tightly sealed and allowed to stand for 48 hours. Drug content uniformity of the formulation was carried out as described in Chapter 2.

### **5.3.2 Varidose experimental set up**

The analysis was performed using Varidose and a Twin Stage Impinger (TSI) in tandem (Copley Scientific Apparatus, Nottingham, UK). The Varidose sensor-rings were placed between the mouthpiece of the inhaler and the entrance of the TSI. The distance between the ring's optical axes was set at 19mm. The varidose was connected to a laptop which had the varidose Software V3.5. The distance between the mouthpiece of the inhaler and the first sensor ring was 25 mm. The settings on the software were: trigger channel 1,

experiment time 2000msec and time out 10000msec. A photograph of the experimental set-up of the varidose rings connected to the TSI is shown in Fig 5.4.



*Figure 5.4 An image of the Varidose-TSI experimental set up.*

### **5.3.3 In vitro aerosolisation studies**

#### **1) Experimental set-up**

The TSI contained 30 ml of mobile phase in stage 2 and 7 ml in stage 1, which at 60 L/min produced a cut-off mass median aerodynamic diameter of  $6.4 \mu\text{m}$  between the two stages. Flow rate was tested prior to operation using a calibrated flow meter. The varidose software settings were: trigger channel 1, experiment time 2000msec and time out 10000msec. The Rotahaler (GlaxoWellcome, UK) was primed by loading a filled capsule ( $33 \pm 4 \text{ mg}$ ) containing the formulation (budesonide and lactose pre-conditioned with 1% w/w MgSt) into the inhaler and twisting to separate the upper and lower sections exposing the formulations to an airstream passing through the device. The inhaler was attached to the cylindrical glass tube of the Varidose via a rubber mouthpiece adaptor. Upon completion of

the capsule firing, the TSI apparatus was then dismantled and each stage was washed with mobile phase into 100ml volumetric flasks. This procedure was carried out until 20 actuations had been conducted. The concentration of the drug was then determined using the HPLC method.

## **2) Addition of a pre-separator to the Varidose setup**

A pre-separator was also added between the USP induction port and the Varidose sensor unit, followed by the TSI without the throat piece, in order to prevent oversized particles from depositing on the glass tube. The Varidose sensor unit was placed in a vertical orientation to the air flow. The pre-separator incorporates two collection surfaces working in tandem. The first (scalper) collection surface is a circular cup, containing 15ml of mobile phase, beneath the inlet of the pre-separator and is intended to remove very large particles like lactose carrier particles. The mobile phase is added to reduce particle re-entrainment from the cup. The scalper is followed by the second collection surface, which has a much sharper cut than the scalper to eliminate most particles that are larger than the cut size of the first stage of the impactor itself, while not removing particles that are of a size to be captured on the second impactor stage.

The pre-separator was required, for the in vitro testing of the formulations containing extrinsic lactose fines. In these formulations a large amount of fines was present, and therefore a pre-separator was used to capture most of the large particles enabling only the small drug particles to pass through it and continue through the varidose device.

### **5.3.3.1 Preparation of carrier based formulations containing fines**

Ten percent of Sorbolac 400 (fines of lactose) was geometrically blended with the untreated (Lactochem) and surface etched lactose (Nanolac) in a ratio 1:67.5 w/w % using the same procedure mentioned above. Briefly, 3.604g of the carrier was weighed out and 0.40024g of Sorbolac 400 and were mixed together by geometric mixing using a Whirlymixer (Fisons Scientific Equipment, Loughborough, UK) for 60 seconds. Upon

completion of the geometric mixing, the blend was placed in a Turbula (Bachofen, Basel, Switzerland) and blended at 46 rev/min for 30 minutes. Then, 3.9743g of this blend was weighed out and geometrically mixed with 0.0257g of budesonide according to the procedure mentioned above. Blends were stored in a tightly sealed container with a saturated salt solution of potassium carbonate, which produced a relative humidity of 44% RH at 25°C. Hard HPMC capsules were filled with  $25 \pm 3$ mg of powder blend.

## 5.4 Results and Discussion

### 5.4.1 Scanning electron microscopy

To examine the relative distribution of the drug particles on the surface of the lactose carrier, scanning electron microscopy was used. Figure 5.7 shows electron micrographs of the surface topography of the blend containing budesonide and lactose, in a 1:67.5 ratio, together with 1%w/w MgSt.

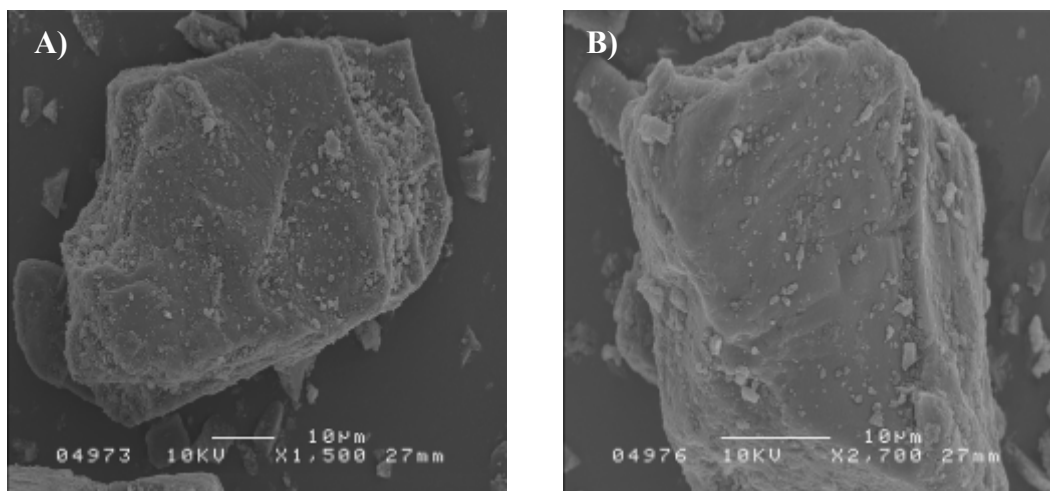


**Figure 5.5** Representative scanning micrographs of blend containing budesonide and lactose pre-conditioned with 1% w/w MgSt at A) x1500 and B) x2700 magnifications.



### 5.4.2 In vitro aerosolization studies

Figure 5.6 shows the variation of the light obscuration for 9 consecutive actuations from a Rotahaler DPI device. There is no noticeable repeated pattern in these actuations, which is indicative of high dose-by-dose variability. Each actuation has been simultaneously characterised by the varidose using two sensor rings. The distance between the two subsequent rings was approximately 4mm. Each ring contains three azimuth sensors ( $120^\circ$  between the sensor axes in the ring plane).

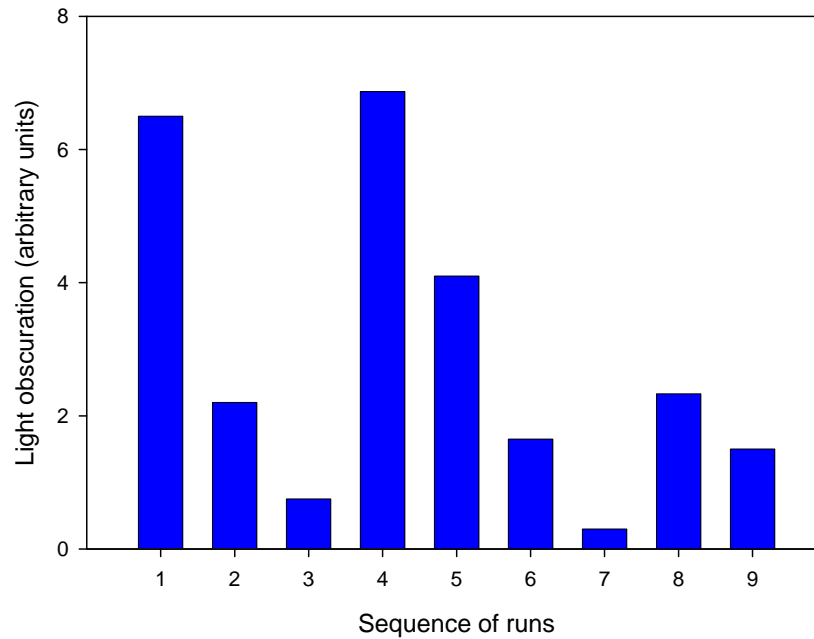


***Figure 5.6 A graph showing the light obscuration values for each actuation estimated by the varidose apparatus.***

The three profiles from the same ring are used to present the 3D visualisation of the optical density of the cloud. The 3D visualisations from the sequent rings indicate the evolution of the cloud during propagation. To describe the cloud evolution in comparative terms, each obscuration profile is characterised by the same parameter. To evaluate the variations in the

light obscuration data from the varidose, the corresponding fine particle delivery of each shot was measured via the twin stage impinger (TSI). The fine particle dose for the nine shots are shown in Figure 5.7. From these data, there is a suggestion that the light obscuration measured with the Varidose strongly correlates with the fine particle dose (FPD) measurements. This agreement is more clearly represented in Figure 5.8.

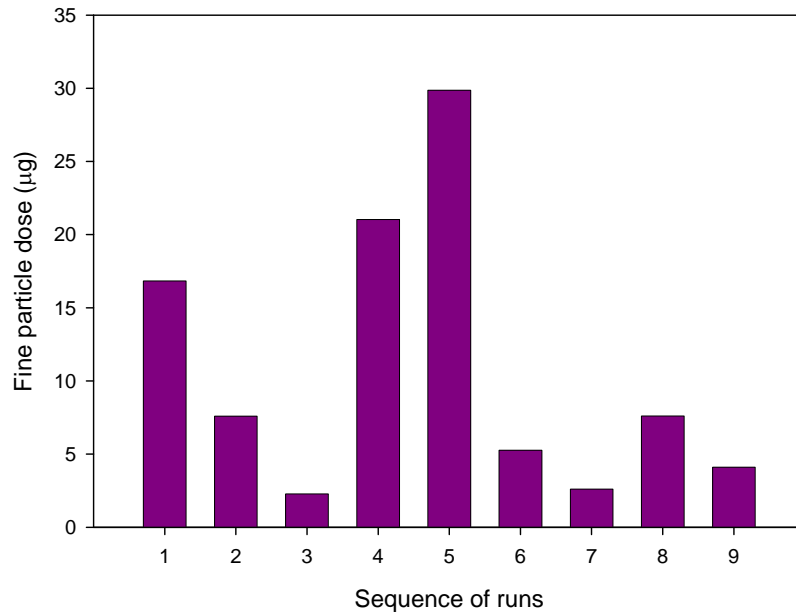


***Figure 5.7 A graph showing the FPD for each actuation calculated with the TSI.***

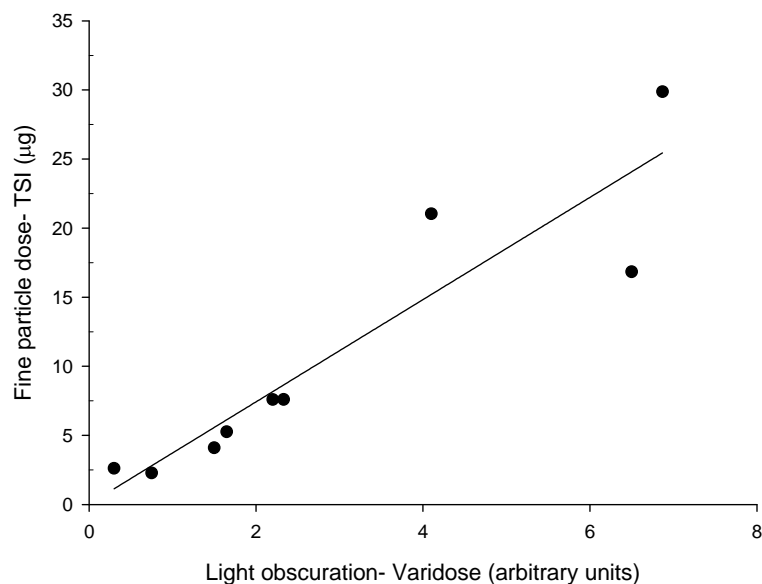


***Figure 5.8 The correlation graph showing the relationship between the FPD estimated by the Varidose and calculated by the TSI.***

As shown, there is a high variability between each actuation in the dose being delivered to the respiratory tract. The observed large variation is consistent with typical dose variations delivered by the Rotahaler DPI device. Furthermore, this variability in the dose shown with the data calculated from the TSI was also observed with the data from the varidose. As shown in Figure 5.8 the TSI data correlates with the data from the varidose; where the fine particle dose was high, the light obscuration was also high and where the fine particle dose was low, the light obscuration was also low. However, there was a noticeable difference between actuations 4 and 5. Actuation 4 had the higher light obscuration as can be seen in figure 5.7 and actuation 7 has the lowest light obscuration. However, actuation 5 has the higher fine particle dose from the TSI measurements. For low doses, the shot by shot measurements correlated well. This rapid means of testing formulations and devices is critically important for testing inhalation systems.

Upon construction of the correlation graph a straight line was observed with  $R^2 = 0.8476$ . There is good correlation between low dose delivery and the light obscuration, but there might be some issue with the higher concentrations which may be in relation to the saturation issues with respect to the obscuration. Nevertheless, these data suggest that the varidose may provide a semi-empirical means of characterising the aerosol cloud produced via an inhalation device and a sensitive means of determining dose-by-dose fluctuations.

The main purpose for using the varidose is to have an estimation of the fine particle dose of a formulation. However, in the presence of significant amount on intrinsic and extrinsic fine excipient material evaluating the dose variability of the drug may be too difficult. To evaluate the influence of fine lactose particles on the varidose response, formulations containing 10%w/w fines were tested. To limit the issues relating to high obscuration, a pre-separator was attached to the end of the throat section of the impinger to remove coarse particles.

The experiment was performed in the same set up as above with the exception of a pre-separator. The addition of a pre-separator should increase the varidose sensitivity to the variation of the drug dose. If the TSI data correlated with the varidose data then the varidose could be used for the investigation of complex powder mixtures.

As shown in figures 5.9, 5.10 and 5.11, 5.12 the peak obscuration data from the varidose did not correlate with the fine particle dose data from the TSI. The varidose data show that all actuations were characterised with a low peak value and a high residue value. In addition, the Nanolac formulation had slightly lower peak obscuration values compared to the lactochem formulation and this could be due to lower amounts of fines scattering the light. It is hard to make any definite conclusions from these data due to the low level of obscuration. While it could be possible that the position of the varidose sensors was not optimal for the purpose of the dose evaluation, it is more likely that the co-removal of extrinsic fines during aerolisation masks the determination of the dose variation of the active pharmaceutical ingredient.

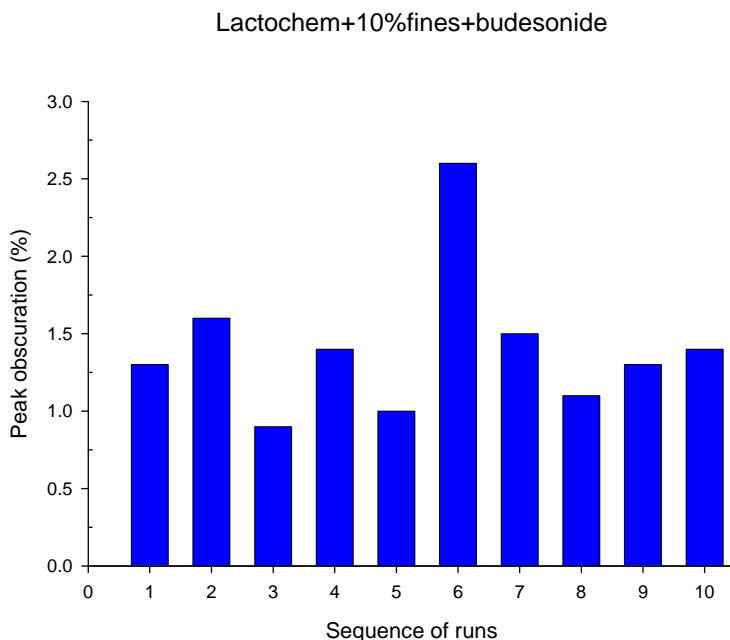


**Figure 5.9** A graph showing the light obscuration values for each actuation estimated by the Varidose for the formulation containing Lactochem+10%fines+budesonide.

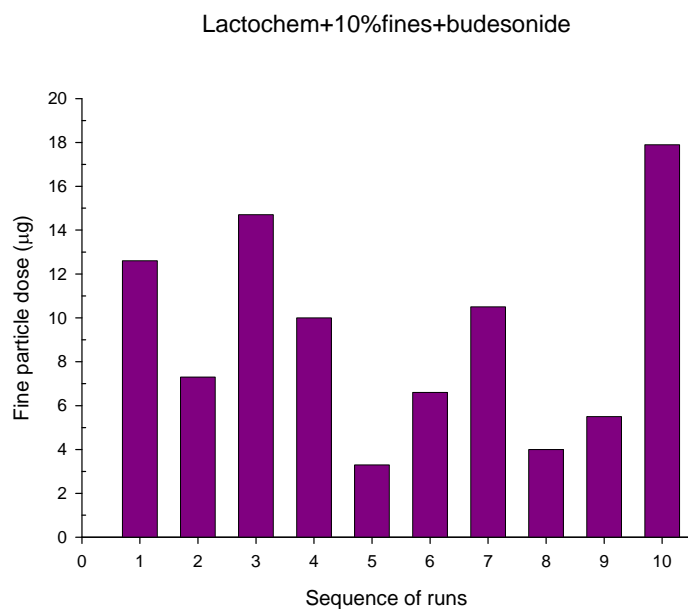


**Figure 5.10** A graph showing the FPD for each actuation calculated with the TSI for the formulation containing Lactochem+10%fines+budesonide.

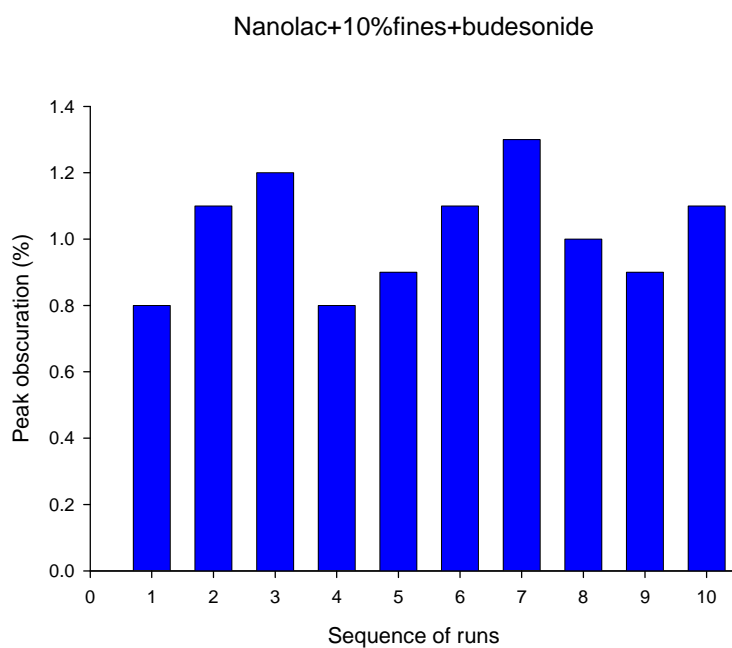


**Figure 5.11** A graph showing the light obscuration values for each actuation estimated by the Varidose for the formulation containing Nanolac+10%fines+budesonide.

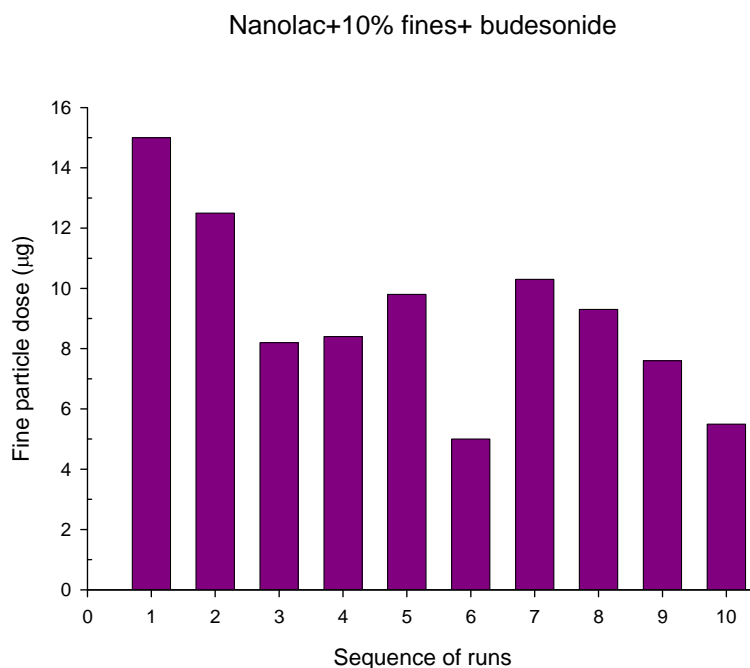


***Figure 5.12 A graph showing the FPD for each actuation calculated with the TSI for the formulation containing Nanolac+10%fines+budesonide.***

A study performed by Kusmartseva et al (2004)<sup>10</sup> utilising the varidose technology showed a strong correlation between the varidose measurements and a Bricanyl® Turbohaler® with the varidose and the TSI, with a correlation coefficient of 0.94 and  $p < 0.0001$  for the assessment of variations in fine particle dose. However, the formulation in this study consisted of pure terbutaline sulphate and no excipients, so each actuation contained 500µg of terbutaline sulphate.

Two types of drug formulations have been investigated simultaneously in this study using the varidose and in vitro testing (TSI). The formulations contained a significant amount of excipients: the carrier particles and lactose intrinsic fines. These types of formulations seriously challenged the varidose assessment. The in vitro data from the formulations containing 1.0% w/w MgSt correlated well with the varidose light obscuration data. However, when conducting further studies, the correlation with increasing % obscuration was not observed.

Therefore the attempt to classify and identify a formulation with good aerosol deposition performance with the varidose at this stage was unsuccessful. Further studies need to be conducted adjusting the experimental set-up and the position of the varidose sensors.

## **5.5 Conclusion**

Pharmaceutical industries are continually investigating easier ways of determining and classifying the performance of their formulations that will save time and resource. Laser diffraction has been shown to be a valuable tool for comparative inhaler evaluation, device development, powder formulation and quality control. The varidose device which is based on laser diffraction has the potential of complying to the requirements needed in such a system by simply analysing the aerosol cloud generated by the inhaler formulation investigated. The varidose technology has been developed and intended for the assessment of efficiency of the pulmonary delivery. It requires only a few seconds to assess a single dose actuation, instead of two hours required for a measurement by a cascade impactor. In addition to that, more detailed and also different information about the aerosol cloud is obtained. It was also designed to be used as an indicator for how well the drug formulation is dispersed during pulmonary delivery and therefore may rapidly measure the delivered dose in-line with a patient. However, the attempt to classify and identify different grades of formulations of good performance with the varidose at this instance was unsuccessful. The main reason for this may relate to the experimental set up. Further studies need to be conducted in order to establish an optimal experimental set-up for different types of formulations.

This study suggested that a relation between the varidose data and the TSI data was not established and at this instance the varidose can not be used as a stand-alone technology for evaluating carrier based formulations. The varidose could potentially be used to make quick assessment of the performance of a formulation, but further studies need to be conducted in order to assure the readings taken from the varidose are accurate and reliable.

## 5.6 References

1. de-Boer A.H, Gjaltema D, Hagedoorn P, Frijlink H.W, “Characterization of inhalation aerosols: a critical evaluation of cascade impactor analysis and laser diffraction technique”, *International Journal of Pharmaceutics* 2002;249:219-231.
2. Meyer W.V, Tin P, Lock J.A, Cannell D.S, Smart A.E, Taylor T.W, “Laser light scattering with multiple scattering suppression used to measure particle sizes”, [www.grc.nasa.gov/www/RT1998/6000/6712meyer.html](http://www.grc.nasa.gov/www/RT1998/6000/6712meyer.html)
3. Puckhaber M, Rothele S, “Laser diffraction: Millenium-link for particle size analysis”, *Powder handling and processing* 1999;11:91-95.
4. Cooper J, “Particle size analysis- The Laser Diffraction technique”, *Materials World* 1998;6:5-7.
5. Hurley P.K, Smye S.W, Cunliffe H, “Assessment of antibiotic aerosol generation using commercial et nebulizers”, *Journal of Aerosol Medicine* 1994;7:217-228.
6. McCallion O.N.M, Taylor K.M.G, Thomas M, Taylor A.J, “Nebulization of fluids of different physiochemical properties with air-jet and ultrasonic nebulizers”, *Pharmaceutical Research* 1995;12:1682-1688.
7. McCallion O.N.M, Taylor K.M.G, Thomas M, Taylor A.J, “The influence of surface tension on aerosols produced by medical nebulizers”, *International Journal of Pharmaceutics* 1996;129:123-136.
8. Bridges P.A, Taylor K.M.G, “Nebulizers for the generation of liposomal aerosols”, *International Journal of Pharmaceutics* 1998;173:117-125.
9. Bohren C.F, Huffman D.R, “Absorption and scattering of light by small particles”, John Wiley & Sons Inc, 1983.
10. Kusmartseva O, Kattige A.S, Price R, Smith P.R, “In-line assessment of pulmonary drug delivery using light obscuration”, *Biosensors and Bioelectronics* 2004;20:468-474.
11. Kusmartseva O, “In-line technology for assessment of pulmonary drug delivery”, PhD thesis, Loughborough University 2005.
12. Marple V.A, Roberts D.L, Romay F.J, Miller N.C, Truman K.G, Van Oort M, Olsson B, Holroyd M.J, Mitchell J.P, Hochrainer D, “Next generation



pharmaceutical impactor (a new impactor for pharmaceutical inhaler testing) Part I: Design", Journal of Aerosol Medicines 2003;16:283-299.

# Chapter 6

## Conclusions

### 6.1 Introduction

Dry powder inhaler formulations consist of small drug particles ( $\leq 5\mu\text{m}$ ) and larger carrier particles. The drug particles are usually blended over the surface of the excipient. Upon aerosolisation, the drug particles detach from the surface of the excipient and penetrate into the lungs. However, in order to achieve this, the adhesive forces that exist between the drug and carrier particles have to be overcome in order to aerosolise the drug particles. One of the major challenges in dry powder inhalation is to achieve a controlled balance of the forces.

Many strategies have been employed in order to improve the aerosolisation efficiency of DPI formulations. These have mainly concentrated on reducing the force of adhesion by manipulating the macroscopic properties of the carrier particles. These include particle size<sup>1</sup>, particle shape<sup>2</sup>, surface rugosity<sup>3</sup> and surface passivation via addition of ternary components<sup>4</sup>.

This study focuses on the addition of a FCA, magnesium stearate (MgSt) and its relationship with the aerosolisation efficiency through modification of the interparticulate forces. It is clear that the addition of MgSt to a formulation modifies the balance between the interparticulate adhesions and the forces acting to overcome them during inhalation, as well as the presence of fines. This study, investigated the relationship between the concentration of MgSt in DPI formulations and their aerosolisation performance. This was achieved by using two different types of carriers in the powder formulations, Nanolac and Lactochem, and changing the concentration of MgSt within them. In addition, these formulations underwent long term stability testing by being stored for 3 months at 25°C, 75%RH and 40°C, 75%RH. Their aerosolisation performance was then re-tested to

examine any changes. Moreover, the VariDose device, which is a new emerging device for rapid drug screening was investigated for a potential indicator for how well the drug formulation is dispersed during pulmonary delivery.

## 6.2 Summary

In order to improve dry powder inhaler formulation delivery performance, the influence of the addition of different concentrations of MgSt to the formulations was investigated. Two different types of carriers were used for the preparation of the formulations: Nanolac and Lactochem, differing in their surface morphology and therefore the interparticulate forces.

The drug particles and the Lactochem surface have weak forces of adhesion between them due to their small surface contact area and therefore only a small amount of energy is required to detach them, making the drug particle detachment easier. In addition, Lactochem contains fines which could occupy the active sites of the carrier, leaving the passive sites to be occupied by the drug particles, facilitating their detachment. On the other hand, Nanolac has a smooth surface with a very small amount of fines in any, having a large surface contact area with the drug particles and therefore a large amount of energy is required to detach them rendering the detachment more difficult than for the lactochem.

With the addition of MgSt, the results showed that the addition of 0.25% w/w MgSt was the optimum concentration for the greatest aerosol deposition performance amongst the Lactochem formulations, while the 0.5% w/w MgSt was the optimum concentration for the greatest aerosolisation efficiency amongst the Nanolac formulations.

The influence of the environmental conditions on the aerosolisation performance of these formulations was then investigated upon storage for 3 months at different conditions; 25°C/44%RH, 25°C/75%RH and 40°C/75%RH. Results show that the addition of 0.5% w/w MgSt in DPI formulations is able to stabilise the powder blends against humidity and temperature. Whereas the controlled formulations which did not contain any MgSt were

heavily affected by moisture, the applied of 0.5% w/w MgSt helps to make the powder blend less susceptible to elevated humidity. The reason could be the formation of a hydrophobic coating by MgSt over the whole surface of the excipient, protecting it from moisture. Therefore, powder stability upon storage at high environmental conditions may be increased by the addition of 0.5% w/w MgSt. The addition of 0.25% w/w MgSt to the Lactochem formulations exhibited the greatest aerosol deposition performance, but however failed to keep this performance upon storage at elevated environmental conditions for a period of 3 months. On the other hand, the addition of 0.5% w/w MgSt to the Nanolac formulations exhibited the greatest aerosolisation performance as well as protecting the formulation from de-stabilising at high RH and temperature and even increasing its aerosolisation efficiency upon storage. Clearly, the environmental conditions under which a formulation may lose its efficacy should be defined, in order to avoid the large variations seen in the aerosol deposition performance of the DPI formulations.

A new emerging technology for an in-line, real-time assessment of the efficiency of pulmonary drug delivery was also investigated. The VariDose technology exploits the phenomenon of light scattering by small particles. Additionally, the technology investigates how the aerosol cloud changes along the propagation path. The experimental results of the first experiment performed show a strong correlation between the VariDose measurements and the conventional in-vitro data. However, upon further testing of more complex powder formulations and the addition of a pre-separator to the experimental set-up the results suggested no correlation between the VariDose measurements and the in-vitro data, failing to give estimations of the fine particle dose.

### **6.3 Suggested future work**

The data presented in this thesis and various previous studies clearly demonstrate that the interparticulate interactions play a major role in drug deposition performance of DPI formulations. However, despite the fact that this factor is quite important, only a very few studies exist in which improvement of the de-agglomeration efficiency is the objective, since most of the studies focus on the control of the adhesive forces in the mixture. It has been described by Amass et al (1996)<sup>5</sup> that different types of de- agglomeration forces can

be used but neither the effectiveness of these forces nor the principles to generate these forces have been studied thoroughly. Clearly, a better understanding of these de-agglomeration forces would possibly lead to a greater aerosolisation efficiency of the DPI formulations.

Moreover, such investigations are more preferably to be conducted concomitantly with extensive long term stability studies. In addition, extended effort may also be undertaken to gain a more valuable insight into the role of fine carrier particulates on aerosolisation behaviour and their mechanism of action since it is still unclear. The second area which would benefit from further study is the relationship between the environmental conditions and formulation performance. A suitable selection of an environmentally-insensitive salt with reduced hygroscopicity<sup>6</sup> that can be added to the formulations in order to avoid the humidity and temperature effects can be investigated. In addition, an acceptable range of temperature and humidity<sup>7</sup> should be determined which will enable the formulation to keep its efficacy over a period of time.

These studies should be repeated using other force control agents like leucine and lecithin and examining their effect on the aerosolisation efficiency of DPI formulations to determine which FCA can provide the greatest delivery performance. Clearly, the future advances in inhalation particle engineering will require a greater understanding of interparticulate interactions at the mesoscopic level<sup>8</sup> and the elucidation of specific physicochemical and environmental factors which govern their variability.

Dry powder inhalation research has been performed since the 1970's, but the sure thing is that the future in this field of research will continue to challenge researchers to develop approaches, devices and formulations that will maximize the clinical efficacy and patient compliance.

## 6.4 References

1. Zeng X.M, Martin G.P, Tee S, Marriott C, “Effects of particle size and adding sequence of fine lactose on the deposition of salbutamol sulphate from a dry powder formulation”, *International Journal of Pharmaceutics* 1999;182:133-144.
2. Zeng X.M, Martin G.P, Marriott C, Pritchard J, “The influence of crystallization conditions on the morphology of lactose intended for use as a carrier for dry powder aerosols”, *Journal of Pharmacy and Pharmacology* 2000;52:633-643.
3. Ganderton D, “The generation of respirable cloud from coarse powder aggregates”, *Journal of Biopharmaceutical Sciences* 1992;3:101-105.
4. Staniforth J.N, “Improvement in dry powder inhaler performance: surface passivation effects”, In: *Proceedings of Drug Delivery to the Lungs*, London, vol.VII, 1996, p.86-89.
5. Amass J.M, “A study of drug carrier interactions in dry powder inhalers”, PhD thesis, University of Essex 1996, UK.
6. Jashnani R.N, Byron P.R, “Dry powder aerosol generation in different environments: performance comparisons of albuterol, albuterol sulfate, albuterol adipate and albuterol stearate”, *International Journal of Pharmaceutics* 1996;130:13-24.
7. Jashnani R.N, Byron P.R, Dalby R.N, “Testing of dry powder aerosol formulations in different environmental conditions”, *International Journal of Pharmaceutics* 1995;113:123-130.
8. Price R, Young P.M, Edge S, Staniforth J.N, “The influence of relative humidity on particulate interactions in carrier-based dry power inhaler formulations”, *International Journal of Pharmaceutics* 2002;246:47-59.

